
Vol. 61 • No. 10
October 2018
Microwave Journal
NEW ENTRANTS PACK A PUNCH IN THE SAW/BAW MARKET
60 YEARS
horizon house
Founded in 1958
mwjournal.com


RUGGED & RELIABLE
MADE IN THE USA FOR OVER 57 YEARS!
M*E*C*A* - MICROWAVE EQUIPMENT COMPONENTS OF AMERICA
Airborne Radar & Communications
Satellite Communications
Test & Measurement
L, S, C, X, Ka & Ku
Missile Guidance
Military Electronic Countermeasures
Research & Development
ML-SERIES PRODUCTS
(COMMERCIAL OFF THE SHELF)
Power Dividers/Combiners
20 MHz - 40 GHz
SMA, 2.92, QMA, N, TNC, BNC,
RPTNC 4.1/9.5 & 7/16 Up to 120 watts
MIL-DT-23971 Available.
Attenuators
Up to 40 GHz
SMA, 2.92, QMA, N,
TNC, BNC, RPTNC & 7/16
Up to 150 watts.
Directional Couplers/Hybrids
0.4 - 40 GHz
SMA, 2.92, QMA, N, TNC, BNC,
RPTNC & 7/16 Up to 500 watts
MIL-DTL-15370 Available.
Bias Tees
Up to 6 & 18 GHz
SMA, 2.92mm, QMA,
N,TNC, RP-TNC & 7/16 DIN.
Terminations
Hz-18 GHz
N, SMA & 7/16 Up to 250 watts
MIL-DTL-3903E
Circulators/Isolators
Up to 40 GHz
SMA, 2.92, N, & 7/16
Up to 250 watts.
MECA Electronics, Inc.
Microwave Equipment & Components of America
Since 1961

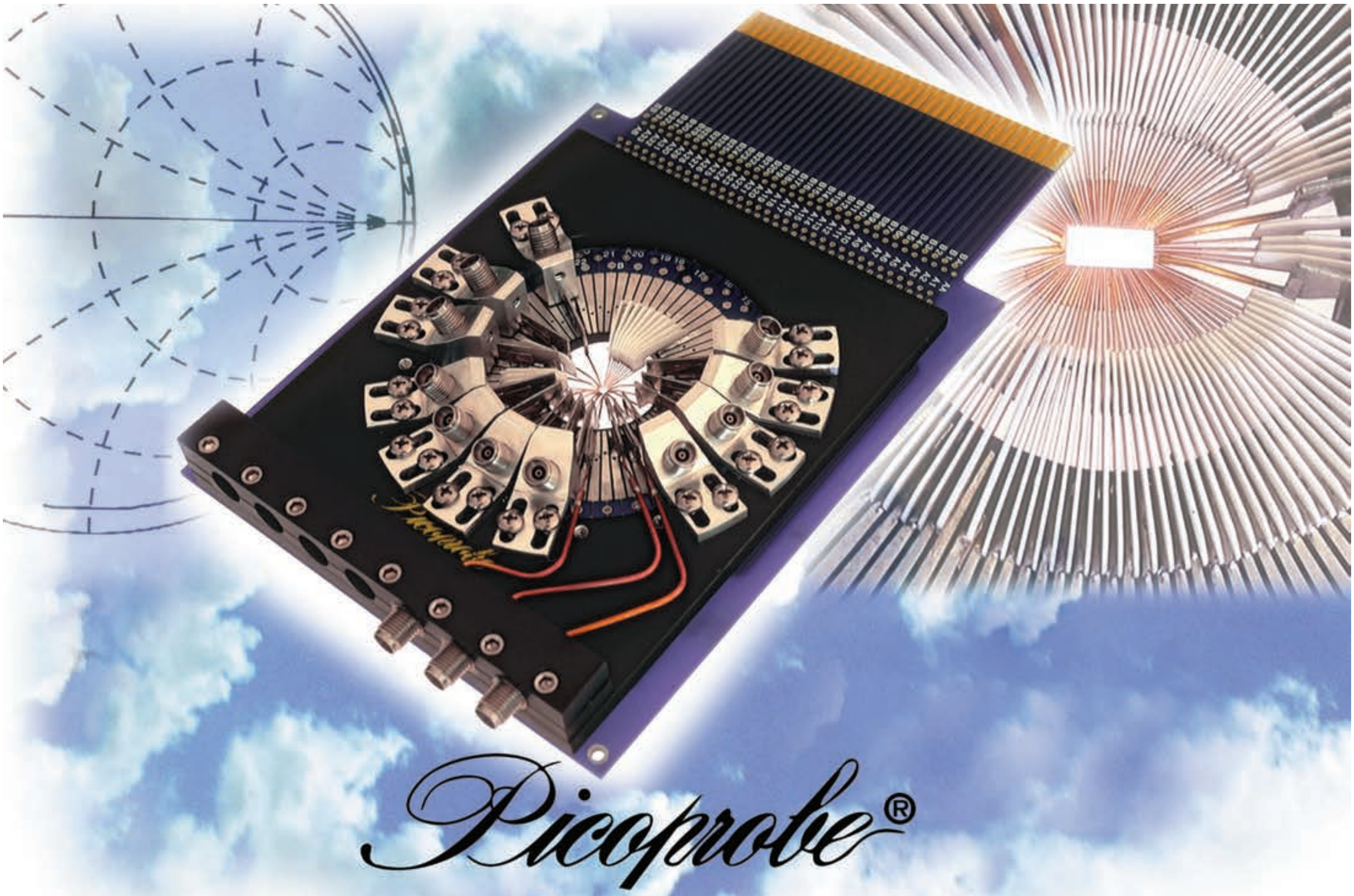

Picoprobe elevates probe cards to a higher level…

(…110 GHz to be exact.)

Since 1981, GGB Industries, Inc., has blazed the on-chip measurement trail with innovative designs, quality craftsmanship, and highly reliable products. Our line of custom microwave probe cards continues our tradition of manufacturing exceptional testing instruments.

Through unique modular design techniques, hundreds of low frequency probe needles and a variety of microwave probes with operating frequencies from DC to 40, 67, or even 110 GHz can be custom configured to your layout.

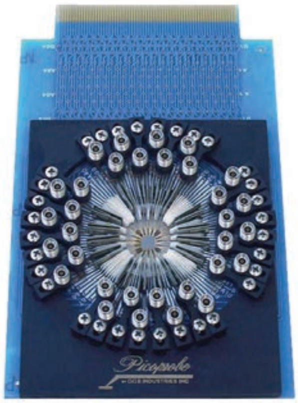

Our patented probe structures provide the precision and ruggedness you require for both production and characterization testing. And only Picoprobe® offers the lowest loss, best match, low inductance power supplies, and current sources on a single probe card.

Our proven probe card design technology allows full visibility with inking capability and ensures reliable contacts, even when probing non-planar structures.

Not only do you get all the attractive features mentioned, but you get personal, professional service, rapid response, and continuous product support--all at an affordable price so your project can be completed on time and within budget.

Typical Specs	10GHz	20GHz	40GHz
Insertion Loss	0.6 dB	0.8 dB	1.3 dB
Return Loss	22 dB	18 dB	15 dB

For technical assistance, custom product designs, or off-the-shelf delivery, call GGB Industries, Inc., at (239) 643-4400.

GGB INDUSTRIES, INC. • P.O. BOX 10958 • NAPLES, FL 34101

Telephone (239) 643-4400 • Fax (239) 643-4403 • E-mail email@ggb.com • www.picoprobe.com


MCL B 744
ADP-2-10
MCL A 745
ADPQ-140
MCL
BPNC
MCL
SBA-2-20
MCL
QBA-12
071638

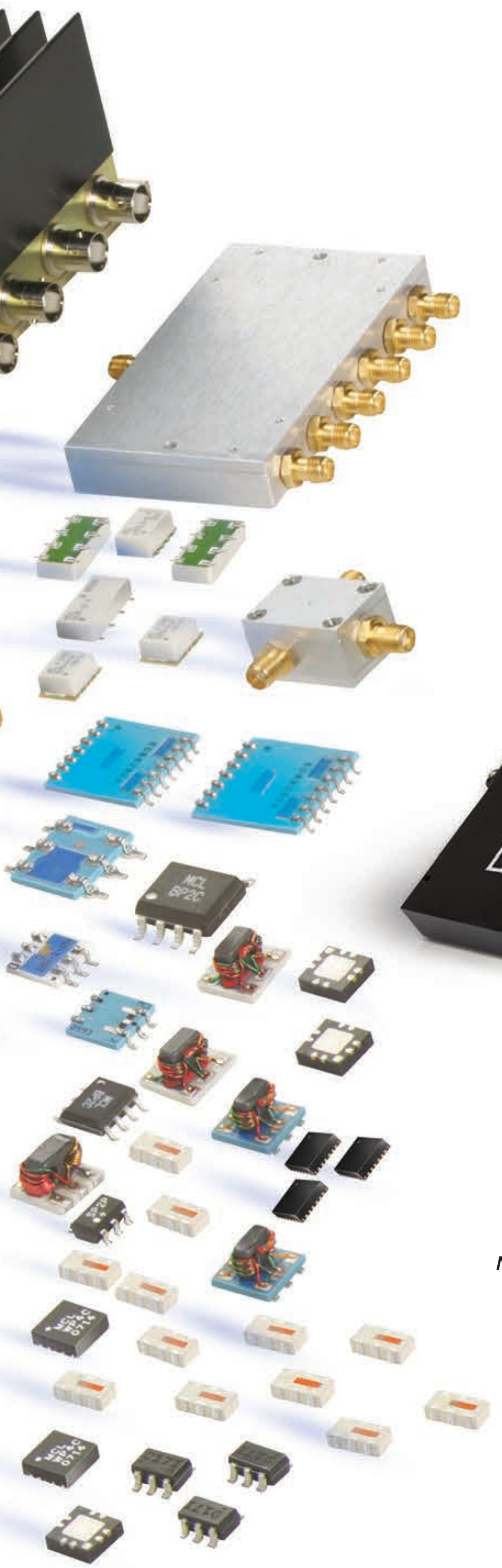

POWER SPLITTERS/ COMBINERS

from **2 kHz to 40 GHz** as low as **89¢** ea. (qty. 1000)

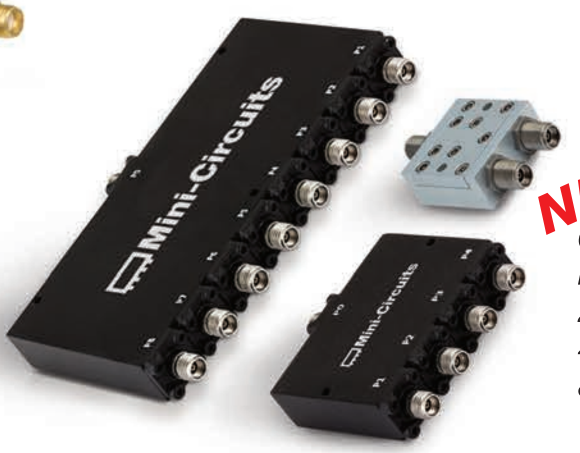

NEW!

COVERING 10 to 40 GHz IN A SINGLE MODEL

2-WAY ZN2PD-K44+
4-WAY ZN4PD-K44+
8-WAY ZN8PD-K44+

The industry's largest selection includes THOUSANDS of models from 2 kHz to 40 GHz, with up to 300 W power handling, in coaxial,flat-pack, surface mount and rack mount housings for 50 and 75Ω systems.

From 2-way through 48-way designs, with 0°, 90°, or 180° phase configurations, Mini-Circuits' power splitter/combiners offer a vast selection of features and capabilities to meet your needs from high power and low insertion loss to ultra-tiny LTCC units and much more.

Need to find the right models fast? Visit minicircuits.com and use Yoni2®! It's our patented search engine that searches actual test data for the models that meet your specific requirements! You'll find test data, S-parameters, PCB layouts, pricing, real-time availability, and everything you need to make a smart decision fast!

All Mini-Circuits' catalog models are available off the shelf for immediate shipment, so check out our website today for delivery as soon as tomorrow!

RoHS Compliant
Product availability is listed on our website.

Mini-Circuits®

www.minicircuits.com P.O. Box 350166, Brooklyn, NY 11235-0003 (718) 934-4500 sales@minicircuits.com 448 Rev U

Designed For 5G MIMO Active Antenna!!!

The World First SMT Microstrip Patented Isolator/Circulator at 28GHz & 38GHz

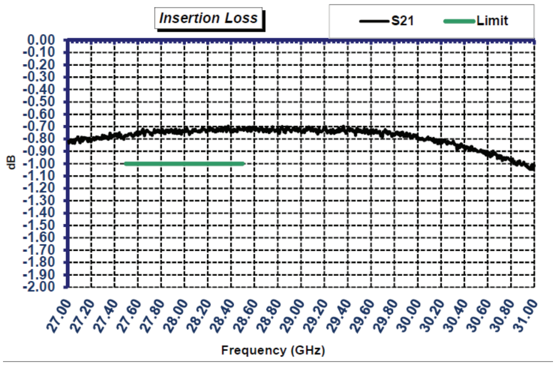

- No Metal Bias Needed
- Easy Reflow Assembly
- No Expensive Wire Bonding

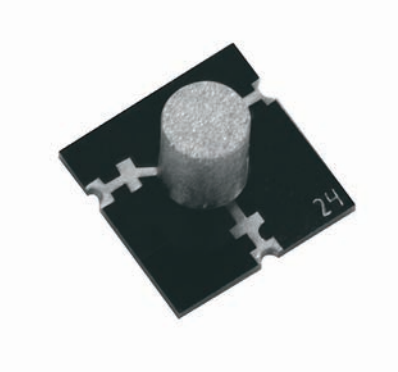

- 200kpcs Sold For Similar Array Application
- Proven Technology

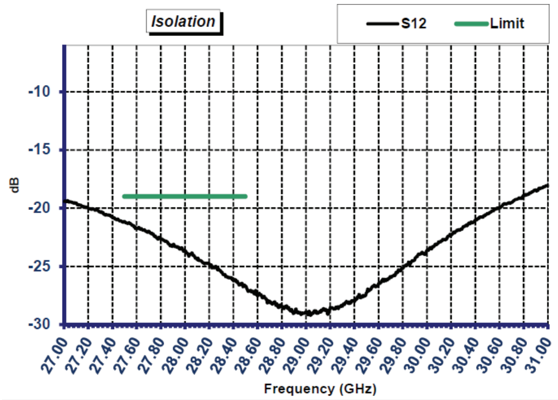

Tel:1(888)236-9828(US&Canada)

www.jqlelectronics.com sales@jqlelectronics.com

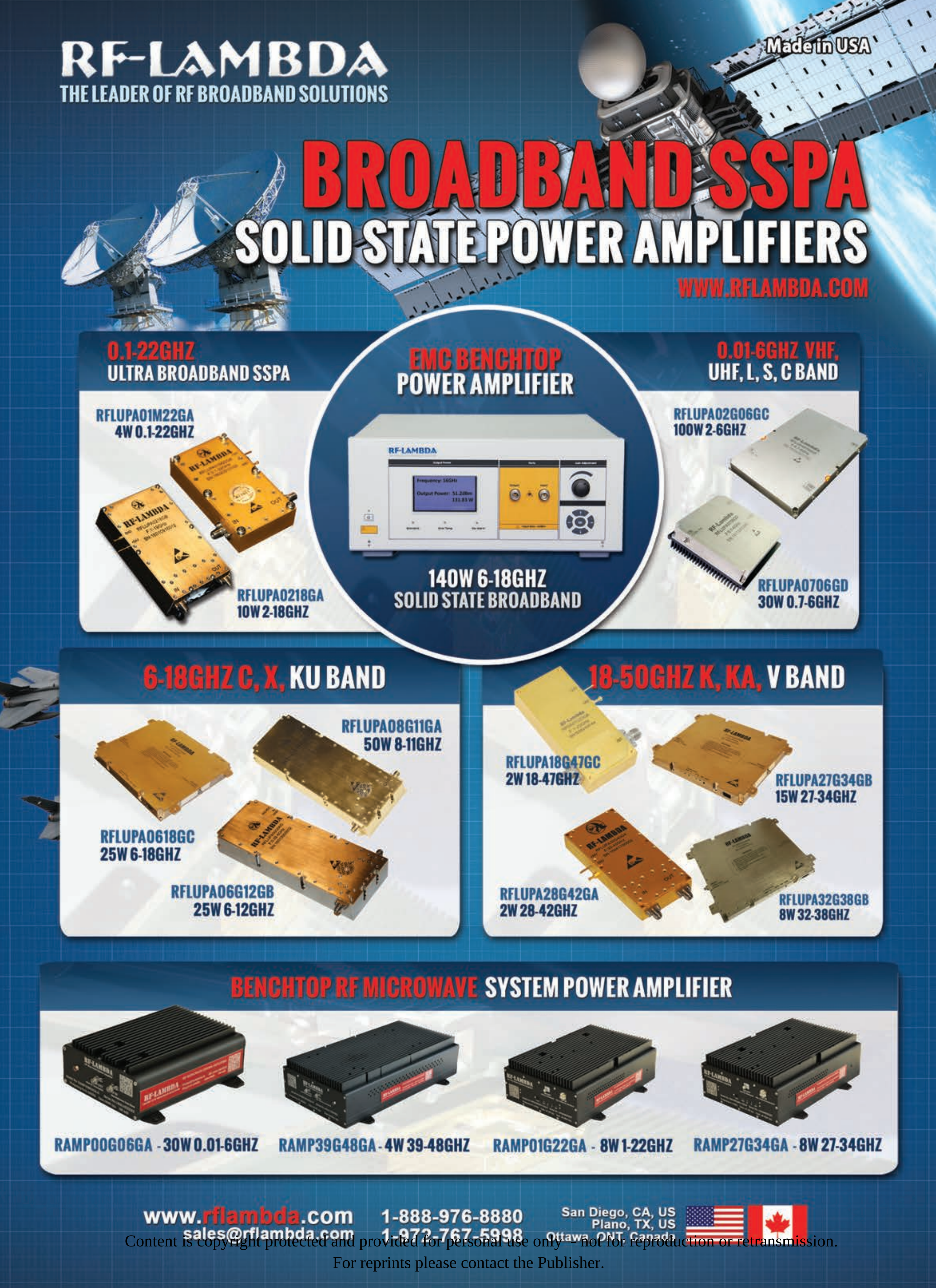
RF-LAMBDA
THE LEADER OF RF BROADBAND SOLUTIONS
Made in USA
BROADBAND SSPA
SOLID STATE POWER AMPLIFIERS
WWW.RFLAMBDA.COM
0.1-22GHZ
ULTRA BROADBAND SSPA
RFLUPA01M22GA
4W 0.1-22GHZ
RFLUPA0218GA
10W 2-18GHZ
EMC BENCHTOP
POWER AMPLIFIER
140W 6-18GHZ
SOLID STATE BROADBAND
0.01-6GHZ VHF,
UHF, L, S, C BAND
RFLUPA02G06GC
100W 2-6GHZ
RFLUPA0706GD
30W 0.7-6GHZ
6-18GHZ C, X, KU BAND
RFLUPA08G11GA
50W 8-11GHZ
RFLUPA0618GC
25W 6-18GHZ
RFLUPA06G12GB
25W 6-12GHZ
18-50GHZ K, KA, V BAND
RFLUPA18G47GC
2W 18-47GHZ
RFLUPA27G34GB
15W 27-34GHZ
RFLUPA28G42GA
2W 28-42GHZ
RFLUPA32G38GB
8W 32-38GHZ
BENCHTOP RF MICROWAVE SYSTEM POWER AMPLIFIER
RAMP00G06GA - 30W 0.01-6GHZ
RAMP39G48GA - 4W 39-48GHZ
RAMP01G22GA - 8W 1-22GHZ
RAMP27G34GA - 8W 27-34GHZ
www.rflambda.com
sales@rflambda.com
1-888-976-8880
1-972-767-5998
San Diego, CA, US
Plano, TX, US
Ottawa, ONT, Canada

Microwave Journal

CONTENTS

October 2018
Vol. 61 • No. 10
Passive & Control Components
mwjournal.com

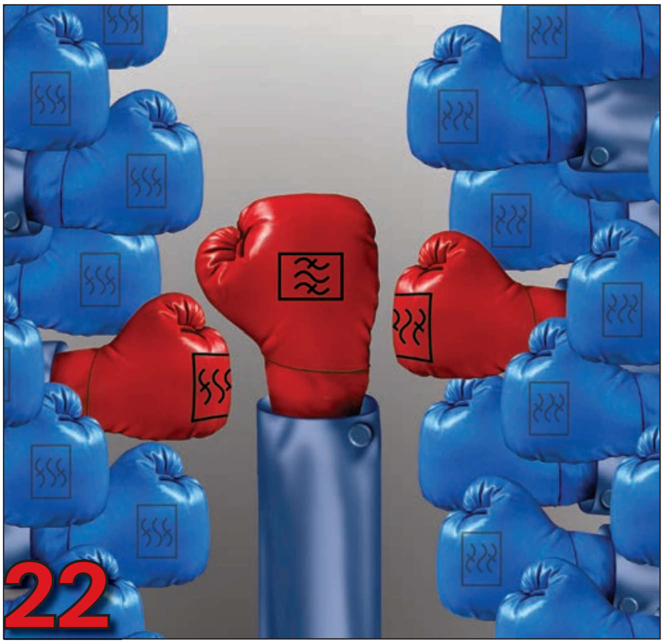

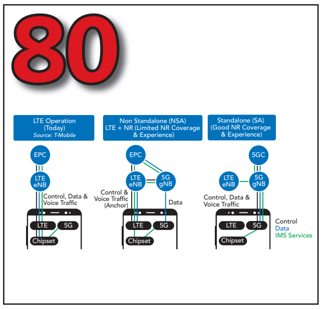

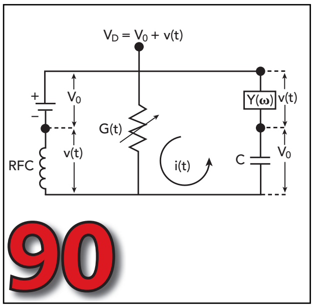

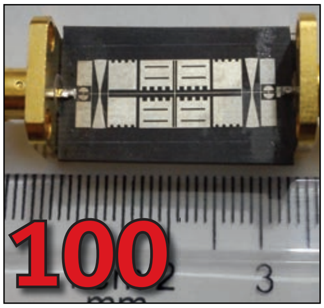

Cover Feature

Technical Features

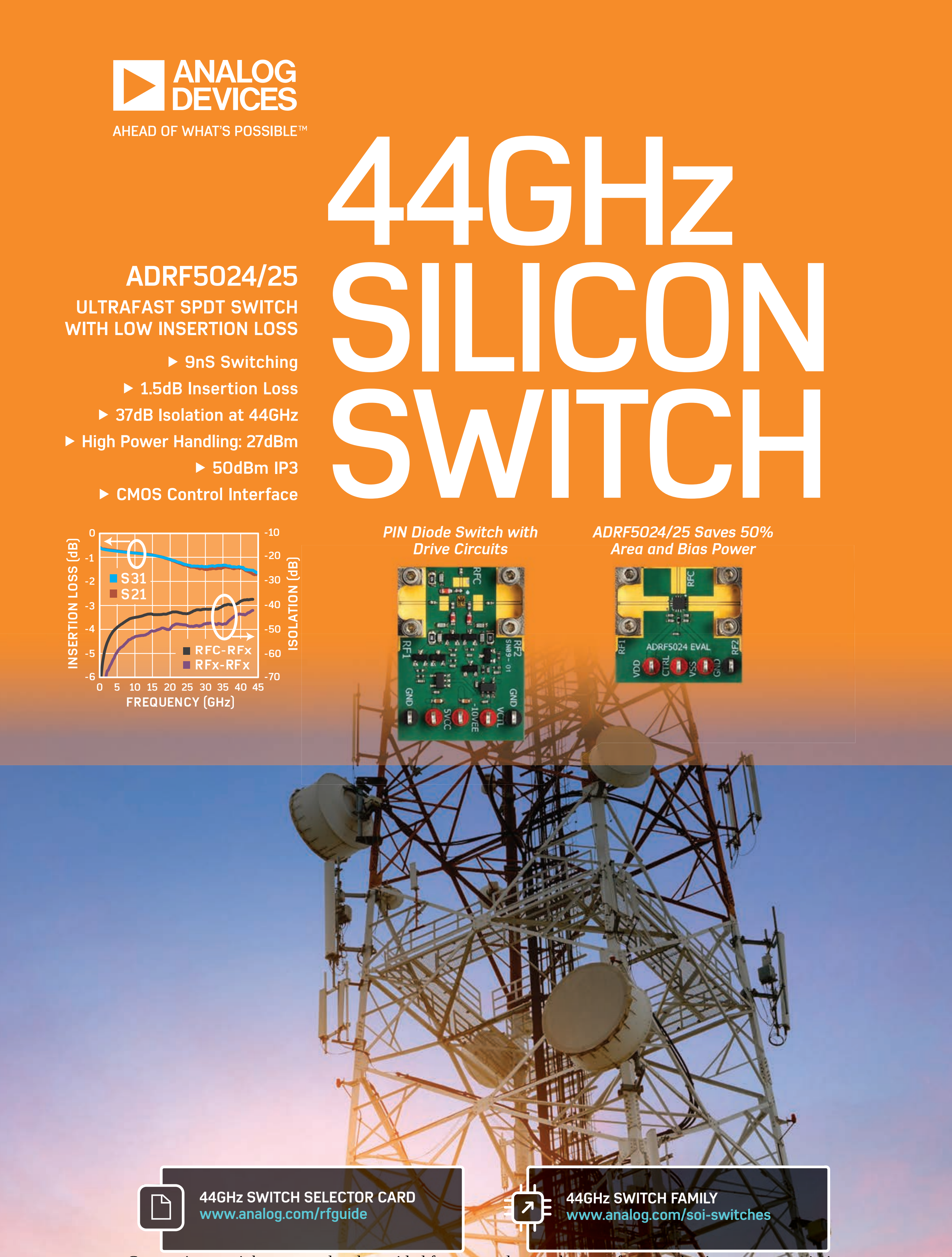
ANALOG DEVICES
AHEAD OF WHAT'S POSSIBLE™
44GHz SILICON SWITCH
ADRF5024/25
ULTRAFAST SPDT SWITCH WITH LOW INSERTION LOSS
▶ 9nS Switching
▶ 1.5dB Insertion Loss
▶ 37dB Isolation at 44GHz
▶ High Power Handling: 27dBm
▶ 50dBm IP3
▶ CMOS Control Interface
INSERTION LOSS (dB)
ISOLATION (dB)
FREQUENCY (GHz)
S31
S21
RFC-RFx
RFx-RFx
PIN Diode Switch with Drive Circuits
ADRF5024/25 Saves 50% Area and Bias Power
ADRF5024 EVAL
44GHz SWITCH SELECTOR CARD
www.analog.com/rfguide
44GHz SWITCH FAMILY
www.analog.com/soi-switches

Microwave Journal

CONTENTS

mwjournal.com

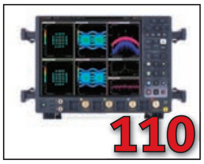

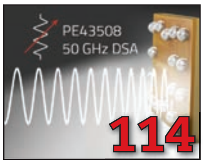

Product Features

Tech Briefs

Departments

Microwave Journal (USPS 396-250) (ISSN 0192-6225) is published monthly by Horizon House Publications Inc., 685 Canton St., Norwood, MA 02062. Periodicals postage paid at Norwood, MA 02062 and additional mailing offices.

POSTMASTER: Send address corrections to Microwave Journal, PO Box 1028, Lowell, MA 01853 or e-mail mwj@e-circ.net.com. Subscription information: (978) 671-0446. This journal is issued without charge upon written request to qualified persons working in the RF & microwave industry. Other subscriptions are: domestic, $120.00 per year, two-year subscriptions, $185.00; foreign, $200.00 per year, two-year subscriptions, $370.00; back issues (if available) and single copies, $10.00 domestic and $20.00 foreign. Claims for missing issues must be filed within 90 days of date of issue for complimentary replacement.

STAFF

Publisher: Carl Sheffres
Editor: Patrick Hindle
Technical Editor: Gary Lerude
Managing Editor: Jennifer DiMarco
Associate Technical Editor: Cliff Drubin
Copy Editor: Ashleigh West
Multimedia Staff Editor: Barbara Walsh
Contributing Editor: Janine Love
Consulting Editor: Harlan Howe, Jr.
Consulting Editor: Frank Bashore
Consulting Editor: David Vye
Consulting Editor: Raymond Pengelly
Electronic Marketing Manager: Chris Stanfa
Digital Content Specialists: Lauren Tully, Jaclyn LaFrance
Audience Development Manager: Carol Spach
Traffic Manager: Edward Kiessling
Director of Production & Distribution: Robert Bass
Art Director: Janice Levenson
Graphic Designer: Ann Pierce

EUROPE

Office Manager: Nina Plesu

CORPORATE STAFF

CEO: William M. Bazzy
President: Ivar Bazzy
Vice President: Jared Bazzy

EXECUTIVE EDITORIAL OFFICE
685 Canton Street, Norwood, MA 02062
Tel: (781) 769-9750
FAX: (781) 769-5037
e-mail: mwj@mwjournal.com

EUROPEAN EDITORIAL OFFICE
16 Sussex Street, London SW1V 4RW, England
Tel: Editorial: +44 207 596 8730 Sales: +44 207 596 8740
FAX: +44 207 596 8749

SUBSCRIPTION SERVICES
Send subscription inquiries and address changes to:
Tel: (978) 671-0446
e-mail: mwj@e-circ.net

www.mwjournal.com

Printed in the USA

Microwave Journal Online

Visit us @ mwjournal.com

E-LEARNING CENTER

An Overview of Glass-Weave Impact on Millimeter-Wave PCB Performance
Sponsored by: Rogers Corp. 10/9

Choosing the Right RF Technology for 5G Infrastructure
Sponsored by: NXP Semiconductors 10/24

Web Survey

Which component design will be the most challenging in sub-6 GHz 5G handsets?

Look for our multiple choice survey online at mwjournal.com/polls

August Survey

Which market is the main strength of Spain's microwave industry?

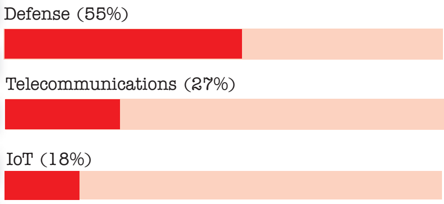

Executive Interviews

Joel Levine, president and co-founder of RF/microwave distributor **RFMW,** discusses the state of the market 15 years after launching RFMW, and how being acquired by TTI will strengthen RFMW and better serve designers.

Lauri Viitas, VP of product and business development at **Guzik Technical Enterprises**, tells how the company's start in magnetic recording evolved into RF and mmWave OTA test systems for 5G and 802.11ad/ay.

WHITE PAPERS

api technologies corp. — Introduction to SAW Filter Theory and Design Techniques

LPKF Laser & Electronics — PCB Substrates: Matching your Design to the Right Material and Rapid Prototyping Process

SKYWORKS — 5G New Radio Solutions: Revolutionary Applications Here Sooner Than You Think

Join Us Online

Follow us @Pathindle @MWJGary @MWJEditor

Join us at the RF and Microwave Community

Become a fan at facebook.com/microwavejournal

.COM

Catch *Frequency Matters*, the industry update from *Microwave Journal*,
microwavejournal.com/FrequencyMatters


Has Amplifier Performance or Delivery Stalled Your Program?
Noise Figure In Select Frequency Bands
Noise Figure (dB)
Frequency (GHz)
4.5dB
4.0dB
2.8dB
2.8dB
2.5dB
1.8dB
1.5dB
1.3dB
1.2dB
1.2dB
0.9dB
0.7dB
0.7dB
0.5dB
0.35dB
B&Z TECHNOLOGIES
Innovating to Excel
www.bnztech.com

NOVEMBER

MARK YOUR CALENDAR

2

Los Angeles, Calif.

CLASTECH highlights recent developments in RF and microwave technologies as a joint effort by the local chapters of the IEEE MTT-S and the APS. **www.clastech.org**

4-9

Williamsburg, Va.

The AMTA is a non-profit, international organization dedicated to the development and dissemination of theory, best practices and applications of antenna, radar signature and other EM measurement technologies.
https://amta2018.org/

5-8

Glendale, Ariz.

ITC is an annual forum and technical exhibition providing telemetry specific short courses, technical papers from professionals and students and exhibits of the industry's leading companies.
www.telemetry.org

6-8

GLOBAL MILSATCOM 2018

6TH NOVEMBER TO 8TH NOVEMBER 2018, LONDON, UNITED KINGDOM

London, U.K.

Global MilSatCom's reputation has been built on the high-level international speakers and decision makers it attracts and the fantastic interactive opportunities offered during the conference sessions, workshops and networking receptions.
www.globalmilsatcom.com

WEBINAR 7

Complete X-Band 2x2 Phased-Array Antenna Design and Simulation

Sponsored by:

NATIONAL INSTRUMENTS | AWR

6-9

APMC 2018 Nov. 6-9 Kyoto Japan

Kyoto, Japan

APMC provides a broad forum for participants from both academia and industries to exchange information, share research results and discuss collaborations in the fields of microwave, mmWave and infrared and optical waves. **www.apmc2018.org**

WEBINAR 13

Signal Integrity Journal

Analysis and Verification of DDR3/DDR4 Interfaces

Mentor
A Siemens Business

13-16

electronica

Munich, Germany

electronica, trade fair and conference, highlights all the latest trends in PCBs, semiconductors, sensors, connectors or displays.
https://electronica.de

WEBINAR 14

Signal Integrity Journal

PAM4 Jitter, Noise and BER Analysis

Sponsored by:

Noisecom

28-30

IMaRC

Kolkata, India

https://imarc-ieee.org

28-30

Microwave Workshops & Exhibition
MWE 2018

Yokohama, Japan

For more than a quarter-century, MWE has provided workshops introducing state-of-the-art technologies and future visions, fundamental educational courses for novice/young engineers and exhibitions of the latest products.
https://apmc-mwe.org/mwe2018/en_index.html

FOR DETAILS, VISIT MWJOURNAL.COM/EVENTS

Coming**Events**

CALL FOR PAPERS

92nd ARFTG Microwave Measurement Symposium
October 26, 2018

CS MANTECH 2019
October 31, 2018

IEEE MTT-S IMS 2019
December 1, 2018

IMBioC 2019
December 6, 2018

IEEE EMC+SIPI 2019
January 6, 2019

EDI CON China 2019
January 10, 2019

EuMCE 2019
January 25, 2019

WAMICON 2019
February 1, 2019

IEEE COMCAS 2019
April 18, 2019

mwjournal.com

OCTOBER

EDI CON USA 2018
October 17–18, 2018 • Santa Clara, Calif.
www.ediconusa.com

MILCOM 2018
October 29–31, 2018 • Los Angeles, Calif.
https://events.afcea.org/MILCOM18/Public/enter.aspx

ESC Minneapolis
October 31–Nov. 1, 2018 • Minneapolis, Minn.
www.escminn.com

NOVEMBER

IEEE CLASTECH 2018
November 2, 2018 • Los Angeles, Calif.
www.clastech.org

AMTA 2018
November 4–9, 2018 • Williamsburg, Va.
https://amta2018.org/

ITC USA
November 5–8, 2018 • Glendale, Ariz.
www.telemetry.org

Global MILSATCOM 2018
November 6–8, 2018 • London, U.K.
www.globalmilsatcom.com

APMC 2018
November 6–9, 2018 • Kyoto, Japan
http://www.apmc2018.org/

electronica 2018
November 13–16, 2018 • Munich, Germany
https://electronica.de/index.html

IEEE IMaRC 2018
November 28–30, 2018 • Kolkata, India
https://imarc-ieee.org

2018 Microwave Workshops & Exhibition
November 28–30, 2018 • Yokohama, Japan
https://apmc-mwe.org/mwe2018/en_index.html

DECEMBER

IEDM 2018
December 1–5, 2018 • San Francisco, Calif.
https://ieee-iedm.org

JANUARY 2019

CES 2019
January 8–11, 2019 • Las Vegas, Nev.
https://www.ces.tech/

92nd ARFTG Microwave Measurement Symposium
January 19–22, 2019 • Orlando, Fla.
www.arftg.org

Radio and Wireless Week 2019
January 20–23, 2019 • Orlando, Fla.
https://radiowirelessweek.org/

DesignCon 2019
January 29–31, 2019 • Santa Clara, Calif.
www.designcon.com

Mobile Deployable Communications 2019
January 31–Feb. 1, 2019 • Warsaw, Poland
www.mobiledeployable.com

FEBRUARY 2019

Mobile World Congress 2019
February 25–28, 2019 • Barcelona, Spain
www.mobileworldcongress.com/

MARCH 2019

EMV 2019
March 19–21, 2019 • Stuttgart, Germany
https//emv.mesago.com/events/en.html

Microwave & RF 2019
March 20–21, 2019 • Paris, France
www.microwave-rf.com

GOMACTech 2019
March 25–28, 2019 • Albuquerque, N.M.
www.gomactech.net/2019/index.html

ANALOG DEVICES

AHEAD OF WHAT'S POSSIBLE™

RadioVerse™

ADRV9008-2

Integrated Dual RF Transmitter with Observation Receiver

High-Performance, Low Power Consumption, Integrated RF Transmitter

Part of the RadioVerse™ technology and design ecosystem, Analog Devices' ADRV9008-2 is a highly-integrated, RF agile transmit subsystem offering dual channel transmitters, observation path receiver, integrated synthesizers and digital signal processing functions.

Key ADRV9008-2 features include:

- 450 MHz max. tunable transmitter synthesis bandwidth
- 450 MHz max. observation receiver bandwidth
- 75-6000 MHz tuning range (center frequency)
- Low power consumption
- Ideal for 2G/3G/4G/5G macro cell base stations and avionics and defense applications

AVAILABLE AT RICHARDSON RFPD

- Integrated wideband RF transceivers
- Evaluation tools & development kits

ANALOG DEVICES
AHEAD OF WHAT'S POSSIBLE™

RadioVerse™
CONCEPT TO CREATION AT LIGHT SPEED

RichardsonRFPD
An Arrow Company

LEARN MORE ABOUT
ANALOG DEVICES' ADRV9008-2
www.richardsonrfpd.com/ADI-radioverse

SCAN ME

Your Global Source for RF, Wireless, IoT & Power Technologies
www.richardsonrfpd.com | 800.737.6937 | 630.262.6800

Enabling Calibration Free Millimeter-Wave 5G for Commercial Deployments

5G is here...

5G is happening now and the industrialization of silicon-based millimeter-wave active antennas is supporting the first true 5G trials and deployments. A radical use case evolution is happening with an explosion of innovation and a tipping point in millimeter-wave Active Antennas that will enable 5G everywhere.

5G antennas that leverage Anokiwave's highly integrated silicon ZERO-CAL® ICs will see a drastic reduction in material and assembly costs by eliminating the need for array calibration. The continued reduction in antenna cost coupled with the ability to optimize and monitor technical performance in the field is paving the way for rapid deployment of 5G systems across the globe.

ZERO-CAL® is one of the many ways Anokiwave is enabling the new world of millimeter-wave 5G at a commercial scale.

mmW Si Core ICs | Active Antenna ASICs | mmW Front End ICs

www.anokiwave.com/5g | innovation@anokiwave.com

Cover Feature
Invited Paper

With Contributions from:
Akoustis Technologies
OnScale
Resonant

SAW/BAW New Market Entrants Offer New Approaches

Editor's Note: With the increasing number of cellular bands for 4G/LTE, the mobile RF front-end's critical component has shifted from the power amplifier to the filter. Surface acoustic wave (SAW), and, more recently, bulk acoustic wave (BAW) filter technology has been addressing the challenges in the mobile RF front-end that currently uses 40+ filters (and growing). This market growth has attracted new market entrants so *Microwave Journal* compiled information from three such companies—Akoustis, OnScale and Resonant—offering new solutions for the SAW/BAW market.

XBAW RF Filter Blazing Into Higher Frequency Spectrum

Dave Aichele
Akoustis Technologies
Huntersville, N.C.

BAW RF filters are high performance semiconductor components primarily used in mobile smart phones. They address the stringent size requirement for high levels of integration and provide superior performance compared to SAW and ceramic filters, therefore improving the battery life and reducing the number of dropped calls to end users. These high performance components offer low insertion loss and high selectivity required to meet the demanding coexistence requirement for difficult FDD and high frequency TDD 4G/LTE and emerging 5G bands. Current multimode, multiband mid- to high-tier smartphones utilize > 50 filters and experts foresee that including 5G bands will push that number to > 70 filters.

Solidly mounted resonator (SMR) and film bulk acoustic resonator (FBAR) are the two dominant BAW resonator technologies currently utilized in BAW RF filters due to their high Q-factor, high operating frequency and good power handling. The BAW RF filter market is currently served by a duopoly that has historically supplied > 95 percent of the market, where both company's core material technology is based on a sputtered poly-crystalline piezo-electric aluminum nitride (AlN) deposited by physical vapor deposition (PVD) techniques.

SINGLE CRYSTAL RF BAW FILTER TECHNOLOGY

Akoustis Technologies is an emerging new entrant in the projected \$5.8 billion BAW filter market dominated by mobile RF filters.[1] Leveraging a patented BAW resonator process (called XBAW) combined with an integrated design and manufacturing (IDM) business model, Akoustis is blazing new territory and focused on becoming the first commercial supplier of BAW RF filters for applications above 3 GHz.

Akoustis has introduced a new approach of utilizing high purity, single crystal piezo-electric

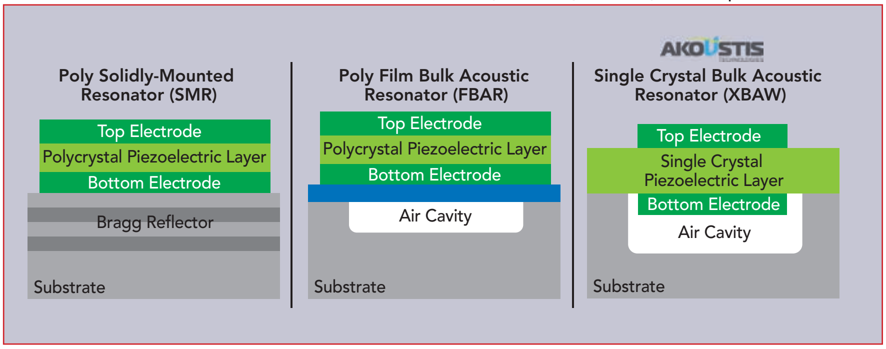

Fig. 1 Cross section images of BAW resonators.

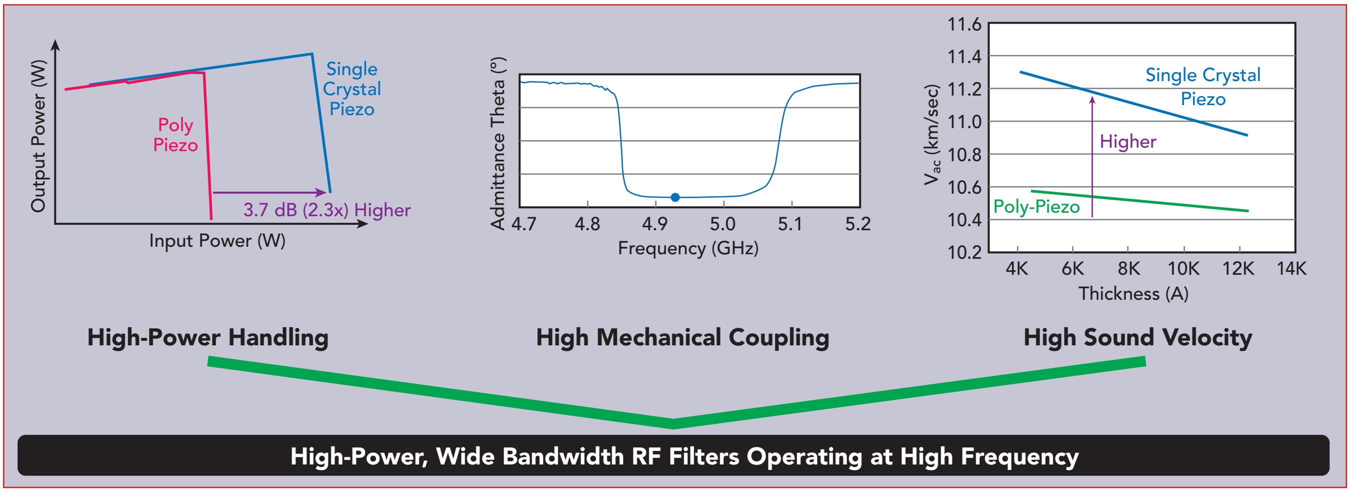

Fig. 2 Three performance features of single crystal piezo-electric material.

AlN material in BAW RF filters (see ***Figure 1***). Epitaxially grown, metal-organic chemical vapor phase deposition (MOCVD) single crystal AlN has inherently higher crystal quality compared to PVD poly-crystal AlN. This improved crystal quality has shown improvements in acoustic velocity and piezo-electric mechanical coupling coefficients. In addition, the thermal conductivity of single crystal AlN is 2× higher than poly-crystal AlN that degrades as film thickness decreases, which may result in a constraint on power capability for traditional FBAR resonators, especially at higher frequencies. In all BAW technologies shown in Figure 1, the resonance frequency is determined by the thickness of the material stack and the effective propagation velocity of the acoustic wave. A higher propagation velocity in the AlN piezo-material results in higher operating frequencies for the same thickness. These three factors; improved acoustic velocity, improved piezo-electric coefficients and improved thermal conductivity enable XBAW RF filters constructed from single crystal, epitaxially grown MOCVD-AlN piezo-electric materials to offer better performance (power handling, insertion loss, bandwidth and skirt steepness) than PVD-AlN based BAW RF filters, especially for high frequency and high-power applications (see ***Figure 2***).

In June 2017, Akoustis completed the strategic acquisition of a MEMS fab located in Canandaigua, N.Y. With this acquisition and subsequent consolidation of all its manufacturing processes, Akoustis now has an internal, ISO-9001 certified 122,000 sq. ft. commercial wafer-manufacturing capability which includes class 100/1000 cleanroom facility, tooled for 150 mm diameter wafers and an operations team to conduct research, development and production of its XBAW RF Filters. In addition, Akoustis is in the process of transitioning DoD Trusted Foundry accreditation for MEMs wafer processing, packaging and assembly, enabling Akoustis to be a supplier for DoD programs requiring specialized filters and Trusted Foundry certification.

RF BAW FILTER MARKETS

Akoustis is the only pure play BAW RF filter company targeting the mobile high band 4G/LTE and emerging 5G applications. This market is by far the largest and made up of filter competitors engaging mobile phone

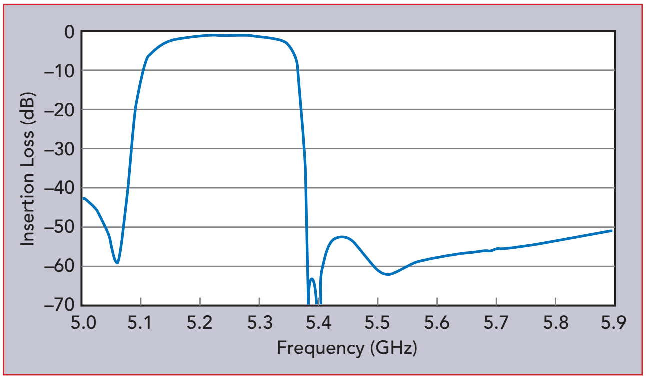

Fig. 3 5.2 GHz BAW RF filter with typical 1.2 IL and > 50 dB attenuation.

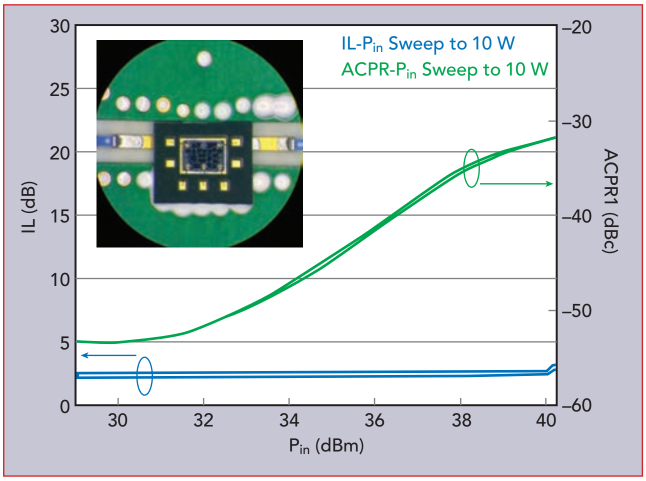

Fig. 4 2.6 GHz BAW RF filter—WCDMA adjacent channel power ratio results.

OEMs and ODMs, RF front-end (RFFE) module manufacturers (some with captive BAW filter technology) and transceiver manufacturers. The push to higher frequency and the wide bandwidth requirement necessary to support the enhanced Mobile Broadband (eMBB) feature of 5G will tax existing SAW and poly-crystal BAW filter technology. Single crystal RF BAW technology will enable the development of higher performance, wider bandwidth BAW RF filters for 5G n41, n77, n78 and n79 bands (or sub bands) operating in 2.6 to 5 GHz spec-

DASSAULT SYSTEMES

SIMULIA

Make the Connection

Find the simple way through complex EM systems with CST Studio Suite

Components don't exist in electromagnetic isolation. They influence their neighbors' performance. They are affected by the enclosure or structure around them. They are susceptible to outside influences. With System Assembly and Modeling, CST Studio Suite helps optimize component and system performance.

Involved in antenna development? You can read about how SIMULIA EM simulation technology is used to simulate antenna performance at **www.cst.com/antenna**.

If you're more interested in filters, couplers, planar and multilayer structures, we've a wide variety of worked application examples live on our website at **www.cst.com/solutions**.

Get the big picture of what's really going on. Ensure your product and components perform in the toughest of environments.

Choose CST Studio Suite – Complete Technology for 3D EM.

CST joins SIMULIA

CST, a Dassault Systèmes company | www.cst.com | SIMULIA.CST.mkt@3ds.com trum with bandwidths that range from 200 to 900 MHz.

Beyond mobile, there are two additional markets that will be well served with access to single crystal RF BAW technology. Advanced Wi-Fi CPE architectures including 802.11ac multi-user MIMO (MU-MIMO) are experiencing faster uptake, driving the demand for smaller components as the complexity within Wi-Fi infrastructure devices is increasing. This trend is expected to continue, especially as 802.11ax is finalized and implemented in next generation tri-band routers that operate at 2.4, 5.2 and 5.6 GHz, simultaneously. Ultra-small passband 5.2 GHz BAW RF filters provide low 1.2 dB typical insertion loss over 160 MHz covering U-NII-1 and U-NII-2A bands with typical 52 dB attenuation across 345 MHz to meet the stringent rejection requirements enabling co-existence with U-NII-2C and U-NII-3 bands (see ***Figure 3***). Incumbent Dielectric Resonator (DR) filters are 23× larger and require shield cans to mitigate interference issues degrading isolation performance.

The infrastructure market is looking at full dimension-MIMO or Massive MIMO architectures which use large antenna array each with its own transceiver configuration to offer much higher spectral efficiency. These new basestation systems will probably be the primary solution for emerging 5G and an alternative to traditional macro-cell BTS for 4.5G and 4.9G LTE networks. FD-MIMO architectures support both FDD and TDD bands and offer 1 to 4 W average powers in 32T32R to 64T64R configurations operating in the 2 to 5 GHz spectrum. These large array systems will need an alternative filter technology to enable size/weight reduction and high volume, surface mount assembly. Traditionally macro-cell style cavity filters are large in size and typically require manual assembly so are not ideal for FD-MIMO systems. Poly-crystal BAW RF filters are used in pico- and micro-cell BTS but may fall short on power handling above 1 W. High-power single crystal technology offers a potential paradigm shift to the major BTS OEMs developing 5G FD-MIMO systems. Akoustis has demonstrated BAW RF filter die mounted on standard laminate capable of handling > 10 W average power at 2.6 GHz (see ***Figure 4***). This power handling provides plenty of power margin headroom for the design of RF BAW filters that offer smaller form factor, surface mount assembly at semiconductor price levels.

SUMMARY

Akoustis Technologies is a new entrant to the multi-billion RF filter market and blazing its own path through material science innovation in single crystal piezo-electric enabling high performance BAW RF filters in the 3 to 6 GHz spectrum for emerging 5G mobile, Wi-Fi and infrastructure applications. Beyond these largest markets, Akoustis is eyeing additional markets such as automotive C-V2X (or DSRC) and military IF/RF filters for L-, S-, C- and X-Band phase radar and communication systems.

Enabling Design of Next-Generation RF Filters for 5G

Gerry Harvey
OnScale
Cupertino, Calif.

While 4G LTE and LTE-Advanced technologies are still being deployed worldwide, the next generation in wireless communication promises a paradigm shift in throughput, latency and scalability. By 2025, the emerging wireless 5G market is expected to reach a total value of $250 billion.[2] SAW filters and BAW filters are already used in 4G devices and will compete for the emerging 5G market. Adoption of 5G will see a significant increase in the number of filters required in a handset, with 4G models already employing 40+ filters. This puts the onus on 5G manufacturers to rapidly innovate new filter designs to capture a share of the growing market. Such innovations tend to offer a "winner take all" prospect such as the FBAR filter ushering in an entirely new product that captured a large percentage of the 4G/LTE market segment.

SAW/BAW DESIGN

To help drive this new level of innovation, OnScale has developed a cloud-enabled simulation platform optimized for Multiphysics analysis of piezoelectric devices such as SAWs and BAWs. This approach is being used to reduce cost, risk and time to market for these products.

Optimization of SAW/BAW filters is a challenging task due to the complexity and size of the devices. OnScale is well-suited for these kinds of problems, taking a highly efficient Finite Element Analysis (FEA) approach and seamlessly deploying this on the cloud. ***Figure 5*** shows a SAW filter with 100 interdigitated pairs and 20 grating fingers modeled in full 3D. The zoomed-in portion shows the simulated surface velocity at a given time-step. The entire model can be run in a matter of hours which is a feat even the most powerful legacy solvers on the market are typically incapable of doing.

Optimization of this design is achieved using the cloud, where hundreds of these models can be simulated simultaneously to allow exploration of a design space defined by the variation of specific parameters. One of these iterations reveals a sweet spot where Q is maximized and spurs are minimized in the impedance of the device. ***Figure 6*** shows the chosen design's impedance versus frequency in this example.

FBAR DESIGN EXAMPLE

FBAR filters, unlike their surface and bulk silicon counterparts, use

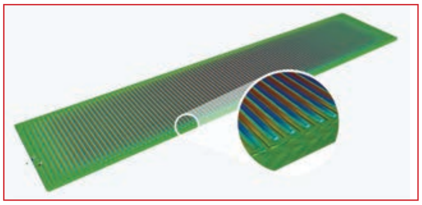

Fig. 5 Full-3D model of a SAW filter in resonance.

piezoelectric thin films over cavities with resonant frequencies between 100 MHz and 10 GHz. A range of different shapes and sizes can be used depending on the performance requirements, with early designs using square shapes and more advanced designs using pentagons. ***Figure 7a*** shows a layout of a pentagonal FBAR resonator that has been imported into OnScale from a GDSII file. An image of the instantaneous surface velocity from the simulation is shown in ***Figure 7b***.

A major challenge for designers is ensuring that filters do not support strong lateral resonances that corrupt passband performance. Resonators with non-parallel sides, such as those shown in ***Figure 8***, support weaker lateral resonances than ones with parallel sides. However, optimizing these shapes empirically is expensive and time consuming. Ideally, an engineer would use full 3D simulation for this optimization process, but this is considered impractical due to the extremely large computational requirements and time demanded by legacy FEM tools. The cloud method solves this problem, delivering rapid insights into these complex electro-mechanical systems and opens entirely new solution spaces for engineers to explore.

To demonstrate this capability, a 3D model of a pentagonal FBAR was constructed and a generic algorithm was used to optimize the design of the filter to minimize lateral resonances. Genetic algorithms mimic the process of natural selection to guide successive populations of candidate designs towards a global optimum. Each population of designs was simulated in parallel on the cloud, as shown in ***Figure 9***.

The model was run for 52 generations and a total of 3,640 designs were investigated. It ran for a total of 68 hours and utilized 8.67 GB of memory. The simulation tool was connected to MATLAB's Global Optimization Toolbox, which allowed various parameters to be tracked during the run including the current best

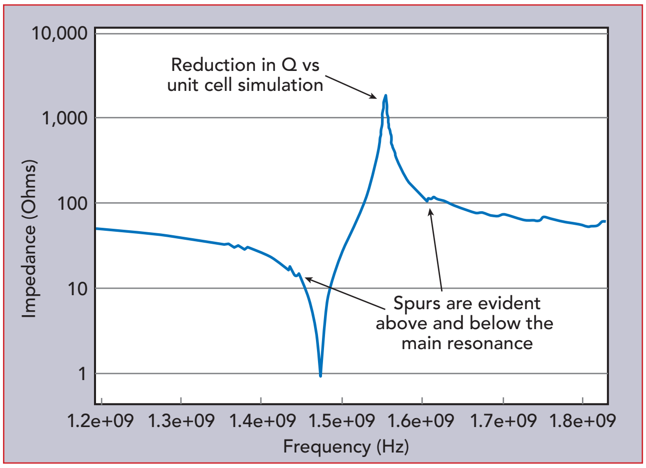

Fig. 6 Impedance plot of an optimized SAW design in full-3D.

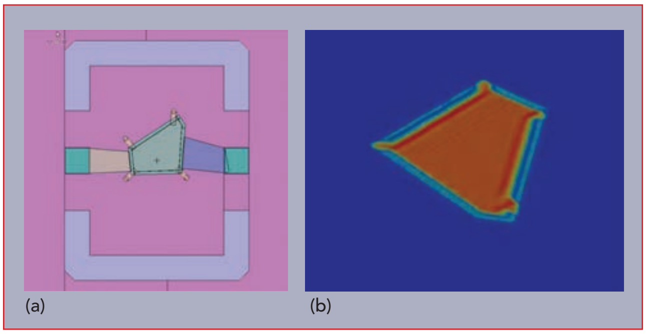

Fig. 7 GDSII import and simulation of a pentagonal FBAR filter.

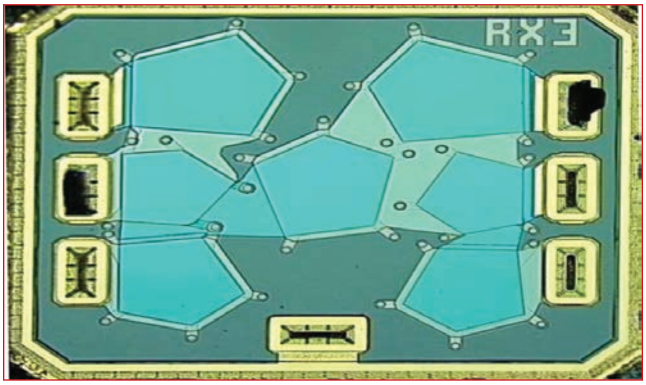

Fig. 8 Die photo of an FBAR employing multiple pentagonal resonators.[3]

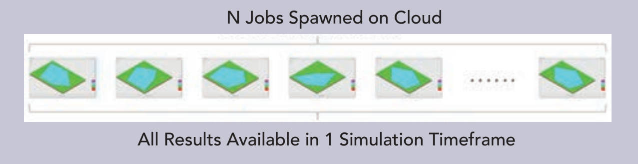

Fig. 9 Parallel design study on the cloud.

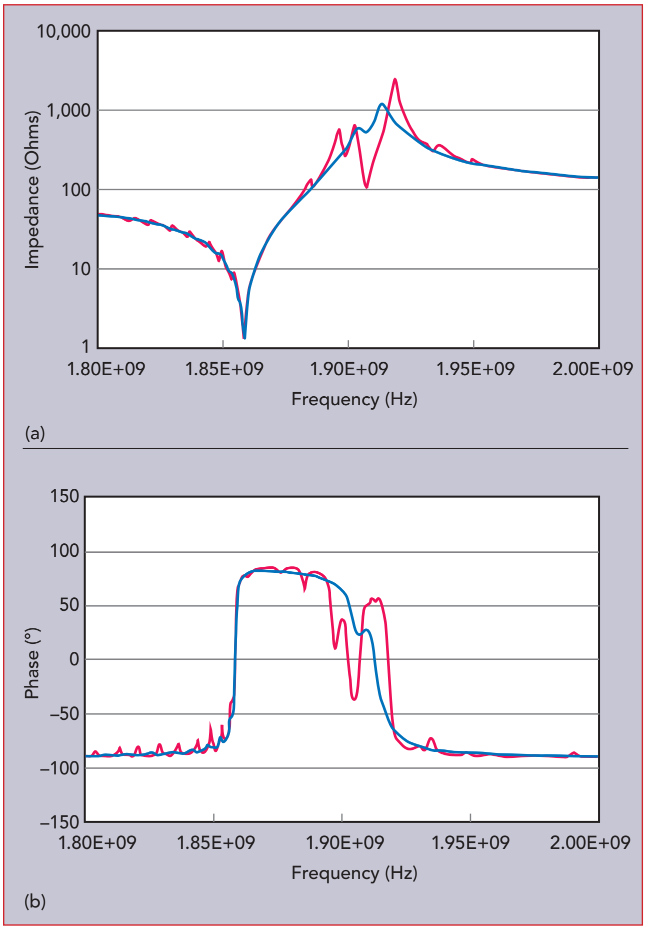

Fig. 10 Comparison of simple square design (red) and optimized pentagonal design (blue).

design. The optimal designs were found to have edges angled relative to the substrate edges to avoid strong reflections, whereas the worst design had three edges close to parallel with the substrate causing increased lateral mode activity.

The results can be seen in ***Figure 10***, where the best pentagonal design shows a significant reduction in ripple when compared to the square device, which was the starting point for the exercise. It is important to note that each of the 3,640 designs were simulated in full 3D, a study that would take a legacy solver nearly a year to complete on the same computing resources. The results provided are indicative of the type of design improvements that can be achieved with cloud based CAE using OnScale's solvers.

SUMMARY

Despite the lack of standards, 5G is promising faster data rates for mobile phones and will be an enabler for autonomous vehicles and the IoT. The move from 4G to 5G represents orders of magnitude higher data rates at frequency bands beyond 3 GHz. However, legacy CAE tools are incapable of performing complete 3D design studies, which are a critical step in optimizing the design and improving the time to market for these highly complex structures. OnScale's cloud solvers open the possibility of doing this analysis in parallel, reducing prototyping costs and speeding time to market.

Infinite Synthesized Networks Deliver RF Filter Design Tools for 5G

Bob Hammond
Resonant
Santa Barbara, Calif.

Where 4G/LTE was a single specification for high speed mobile device services, 5G is a family of technologies designed to serve different use cases ranging from ultra-broadband fixed wireless to low data-rate IoT services. The transition to this new network technology will result in dramatic increases in filter and RFFE complexity.

5G devices will exist in a mobile device environment that includes more complexity, more components (particularly filters), more performance demands, smaller size and lower cost components, plus dual connectivity between cellular and Wi-Fi networks. More bandwidth will be needed, which will require higher frequency components, more carrier aggregation (CA), more complex MIMO antennas, new and adaptable waveforms and improved interference mitigation.

5G RFFE designs for all wireless-enabled products will be driven by cost, power efficiency and available space within the mobile device. The requirements for 5G filters will include complex multiplexing, increasing integration, more filters and the capability to handle much higher frequencies than are currently in use.

RESONANT INFINITE SYNTHESIZED NETWORKS

To address these needs, Resonant has developed a comprehenapi technologies corp.

Solutions for mission critical radar, military defense, EW, communications & SATCOM systems, avionics, & space platforms.

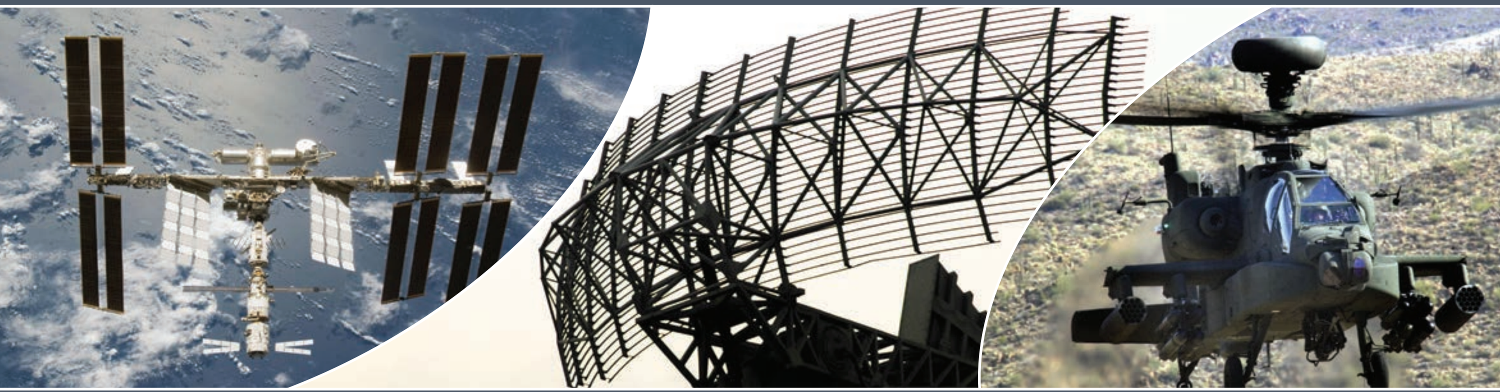

RF, Microwave, Microelectronics & Power Solutions

Components, Modules, Integrated Assemblies & Subsystems

- Amplifiers, Filters, and Passive & Active Components
- Integrated Microwave Assemblies
- SAW Filters & Oscillators
- Optoelectronic Solutions
- High Temperature Microelectronics
- Power Conversion & Distribution

Call +1 (855) 294 3800 or visit micro.apitech.com | Check us out on social:

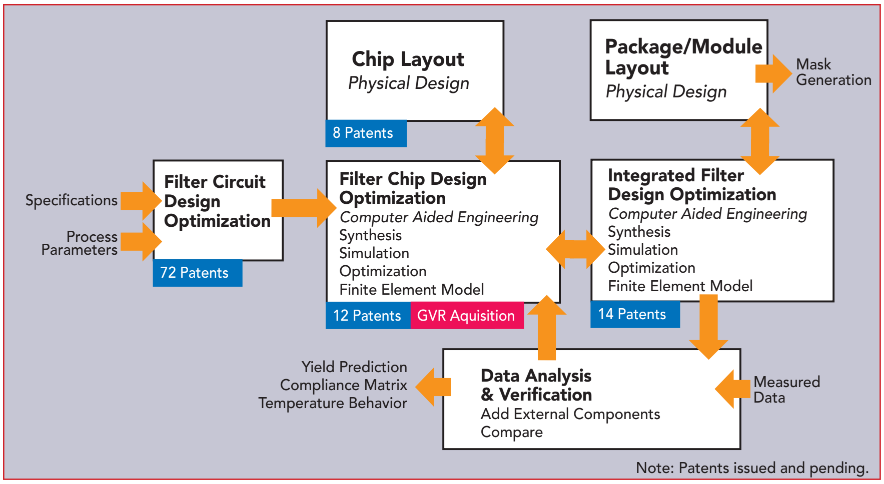

Fig. 11 ISN schematic, showing process flow from initial design to completed mask.

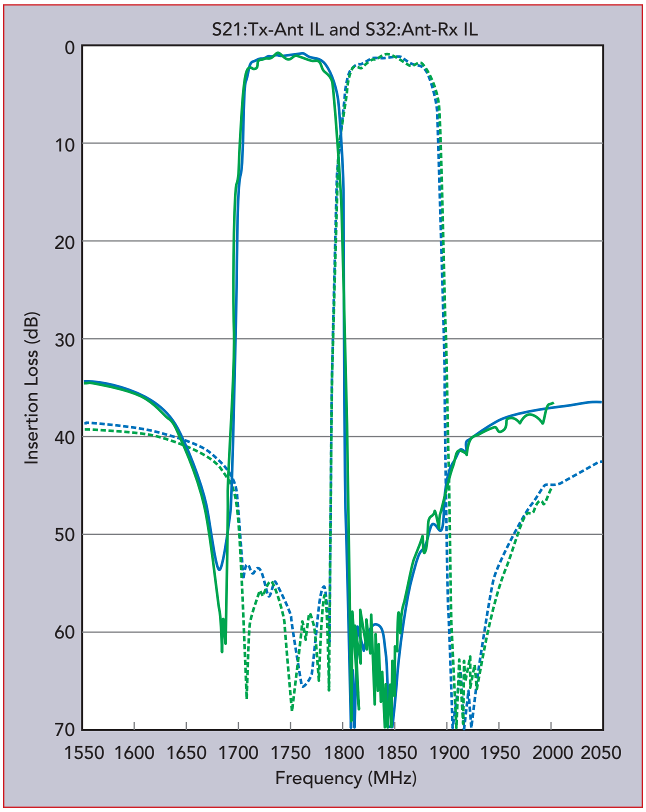

Fig. 12 Measured (blue trace) and modeled (green trace) duplexer performance.

sive filter Electronic Design Automation (EDA) platform called Infinite Synthesized Networks (ISN). Resonant's ISN platform brings together the following elements:

- Modern filter theory.
- Finite element modeling, both electro-magnetic and acoustic.
- Novel optimization algorithms.
- Ecosystem of foundry and packaging/back-end partners.

ISN was initially focused on designing acoustic wave filters, which are a key design block for the RFFE.

ISN is specifically intended to solve many of the 5G challenges that will face design engineers: speed, flexibility and tools that drive down system cost. As of August 2018, more than 10 companies have committed to produce more than 60 devices using ISN.

Figure 11 is a schematic that shows the design-to-mask flow through the ISN process. Testing has proven that ISN's models are highly accurate and reflect physical details of the filter structures, matching the measured performance of manufactured filters, not only in loss and isolation but also in power handling and linearity. Thus, ISN is a capable platform for quickly, efficiently and cost-effectively scaling filter design to meet emerging 5G demand.

Traditional acoustic wave filter design uses a ladder structure and empirical models (linked to a particular fab manufacturer). This typically results in an iterative approach to filter development that involves multiple foundry runs and can take months or more. The ISN platform enables filter design teams to create novel filter structures that outperform traditional filter designs, in a smaller footprint and using lower-cost technologies. ***Figure 12*** shows how closely ISN-modeled performance tracks the actual data measured on a Band 3 duplexer.

ISN's grounding in fundamental materials physics, while optimizing for high-volume design screening, enables designs that are unconstrained by traditional acoustic wave filter design techniques. Consequently, a designer using ISN can create multiplexers, wide passbands and high-power performance, and predict manufacturing yields as well, before a design is committed to mass production.

Thousands of designs can be developed simultaneously and screened to maximize the ultimate performance of the device. Leveraging the expertise of filter design engineers for an increasing number of more complex designs can be achieved using ISN.

IMPLICATIONS FOR THE 5G RF FRONT-END

ISN can be used to develop RF filters for 4G/LTE and other wireless networks, but it is especially impactful for 5G designs that need the high performance, small size and complex passband design benefits of the design tool.

The current state-of-the-art for a 4G/LTE mobile smartphone RFFE separates the frequency spectrum into low-band (698 to 960 MHz), mid-band (1710 to 2200 MHz) and high-band (2400 to 3800 MHz) frequencies, which isolates the RF components, minimizes cross-talk and optimizes the entire power amplifier-filter-switch path (see ***Figure 13***). Although integration of components is logical, the increasing complexity of 5G limits the number of manufacturers that have the expertise to execute on such a complex RF sub-system.

5G RFFEs for all wireless-enabled products will be driven by cost, power efficiency and available space within the unit. So they will need to be small, highly efficient and able to be manufactured in large quantities to meet fast-growing global demand. To commercialize afford-

New ATC 560L Ultra-Broadband UBC™ SMT Capacitors

Ultra-Broadband Performance from 16 KHz to 40+ GHz

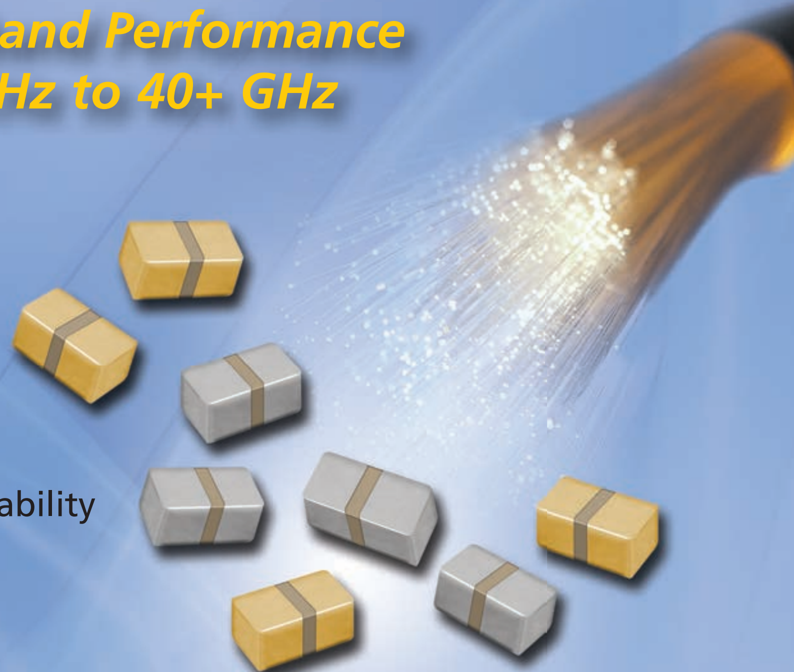

Advantages:

- Ultra-Broadband Performance
- Ultra-Low Insertion Loss
- Flat Frequency Response
- Excellent Return Loss
- Rugged Ceramic Construction
- Unit-to-Unit Performance Repeatability

Features:

- EIA 00402Case Size
- Capacitance: 100 nF
- Operating Frequency: 16 KHz to 40+ GHz
- Insertion Loss: <0.6 dB typ.
- Orientation Insensitive
- One Piece Construction
- Voltage Rating: 16 WVDC
- Gold Complaint Terminations
- RoHS Compliant

Applications:

- Optoelectronics / High Speed Data
- Transimpedance Amplifiers
- ROSA / TOSA†
- SONET††
- Broadband Test Equipment
- Broadband Microwave Millimeter-wave

† Receive and Transmit Optical Sub-Assembly
†† Synchronous Optical Network

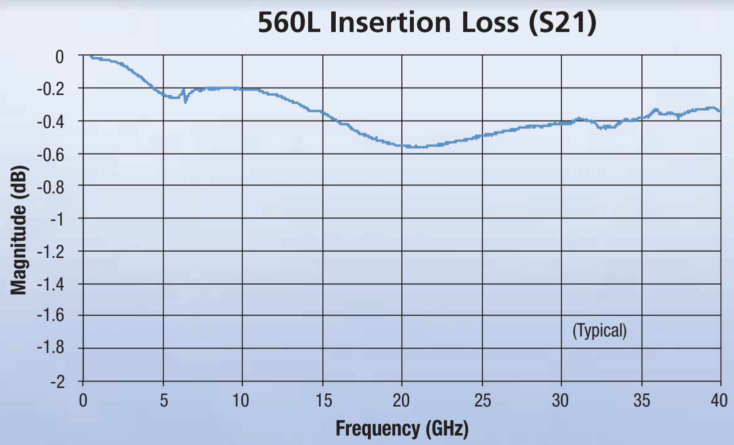

AMERICAN TECHNICAL CERAMICS

ATC North America
sales@atceramics.com

ATC Europe
saleseur@atceramics.com

ATC Asia
sales@atceramics-asia.com

THE ENGINEERS' CHOICE®
ISO 9001 REGISTERED COMPANY

RoHS Compliant

THE ENGINEERS' CHOICE® www.atceramics.com

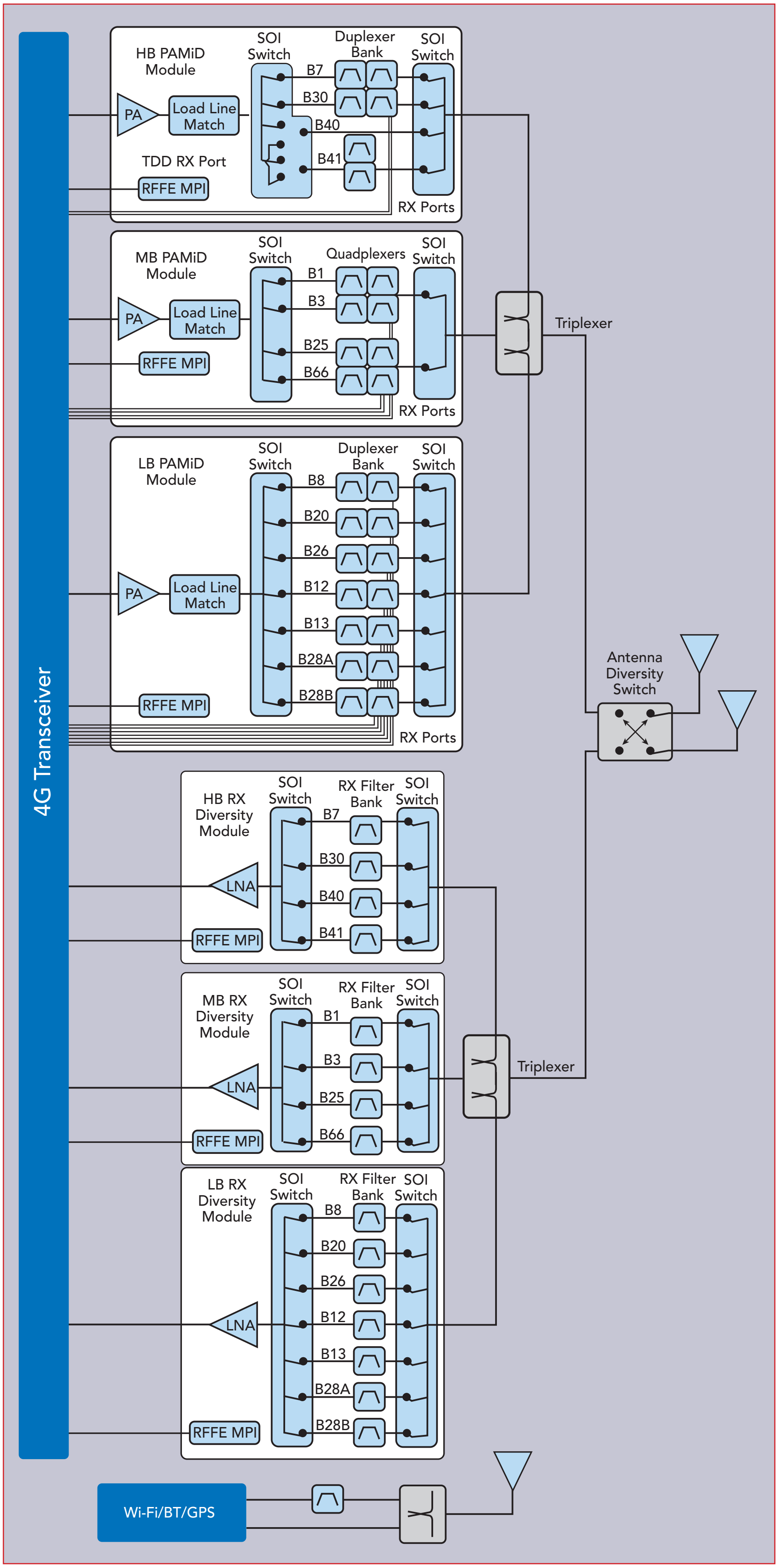

▲ Fig. 13 **Current state-of-the-art RF front-end architecture.**

able custom parts for IoT devices in particular, RFFEs will need to be designed with a minimum number of components and manufacturing volumes will have to increase dramatically from current levels to reduce per-unit cost. In the current environment, most IoT devices are being built with low-cost parts originally developed for high-volume mobile phone production.

As we move toward 5G, the complexity of the RFFE continues to increase. For instance, in addition to the main antenna path modules, diversity antennas provide both link robustness and increased downlink data rates. Designers are increasingly using receive diversity modules to process the diversity path, comprised of receive (Rx) filters and switches (and increasingly incorporating LNAs). Wireless carriers demanding higher 5G data rates will drive more carrier aggregation, creating more potential interference. Consequently, the onus on RFFE designers moving forward will be to reduce complexity, reduce cost, while at the same time improving performance.

5G FILTER REQUIREMENTS

The growth in the number of filters, and the ever more demanding performance requirements, make RF filtering the critical pain point of the RFFE. The basic requirements for a 5G filter includes complex multiplexing driven by CA and increasing integration to maintain high performance of the RFFE. Maximizing PA efficiency on the uplink, and receiver sensitivity on the downlink, will require optimization of the entire RF chain. As complexity increases, it will be crucial to understand the RF chain and any interactions between elements.

Isolation, loss and power handling requirements continue to create new performance challenges. Filters in the RF chain are a major contributor to loss, which is critical for total Tx efficiency (and ultimately for the current draw for the PA and battery life), and the total noise figure in the Rx path (and ultimately for the SNR and the data rate). ***Figure 14*** shows the estimated losses from each component in the Tx path.

WHEN 5G MASSIVE MIMO DEMANDS PERFORMANCE IN TINY PACKAGES

OUR ENGINEERS DELIVER!

Introducing the all-new high power 0805 (5W CW) form factor coupler product family

- Constructed from organic substrates
- Electrical and mechanical stability up to +105C (AEC-Qxx)
- Footprint optimized couplers for increased power and superior RF performance
- Specifically designed for all applications where high power is essential

Samples are available. Order yours today!

Scan the QR code below for more information.

Available in 2dB, 3dB, 4dB, 5dB, 10dB and 20dB coupling

Anaren®

A TTM Technologies COMPANY

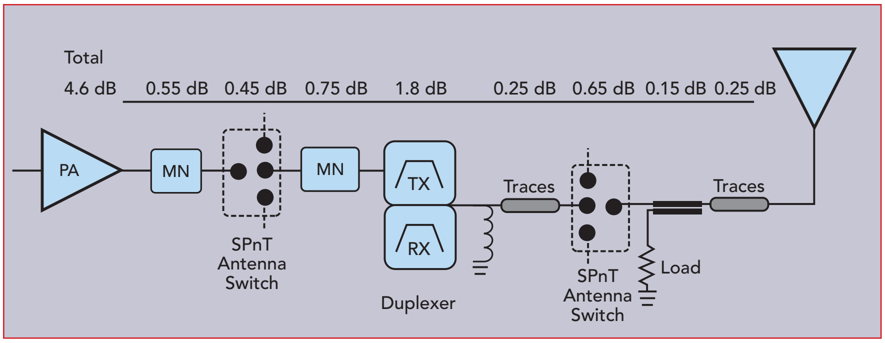

Fig. 14 TX path component line-up with estimated losses.

LTE, which is optimized for high speed data, demanded significantly higher power than 3G protocols such as CDMA. And as such, the requirements for isolation and minimizing leakage into the Rx path, and vice versa, grew. This will only be further exacerbated by high-power user equipment (HPUE), which uses more Tx power for improved cell edge coverage. In addition, power durability of progressively smaller filters becomes a major concern.

For 5G, frequencies greater than 6 GHz will require different filter technology than the current acoustic wave filters used in mobile devices. Significant advances will be needed to reduce size and cost. The 5G RFFE for mobile broadband will be extremely complex and that the goal for filter design will be to both simplify the design process and the RFFE itself.

Innovations that enable 5G RFFEs will need to include a low-loss triplexer (to minimize the number of antennas), multi-mode, multi-band PAs and multi-band filters (to reduce the number of filters and switches), all of which will need to be optimized as a complete system to reduce matching components.

SUMMARY

With RF complexity expected to grow significantly in 5G devices, the time is right for a filter design tool that can design better, more complex components in a time and capital efficient way. ISN delivers on this need with highly accurate, highly integrated and highly manufacturable filters with complex features.■

References

1. "RF Front-Ends for Mobile Devices 2018," *Mobile Experts Inc.*, 2018.
2. "5G Wireless Market Worth $250 Billion by 2025: $6 Billion Spend Forecast on R&D for 2015–2020," *PR Newswire*, March 2016.
3. R. Ruby, "A Decade of FBAR Success and What Is Needed for Another Successful Decade," *2011 Symposium on Piezoelectricity, Acoustic Waves and Device Applications (SPAWDA)*, 2011, pp. 365–369.

Women in SATCOM to Discuss the National Defence Authorization Act 2018 at Global MilSatCom

The 20th annual Global MilSatCom conference, taking place 6-8 November 2018 in London, will feature a new, all-female panel discussion on "What the National Defence Authorisation Act 2018 Means for SATCOM."

Led by senior military and industry representatives from the U.S., the panellists include:

- Deanna Ryals, Chief, International Programmes Division, Military Satellite Communications Systems (MILSATCOM) Directorate, Space and Missiles System Center (SMC), Air Force Space Command, U.S. Air Force
- Sandra Erwin, National Security Reporter, *SpaceNews*
- Clare Grason, Division Chief, Satellite Communications, Defense Information Systems Agency (DISA)
- Andrea Loper, Acquisition Program Manager, Air Force Research Laboratory Space Vehicles Directorate, U.S. Air Force

Key talking points of the panel discussion include:

- SATCOM in a contested world—current communication challenges and where they can be overcome
- National Security Space Provisions within the legislation, moving towards consideration of space as a unique domain
- Protected SATCOM services within NDAA, an overview of assessments of waveforms, terminals and ground segment sections
- What NDAA means for government-industry cooperation in space and enhancing U.S. space enterprise
- How the Warfighter Information Network-Tactical (WIN-T) will be developed in the wake of NDAA—ring-fencing survivability and security requirements
- An outline of the roadmap for military satellite requirement and enhancing the use of commercial constellations.

When discussing the panel, Sandra Erwin, national security reporter at *SpaceNews*, said: "It's a pivotal time for U.S. military SATCOM. The Defense Department just completed an analysis of alternatives for wideband communications—and at the same time it is being directed by the Congress to submit a strategy and create a program office for commercial SATCOM services. Yes, a lot to digest. I look forward to the discussion at Global MilSatCom."

Andrea Loper, acquisition program manager, Air Force Research Laboratory Space Vehicles Directorate, U.S. Air Force, also said: "Since I began working for the Air Force in 2008, there has been much rhetoric at space symposia and conferences identifying the problems resulting from an increasingly contested, congested and competitive space environment. However, it has not been until the last two to three years that any change addressing the problems at the root—guiding U.S. regulations and policies undergirding standard acquisition practices and Military Commanders' Intent—resulted in action to address the problems identified.

"We are in an era of disruption within the space environment in which new entrants—ranging from the commercial sector to the emerging state actors—can access space capabilities and prosper from the multitude of benefits space assets afford. Consequently, the U.S. can no longer maintain Cold War era policies that support the development of overly complex, redundant and unique systems, interoperable with few allies. The need for speed and agility is the new of the coin of the realm in military space and, if the U.S. wishes to remain relevant, policies, guidance and a culture adverse to risk must evolve to: enable international partnerships, develop new applications and acquire rapidly space-based assets."

The three-day event is an ideal forum to raise questions, to share the experience and knowledge among 500+ decision makers from the government and military, as well as leading international industry professionals.

There will also be a pre-conference focus day on Monday, 5 November, entitled: "Small Satellites and Disruptive Technology." More information on the conference and focus day can be found on the event website.

Visit the website to book your place, download exclusive event content and view the latest agenda at: www.globalmilsatcom.com/mjpr.

Lead Sponsor: SES Networks | Gold Sponsor: Airbus | Sponsors: COMSAT, Eutelsat, GOVSAT, Hughes, Intelsat General (IGC), Kratos, Laser Communications Coalition, Lockheed Martin, Newtec, Raytheon, SES GS, Thales, Viasat | Exhibitors: Baader Planetarium GMBH, Comtech Telecommunications Corp., Datapath, Inster, Integrasys, SCISYS, XTAR, U.S. Air Force.

Opportunities for industry to sponsor, exhibit and contribute to the conference are extremely limited. For details on how your company can get involved please contact Alia Malick at +44 (0) 207 827 6168 or email: amalick@smi-online.co.uk.

For More Information Visit mwjournal.com for more defense news.

RADA's Multi-Mission Hemispheric Radar at the Heart of Rafael's "Drone Dome"

RADA Electronic Industries Ltd.'s Multi-Mission Hemispheric Radar (MHR), embedded in the Rafael Advanced Defense Systems Drone Dome counter-drone solution, will be delivered to the British Army in the coming months.

These systems will be used to protect some sensitive facilities and sites, on which British armed forces are deployed, from airborne drones. The British Army is the first customer for this new and advanced Drone Dome system. Several initial systems are being purchased, with the potential for significant further orders expected.

RADA (Source: RADA Electronic Industries Ltd.)

RADA's MHR provides 360-degree surveillance and detects drones at distances of 3 to 5 km. Signal intelligence and electro-optical sensors provide additional layers of threat classification and identification, while RF jamming provides the soft-kill layer.

US Air Force First Advanced GPS III to Launch

On August 20, Lockheed Martin shipped the U.S. Air Force's first GPS III space vehicle (GPS III SV01) to Cape Canaveral for its expected launch this December. GPS III will be the most powerful and resilient GPS satellite ever put in orbit.

Developed with an entirely new design for U.S. and allied forces, it will have 3× greater accuracy and up to 8× improved anti-jamming capabilities over the previous GPS II satellite design block, which makes up today's GPS constellation.

GPS III also will be the first GPS satellite to broadcast the new L1C civil signal. Shared by other international global navigation satellite systems, like Galileo, the L1C signal will improve future connectivity worldwide for commercial and civilian users.

GPS III SV01 is the first of 10 new GPS III satellites under contract and in full production at Lockheed Martin.

Reactel, Incorporated

Reacting First to All Your Filter Needs.

When Being the First to React Makes all the Difference in the World

- **RF & Microwave Filters**

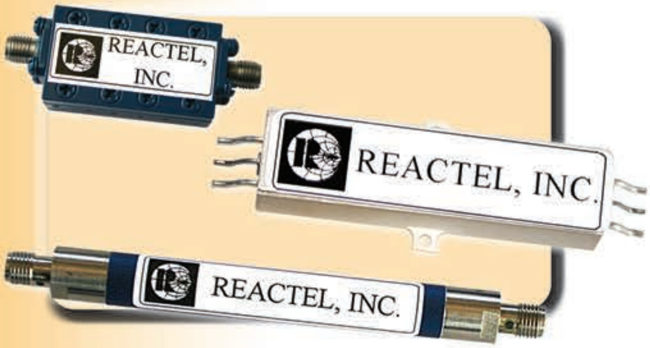

- **Diplexers & Multiplexers**

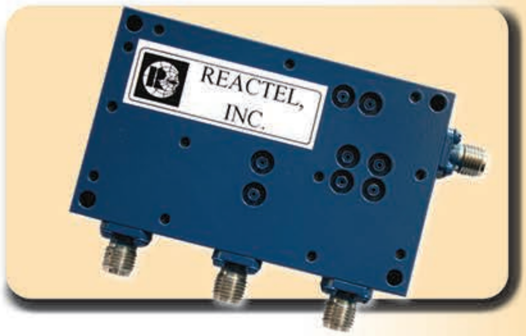

- **Multifunction Assemblies**

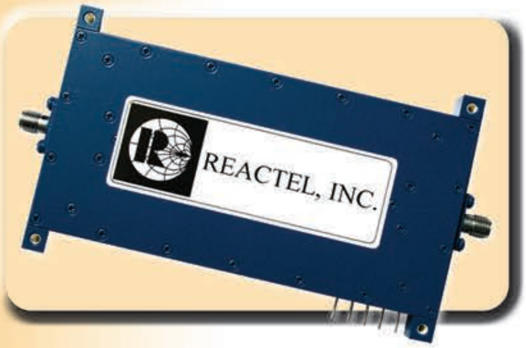

- **Ceramic Filters**

Reactel, Incorporated is your source for RF & Microwave Filters, Multiplexers and Multifunction Assemblies covering DC - 50 GHz.
Trust in Reactel's highly skilled engineers and technicians to quickly develop and produce the most reliable products for your filter requirements.

8031 Cessna Avenue • Gaithersburg, Maryland 20879 • Phone: (301) 519-3660
For general inquiries, please email reactel@reactel.com • http://twitter.com/reacteljim
Go online to www.reactel.com to download your Reactel catalog today.

Intertek   RoHS Compliant 2002/95/EC   @reacteljim


SP4T
SP6T
NEW!
SP8T
SPDT
Absorptive
Transfer
Switches
SPDT
Reflective

RF Power Semiconductors for Wireless Infrastructure Over $1B for 2018 with GaN Grabbing More Share

RF power semiconductors for wireless infrastructure (< 4 GHz and > 3 W) was over a $1 billion business for 2018. The segment was essentially revenue flat, but GaN continues to make inroads into this segment

"GaN should continue to gain share over the next few years," noted Lance Wilson, director at ABI Research. "It bridges the gap between two older technologies, exhibiting the high frequency performance of GaAs combined with the power handling capabilities of Silicon LDMOS. It is now a mainstream technology which has achieved measurable market share and, in the future, will capture a significant part of the market."

> GaN grabbing greater market share.

The wireless infrastructure sub-segment while representing about two-thirds of total RF power device sales has been anemic recently but is still holding its own. The eventual deployment of 5G also offers an upside for the wireless infrastructure segment. The main issue is one of timing on a large-scale rollout.

"The business environment for the RF power semiconductor devices has become more complex with potential trade tariffs, merger and acquisition troubles and other similar issues clouding the market," Wilson added.

Next-Generation Network Market Worth $32.81B by 2023

According to a new MarketsandMarkets research report, the next-generation network (NGN) will grow from $21.86 billion in 2018 to $32.81 billion by 2023, at a CAGR of 7 percent.

Demand for high speed services, increase in public private partnerships for NGN developments and low operational cost are among the driving factors. Telecommunications companies are increasingly adopting NGN to meet the growing requirements for high speed data services. The exponential growth in IP and mobile data traffic has been the major driver. As the number of smartphone and tablet users increases day by day, demand for high speed data services grows significantly. Also, the rising trend of Voice over Internet Protocol (VoIP) promotes services pertaining to data quality as well as quantity. Many companies in this industry proactively provide NGN products and services and are likely to transform traditional networks to high speed packet-based NGN.

The major hardware devices required include routers, switches and gateways. To upgrade traditional networks, the hardware must be replaced with advanced capabilities including huge data handling, compatibility for software interfaces and support for legacy networks. The growth for new hardware is primarily attributed to the rise in network data traffic and increases in virtualization and technological advancement to reduce operational expenditures. Moreover, growing IoT and cloud-based services are expected to create further opportunities for the NGN market.

> Growth particularly strong in the Asia-Pacific region.

The Asia-Pacific region (APAC) is expected to retain a major share of the market. Growth is attributed to increasing network upgrade activities and growing public-private partnerships to offer high speed data connectivity. APAC has the highest number of mobile subscribers, and the number is expected to grow at a faster rate in the coming years. It is a diversified region with a range of countries moving toward the digital transformation. The NGN market, including 4G, is in a high growth phase in the region driven by a large number of mobile subscribers and a huge demand for high speed data connectivity.

Cisco (U.S.), Huawei (China), ZTE (China), Ericsson (Sweden), Nokia (Finland), Juniper Network (U.S.), NEC Corp. (Japan), Samsung Electronics (South Korea), IBM (U.S.), Ciena Corp. (U.S.), Hewlett Packard Enterprise (U.S.), AT&T (U.S.), ADTRAN (U.S.), TELES (Germany), KPN International (Netherlands), Infradata (Netherlands), PortaOne (Canada), TelcoBridges (Canada), CommVerge Solutions (Hong Kong) and Extreme Networks (U.S.) are among the major players in the NGN market.

Supply Chain Complexity Driving Transportation Management System Revenues to $25B by 2023

A robust Transportation Management System (TMS) is a strategic enabler of the supply chain through reliable planning and execu-

For More Information Visit mwjournal.com for more commercial market news.

tion (empowered by advanced analytics and real-time visibility), as well as innovation in emerging areas such as machine learning, automation and blockchain. Key vendors provide the ability to scale across multimodal and global markets as well as provide cloud and mobile solutions. In fact, numerous established companies are eyeing potential acquisitions to bolster cloud, geographic and modal coverage. This creates a significant opportunity over the next five years to use cloud platforms and level the playing field, according to new research from ABI Research. Continued complexity from regulations, taxes, staffing and e-commerce expectations will continue to challenge goods transport across the globe.

> Revenues to grow to $25 billion by 2023.

"Vendors that focus on a given geography, mode or enterprise need to partner, acquire or develop more extensive solutions to provide flexible, end-to-end coverage," said Susan Beardslee, principal analyst at ABI Research. Established companies need to "future-proof" through developments in predictive analytics, blockchain, emerging transit modes and communication technologies (e.g., 5G and satellite).

A further shift away from on-premise, high-investment and lengthy training/upgrade cycles will continue to ramp toward cloud-based, scalable "as-a-service" models, with cloud-hosted platforms expected to begin to surpass those of on-premise adoption by next year and exceed 70 percent of the market by 2022. TMS revenues are roughly split between licensing, subscriptions and professional services.

A host of new solutions are going to market from both startups and well-established market leads. Enterprise resource planning (ERP) and supply chain management (SCM) vendors such as SAP, JDA Software and Oracle are integrating more TMS processes to help shippers align and enhance manufacturing and production along with their logistics processes. Third-party logistics and telematics vendors driving TMS include C.H. Robinson, Trimble, Omnitracs and Cerasis. Small and medium business and "freemium" focused business models include Kuebix and Cloud Logistics. Omni-mode TMS suppliers such as Amber Road, One Network Enterprises and MercuryGate are finding traction in TMS. Disruption lies ahead from dominant scaling players like Amazon and Alibaba as well as machine learning/AI solutions from ClearMetal.

Around the **Circuit**

Barbara Walsh, Multimedia Staff Editor

MERGERS & ACQUISITIONS

HEICO Corp. announced that a subsidiary of its Flight Support Group has acquired 100 percent of the business and assets of **Optical Display Engineering** in an all cash transaction. HEICO stated that it expects the acquisition to be accretive to its earnings in the year following the purchase. Further financial terms and details were not disclosed. ODE is an FAA-authorized Part 145 Repair Station focusing on the repair of LCD screens and display modules for aviation displays used in civilian and military aircraft. ODE also holds FAA-PMA authority to supply products that it repairs.

CORE Industrial Partners, a Chicago-based private equity firm, announced that it has acquired **Midwest Composite Technologies Inc.**, an additive manufacturer of prototype and low-volume production components, establishing an industry technology 4.0 platform that it plans to build upon. Financial terms of the transaction were not disclosed. Industry 4.0 refers to the Fourth Industrial Revolution, where companies use automation and data sharing in a cyber-physical system to communicate and cooperate in the manufacturing process over the IoT in a smart factory.

COLLABORATIONS

Keysight Technologies Inc. announced that it has signed a MoU with **CMCC (China Mobile Communication Corp.)** in support of the 5G Device Forerunner Initiative project. The program's large-scale 5G trials aim to accelerate development and industry maturity of 5G devices. The 5G Device Forerunner Initiative, established by CMCC at MWC 2018, brings together more than 20 of the industry's most influential and capable chipset manufacturers, component manufacturers and end-solution providers to form a strong industry ecosystem, encouraging 5G device innovation and accelerating 5G device commercialization.

The Nevada Institute for Autonomous Systems (NIAS), an FAA-designated UAS Test Site, announced they have signed a LOI with the EU's largest Polish coking (coal) producing company, **JSW SA**. The UAS commercial drone industry in Poland is currently booming, similar to the one being seen in the U.S. One of the leading entities in this commercial autonomous systems market is JSW SA, a company that makes the core ingredient for steel with a $2.5 billion market capitalization.

Steradian Semiconductor is providing IP to enable **IDT**'s SenseVerse radar transceiver ICs. The two companies are collaborating on a family of increasingly integrated ICs, and they plan to offer radar modules with integrated antennas, SVR transceivers, radar processing ICs and DSP algorithms. IDT's initial transceiver, the SenseVerse SVR4410, is a multi-channel—IDT says the highest number of channels in the industry—radar operating in the 76 to 81 GHz automotive radar band. With integrated beamforming and support for multi-device aggregation, the SVR4410 provides what IDT says is "superior interference performance" and "best-in-class" angular resolution, range and power consumption in a small form factor.

ACHIEVEMENTS

Rohde & Schwarz is a partner in the Providentia research project on the "proactive video-based use of telecommunications technologies in innovative highway scenario." The project creates the conditions necessary for adding a new dimension to local environment analysis. Based on data from distributed sensors, drivers and automated vehicles receive a digital image of the traffic situation that allows them to see what is coming up far ahead and ensures a smooth traffic flow. To achieve this, the vehicles must be connected to a wide area network via a high performance mobile communications infrastructure.

Nokia signed a EUR 500 million loan transaction with the European Investment Bank (EIB), supported by the European Fund for Strategic Investments (EFSI), a key element of the Investment Plan for Europe, also known as the Juncker Plan. Nokia will use the loan to further accelerate its research and development of 5G technology. The EFSI-supported loan from the EIB supports a key European technology provider, Nokia, that invests heavily in research, development and innovation in an area which can produce enabling technologies for innovation and growth in Europe.

Würth Elektronik has been distinguished in the category for "Electronics & electrical engineering, automation & measurement technology." The company promotes technical innovations with diverse activities in the field of research and development, as well as professional innovation management. Objective evidence of this strong innovation culture is provided by the rapidly increasing numbers of patents. Inclusion in "The Best List of the Most Innovative Companies" now also demonstrates that the innovative performance is recognized by customers and industry experts alike. Würth Elektronik evidently succeeds in matching the needs of its customers for products and systems with creativity and passion in an anticipatory manner.

Custom MMIC announced their growing corporate facility at 300 Apollo Drive, Chelmsford, Mass. has recently been certified by Nemko as meeting the standards of ISO 9001:2015. This achievement is an evolution from the company's previous certification to ISO 9001:2008 standards in 2012 and 2015. Custom MMIC continues its expansion with the recent acquisition of additional high volume production equipment. The new network analyzers, test handlers and automatic die probers will

For More Information For up-to-date news briefs, visit mwjournal.com

Exceptional
Phase Noise Performance
Dielectric Resonator Oscillator

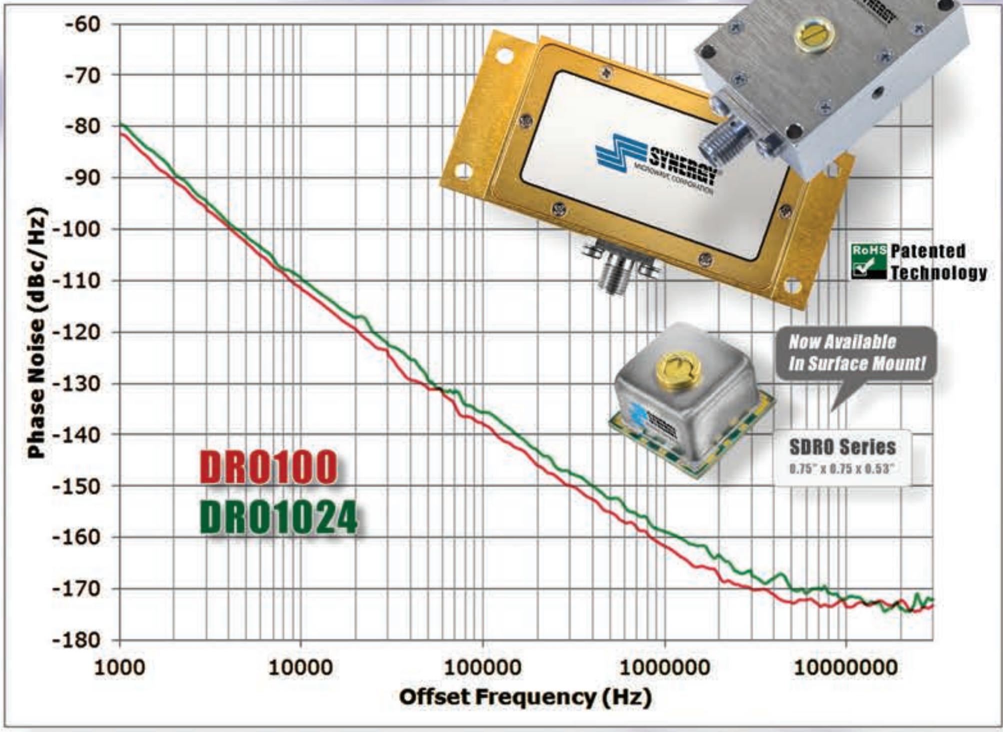

Model	Frequency (GHz)	Tuning Voltage (VDC)	DC Bias (VDC)	Typical Phase Noise @ 10 kHz (dBc/Hz)
Surface Mount Models				
SDRO1000-8	10.000	1 - 15	+8.0 @ 25 mA	-107
SDRO1024-8	10.240	1 - 15	+8.0 @ 25 mA	-105
SDRO1118-7	11.180	1 - 12	+5.5 - +7.5 @ 25 mA	-104
SDRO1121-7	11.217	1 - 12	+5.5 - +7.5 @ 25 mA	-104
SDRO1130-7	11.303	1 - 12	+5.5 - +7.5 @ 25 mA	-104
SDRO1134-7	11.340	1 - 12	+5.5 - +7.5 @ 25 mA	-104
SDRO1250-8	12.500	1 - 15	+8.0 @ 25 mA	-105
Connectorized Models				
DRO80	8.000	1 - 15	+7.0 - +10 @ 70 mA	-114
DRO100	10.000	1 - 15	+7.0 - +10 @ 70 mA	-111
DRO1024	10.240	1 - 15	+7.0 - +10 @ 70 mA	-109
KDRO145-15-411M	14.500	*	+7.5 @ 60 mA	-100

*Mechanical tuning only ±4 MHz

Talk To Us About Your Custom Requirements.

SYNERGY®
MICROWAVE CORPORATION

Phone: (973) 881-8800 | Fax: (973) 881-8361
E-mail: sales@synergymwave.com
Web: WWW.SYNERGYMWAVE.COM
Mail: 201 McLean Boulevard, Paterson, NJ 07504

position Custom MMIC for servicing high volume orders with ease.

Edge Electronics Inc., an authorized distributor of electronic components and LCD solutions for industrial, military, security, aerospace and medical applications, achieved Lockheed Martin Rotary and Mission Systems (RMS) "Elite" supplier status for excellent performance. The certified Women's Business Enterprise (WBE) is internationally recognized for providing unmatched engineering, inventory and customer support services to technology leaders. The RMS Elite Suppliers Program identifies Lockheed Martin's top suppliers through evaluating quality and delivery of performance, ability to meet RMS standards and requirements and contributions made to national defense in the RMS business area.

CONTRACTS

Boeing will build the **U.S. Navy's** first operational carrier-based unmanned aircraft, the MQ-25 aerial refueler, through an $805 million contract. Boeing was awarded the engineering and manufacturing development contract to provide four aircraft. Boeing plans to perform the MQ-25 work in St. Louis. MQ-25 is designed to provide the U.S. Navy with a much-needed refueling capability. According to the U.S. Navy, the MQ-25 Stingray will allow for better use of combat strike fighters by extending the range of deployed Boeing F/A-18 Super Hornet, Boeing EA-18G Growler and Lockheed Martin F-35C aircraft. MQ-25 will also seamlessly integrate with a carrier's catapult and launch and recovery systems.

The U.S. Defense Information Systems Agency (DISA) has officially awarded global communications company **Viasat** an eight-year, firm-fixed price contract to provide U.S. Government Senior Leader and VIP aircraft with in-flight broadband and connectivity services. The base year award value is $55.6 million. The period of performance for the base year award is through August 31, 2019. The base year and seven 12-month option periods have a total cumulative value of $559.8 million. Over the past two and a half years, Viasat has provided in-flight broadband and connectivity services to senior leader aircraft under the AMSS IIa contract, demonstrating its unique SATCOM capabilities.

The Department of Defense awarded **DynCorp International (DI)** a contract to support the U.S. Air Force at Joint Base Andrews in Maryland. DI will provide executive airlift maintenance support for all management, personnel and equipment. Services performed will include fixed-wing flight line and back shop maintenance for the 89th Airlift Wing aircraft, as well as back shop support services to the 811th Operations Group rotary-wing aircraft. The competitively-awarded, firm-fixed-price contract has a base year plus four option years and an additional six-month option period, valued at $203.1 million if all options are exercised. The period of performance is through February 29, 2024.

CACI International Inc. announced that it was awarded a task order with a ceiling value of $75 million by **Space and Naval Warfare Systems Center Atlantic** to deliver defense health readiness engineering support for the U.S. Navy, U.S. Marine Corps and U.S. Air Force. The five-year task order was awarded under the SeaPort-e vehicle and represents continuing work for CACI in its health market area. SPAWAR Systems Center Atlantic provides advanced health information technology solutions that support the nation's military. Under the task order, CACI will provide system integration, training and support for readiness and operational health information management systems.

Sparton Corp. and **Ultra Electronics Holdings plc** announced the award of subcontracts valued at $64.6 million to their ERAPSCO joint venture, for the manufacture of sonobuoys for the U.S. Navy. The award is a GFY18 ERAPSCO IDIQ contract release for sonobuoy requirements under ERAPSCO's five-year contract. ERAPSCO will provide production subcontracts in the amount of $30.3 and $34.3 million to Ultra Electronics USSI and Sparton DeLeon Springs LLC, respectively. Production will take place at Ultra Electronics USSI's Columbia City, Ind. facility and Sparton's DeLeon Springs, Fla. facility and is expected to be completed by April 2020.

Cubic Corp. announced its **Cubic Mission Solutions (CMS)** business division received orders worth more than $55 million to deliver its inflatable SATCOM and networking systems to the **U.S. Army**. These orders will satisfy the Army's upcoming fielding need for 1.2 and 2.4 m GATR systems, associated spares as well as training and sustainment support. Cubic's solution provides robust high speed links that enable secure network communications, sustainment support and mission command across the full spectrum of operations, from initial entry to sustained operations.

Altamira Technologies Corp. has been awarded a $25 million contract to support the enhancement of a mission critical system for the **U.S. Intelligence Community**. Under this multi-year contract, Altamira will provide enterprise system modernization to improve system sustainability in line with recent IC mandates and maintain the highest level of national security readiness.

Smiths Detection Inc. announced an order of more than $10 million to supply its RadSeeker handheld radioisotope detectors and identifiers for screening at **Customs and Border Protection (CBP)** ports of entry. The order is part of a five-year IDIQ contract with DHS Domestic Nuclear Detection Office (DNDO), which was announced in January 2016. RadSeeker is a next-generation, highly accurate radiation detection and identification system. It can locate the source of radiological material and identifies if it is harmful or naturally occurring.

Mercury Systems Inc. announced it received an $8.4 million order from a leading defense prime contractor for precision-engineered RF converter subsystems for an advanced airborne electronic protection application. The order was booked in the company's fiscal 2018 fourth quarter and is expected to be shipped over the next several quarters. With advanced state-

of-the-art modeling tools and scalable Advanced Microelectronics Centers, Mercury Systems is the leading commercial supplier of affordable RF and microwave solutions for electronic warfare (EW) applications. The company's advanced miniaturization and ruggedization capabilities are ideally suited to address the needs of SWaP-constrained applications while delivering the highest levels of performance to military forces.

Norden Millimeter announced that it has received a $5.5 million award for advanced frequency conversion modules. Norden received the award from a prime contractor supporting a military test facility. The order was booked in the fiscal 2018 third quarter and is expected to ship in 2019. The work will be performed at Norden's facility in Placerville, Calif.

Engility Holdings Inc. won a prime contractor position in July for all four functional areas on the **U.S. Army's Armament Research Development and Engineering Center, Armament Software Engineering Center** IDIQ services contract. The company also won two of the first four task orders valued at $2.8 million, if all options are exercised. Over the life of the contract, Engility will provide software development, sustainment and process assurance services for weapons, training and combat support systems. Engility has been supporting Picatinny for 20 years with armament fire control software development, systems engineering and information technology environment support.

SG Blocks Inc., a designer, fabricator and innovator of container-based structures, has been selected to design and construct new container-based office facilities for the **U.S. Navy**, representing an estimated revenue opportunity of $2.2 million in 2018. The office modules, will be prefabricated and delivered by the end of the year and the Navy will utilize the facilities at various locations in Portsmouth, Va. both ashore and afloat.

TMD Technologies Ltd. has received a £2 million overseas order for travelling wave tubes (TWT) for an airborne search and rescue radar application. Based on TMD's innovative, proven ring loop development, this top performance, high-power TWT operates in X-Band with exceptional reliability, featuring an advanced electron gun with long life dispenser cathode and sophisticated grid design.

PEOPLE

▲ *Michelle Roe*

Southwest Microwave Inc., a global leader in high performance outdoor perimeter security technologies and microwave interconnect products, announced the appointment of **Michelle Roe** as president. In her new role, Roe will oversee international operations of both the Security Systems and Microwave Products divisions, including Southwest Microwave Ltd. based in Worcestershire, U.K. Roe began at Southwest Microwave

as controller in 2010, and was later promoted to director and CFO in 2016. She has been instrumental in guiding the continuing success of the organization with initiatives that have reduced company expenditures while improving profitability and operational efficiencies.

Teledyne Technologies Inc. announced the following executive promotions within Teledyne's Environmental and Electronic Measurement Instrumentation (EEMI) group, effective immediately. Sean B. O'Connor will assume management responsibility for the EEMI group as COO and CFO. **Kevin Prusso** will become vice president and general manager of Teledyne LeCroy, also known as Teledyne Test & Measurement Instrumentation. **Vicki Benne** will become vice president and general manager of Teledyne Environmental Instrumentation. **Thomas H. Reslewic**, group president, EEMI and Defense Electronics and vice president, Teledyne, has resigned, effective immediately, to pursue other professional opportunities.

▲ *General Ellen M. Pawlikowski*

The board of directors of **Raytheon Co.** has elected **General Ellen M. Pawlikowski**, USAF, Retired, as a director, effective immediately. Pawlikowski retired as Commander, U.S. Air Force Materiel Command, Wright-Patterson Air Force Base, Ohio, on September 1. During her command, she executed the critical mission of warfighter support through leading-edge science and technology, complete life cycle weapons systems management, world-class developmental test and evaluation and depot maintenance and supply chain management. Pawlikowski entered the U.S. Air Force in 1978 through the ROTC program at the New Jersey Institute of Technology.

REP APPOINTMENTS

Epsilon Electronics Inc., a state-of-the-art mobile and audio electronics company, recently appointed **Southwest Sales and Marketing (SWSM)** as their Southwest region manufacturer's representative. Epsilon's brands include SoundStream, Power Acoustik, Precision Power, Farenheit and more. The company has been creating innovative audio electronics for more than 37 years. SWSM brings a four-person team of seasoned industry veterans together to represent the Epsilon family of products. Scott Ringo, CEO of SWSM, started the firm in March 2016, utilizing his 35 years of experience as a representative in the mobile electronics industry.

Mouser Electronics Inc., a leading new product introduction (NPI) distributor with the widest selection of semiconductors and electronic components, announced a global distribution agreement with **Marvell Semiconductor Inc.**, a provider of storage, processing, networking, security and connectivity semiconductor solutions. Mouser will distribute Marvell® industry-leading Fast Ethernet and Alaska® Gigabit Ethernet physical layer (PHY) transceivers. The Marvell Fast Ethernet PHY trans-

5G: Higher Frequencies!

Do you have the **right** circuit materials?

Frequencies at 28 GHz and higher will soon be used in Fifth Generation (5G) wireless communications networks. 5G infrastructure will depend on low-loss circuit materials engineered for high frequencies, materials such as RO4835T™ laminates and RO4450T™ bonding materials from Rogers Corporation!

Rogers RO4835T spread-glass-reinforced, ceramic-filled laminates are low-loss materials in 2.5, 3.0, and 4.0 mil thicknesses. They are well suited for millimeter-wave frequencies as part of the inner cores of 5G hybrid multilayer PCBs. They can work with other materials to provide the many functions needed by 5G wireless base stations, including power, signal control and signal transfers.

Rogers RO4450T bonding materials are available in 3, 4, and 5 mil thicknesses to help construct those 5G hybrid multilayer circuits. These spread-glass-reinforced, ceramic-filled bonding materials complement the different materials that will form these hybrid circuits, including RO4835T and RO4000® laminates. And for many 5G hybrid multilayer circuits, Rogers CU4000™ and CU4000 LoPro® foils will provide a suitable finishing touch for many hybrid multilayer circuit foil lamination designs.

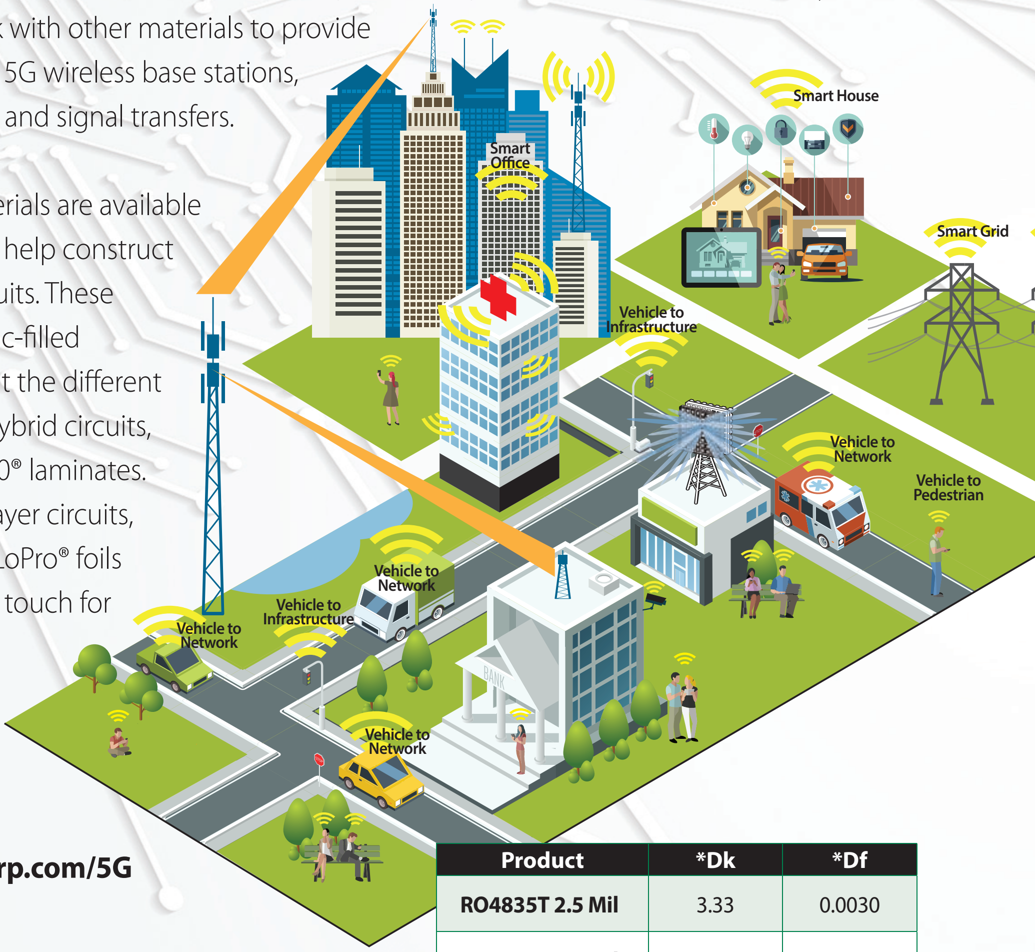

5G is coming! Do you have the right circuit materials?

Learn more at **www.rogerscorp.com/5G**

Product	*Dk	*Df
RO4835T 2.5 Mil	3.33	0.0030
RO4835T 3.0 Mil	3.33	0.0034
RO4835T 4.0 Mil	3.32	0.0036
RO4450T 3.0 Mil	3.23	0.0039
RO4450T 4.0 Mil	3.35	0.0040
RO4450T 5.0 Mil	3.28	0.0038

** IPC TM-650 2.5.5.5 Clamped Stripline at 10 GHz - 23˚C*

ROGERS CORPORATION

Advanced Connectivity Solutions

USA - AZ, tel. +1 480-961-1382 • EUROPE - BELGIUM, tel. +32 9 235 3611

www.rogerscorp.com

ceivers offer low power dissipation, small form factor, high performance and an advanced feature set. The octal Fast Ethernet PHY family, including the 88E3082 and 88E3083 devices, features significantly lower power consumption (under 150 mW per port), enabling network systems manufacturers to decrease system costs by reducing both power supply and fan requirements.

PLACES

Isola Group announced it has reached an agreement to sell its Chandler, Ariz. production facility to **Rogers Corp.** The sale does not include products, technology or other assets related to Isola's continuing business operations. Isola also announced plans to build a new state-of-the-art facility in the Chandler area that will be optimized for the quick-turn PCB market that drives much of the product innovation in North America. Timing for the opening of the new production facility is targeted for early 2020. Isola will transition out of its existing facility over the course of 2019 and will work closely with its customers and distributors to manage the transition period to the new facility.

NAI, a manufacturer of global connectivity solutions for high performance systems used in the industrial technology, telecom and medical industries, has announced the opening of a new manufacturing facility in Suzhou, China, designed to cut lead times for domestic customers in China. The new plant will be located "within" China. NAI's current 126,200 sq. ft. manufacturing plant in Suzhou is located "outside" China in a duty-bonded zone in order to trade in U.S. dollars. The new operation "within" China, called the NAI Communication Technology Innovation (Suzhou) Co. Ltd., will conduct business in local Ren Min Bi (RMB) currency.

Swagelok Co., a global developer and manufacturer of fluid system solutions, announced that its Board of Directors has approved Solon, Ohio as the location of its new $30 to $50 million Global Headquarters and Innovation Center, following a three-month competitive site selection process. The City of Solon and JobsOhio are both partnering with Swagelok to support the company's growth and enable Swagelok to expand in Solon. Solon City Council has approved its economic development package. Pending Ohio Tax Credit Authority and JobsOhio approvals, the new campus will be built at Swagelok's present location at 29500 Solon Road in Solon, where the company has been headquartered since 1965.

Toshiba Memory Corp. and **Western Digital Corp.** celebrated the opening of a new state-of-the-art semiconductor fabrication facility, Fab 6, and the Memory R&D Center, at Yokkaichi operations in Mie Prefecture, Japan. Toshiba Memory started construction of Fab 6, a dedicated 3D flash memory fabrication facility, in February 2017. Toshiba Memory and Western Digital have installed cutting-edge manufacturing equipment for key production processes including deposition and etching.

WIDEBAND DIGITAL ATTENUATORS

CMD280C3	CMD281C3	CMD282
DC-18 GHz FREQUENCY RANGE	DC-22 GHz FREQUENCY RANGE	DC-40 GHz FREQUENCY RANGE
0.5 dB STEP SIZE	2 dB STEP SIZE	4 dB STEP SIZE
15.5 dB ATTENUATION RANGE	6 dB ATTENUATION RANGE	12 dB ATTENUATION RANGE

Check Out our Attenuation Calculator

Quickly calculate the resistor values for PI, TEE, and BRIDGED-TEE attenuators. It's part of our free suite of design calculators at:

CustomMMIC.com/ Calculators

Bring your equipment to a new level with high-performance DATTs.

Allowing for both coarse and fine control, our family of eight new digital attenuators (DATTs) deliver unprecedented accuracy for next-generation wideband equipment designs. Download data sheets and S-parameters from our website today.

Where can we take you next?

Custom MMIC
CustomMMIC.com

INVITED PAPER

Optoelectronic Oscillators: Recent and Emerging Trends

Afshin S. Daryoush,[1] Ajay Poddar,[2] Tianchi Sun[1] and Ulrich L. Rohde [2]
Drexel University,[1] Philadelphia, Pa.
Synergy Microwave Corp., [2] Patterson, N.J.

Highly stable oscillators are key components in many important applications where coherent processing is performed for improved detection. The optoelectronic oscillator (OEO) exhibits low phase noise at microwave and mmWave frequencies, which is attractive for applications such as synthetic aperture radar, space communications, navigation and meteorology, as well as for communications carriers operating at frequencies above 10 GHz, with the advent of high data rate wireless for high speed data transmission. The conventional OEO suffers from a large number of unwanted, closely-spaced oscillation modes, large size and thermal drift. State-of-the-art performance is reported for X- and K-Band OEO synthesizers incorporating a novel forced technique of self-injection locking, double self phase-locking. This technique reduces phase noise both close-in and far-away from the carrier, while suppressing side modes observed in standard OEOs. As an example, frequency synthesizers at X-Band (8 to 12 GHz) and K-Band (16 to 24 GHz) are demonstrated, typically exhibiting phase noise at 10 kHz offset from the carrier better than −138 and −128 dBc/Hz, respectively. A fully integrated version of a forced tunable low phase noise OEO is also being developed for 5G applications, featuring reduced size and power consumption, less sensitivity to environmental effects and low cost.

Electronic oscillators generate low phase noise signals up to a few GHz but suffer phase noise degradation at higher frequencies, principally due to low Q-factor resonators. The conventional approach for high frequency signal generation is a frequency multiplier technique, but this suffers from higher phase noise due to AM-PM noise conversion[1] and sub-harmonic generation.[2] There are different types of resonators used in electronic oscillator circuits, such as printed coupled transmission line resonators using surface acoustic wave resonators, dielectric resonators, ceramic coaxial resonators, yttrium iron garnet (YIG) resonators and sapphire-loaded cavity (SLC) resonators. All have their unique characteristics and limitations. They typically operate from 500 MHz to 20 GHz; however, their Qs degrade as operating frequency increases and are, at best, limited to $f \times Q < 10^{14}$. SLC based oscillators offer low phase noise signal generation but have limited tuning capability and require precise low temperature cooling systems, which makes them expensive.

Emerging technologies focus on metamaterial resonator oscillators for microwave and mmWave applications.[3] Efforts to improve phase noise performance and tuning


Making the Connection in Handheld Solutions
*Available in WR-28, WR-15, WR-12 & Ext. WR-12 (56-96)
*For measurements in: 5G, WiGig, Auto Radar & E-Band Backhaul
RF OUT
S12H6DC5696
56 GHz to 96 GHz
Extended WR12 Source Module
OML Inc.
Ser Nr. 170522-01
Morgan Hill, CA. USA 95037
RF IN
9.33 – 16.0 GHz
Pin -10 dBm
+5VDC
*No external LO source or DC Power required
Introducing the first mini-portable "MP" solution for millimeter wave signal source.
Innovation in Millimeter Wave Solutions
www.omlinc.com
(408) 779-2698
OML

range of metamaterial resonator oscillators led to the exploration of Möbius topologies for high frequency signal generation and signal processing.[4] ***Figure 1*** shows a typical layout of a printed Möbius metamaterial strips (MMS) resonator and its equivalent lumped LC circuit model. ***Figure 2*** shows the phase noise measurement setup for an MMS inspired X-Band oscillator. The measured phase noise is −139 dBc/Hz at 10 kHz for a 10.24 GHz carrier (see ***Figure 3***), where a narrow tuning range of about 5 percent is achieved with varactor diodes.[4]

The novel approach for generating a low phase noise synthesized signal source demonstrated in Figures 1 through 3 trades phase noise for tuning and, therefore, is not suitable for wideband applications. The OEO offers a promising solution. It has a high Q-factor due to a long storage delay using low loss optical fiber, the potential for high frequency operation, due to inherently broadband electro-optic and optoelectronic transducers and a high immunity to electromagnetic interference.

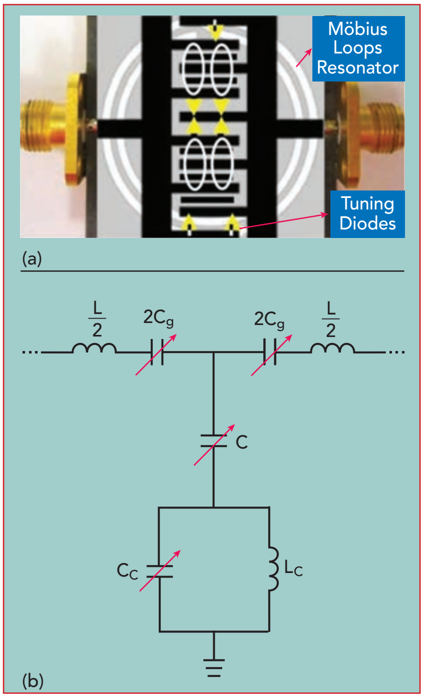

Fig. 1 Typical metamaterial Möbius strips resonator: layout (a) and lumped circuit model (b).

Fig. 2 Phase noise measurement setup for the 10.24 GHz synthesizer using MMS inspired oscillator.

CURRENT OEO TECHNOLOGY

A typical OEO is a hybrid electronic and microwave photonic system using an augmented positive feedback loop to facilitate low phase noise, high frequency signal generation. Yao and Maleki[5-7] first reported microwave signal generation using optical fiber delay lines in 1996. Their methods, based on converting the continuous light energy from

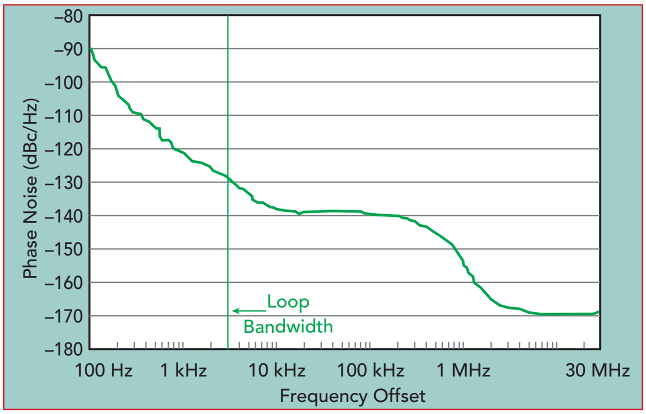

Fig. 3 Measured phase noise of the 10.24 GHz synthesizer.

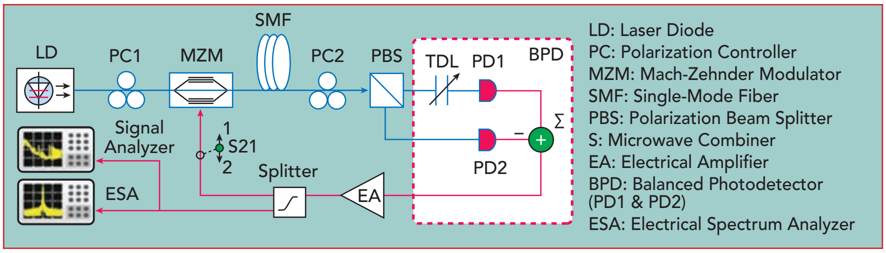

Fig. 4 Block diagram of the PT-symmetric OEO.[8]

Blue Chip Performers

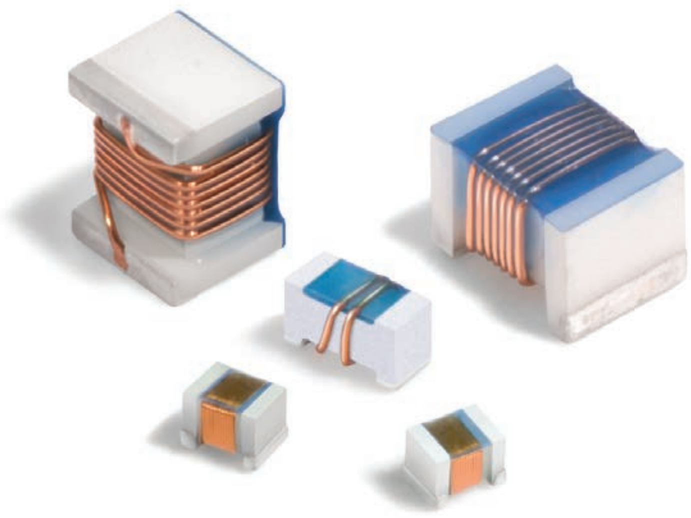

Exceptionally high Q, low DCR and a wide range of inductance values make our wirewound chip inductors a sure bet!

Engineers love our high-performance, low-cost, wirewound ceramic chip inductors; considered by most to be the best performing wirewounds available.

For example, our 0201HL Series is offered in seven inductance values ranging from 22 to 51 nH – the highest currently offered in an 0201 (0603) package – making them fully optimized for impedance matching in 700 MHz band LTE and 5G applications.

Our 0402DC and 0805HP Series provide the industry's highest Q factors in their respective sizes for super low loss in high frequency circuits. Select values from 2.6 to 820 nH, including 0.1 nH increments from 2.8 to 10 nH in the 0402DC Series.

Find out why our customers are so bullish on our wirewound ceramic chip inductors. Order your free samples today at **www.coilcraft.com.**

Coilcraft®

coilcraftdirect.com
No min order. Next day delivery.

WWW.COILCRAFT.COM

a pump laser to RF and microwave signals, may use optical fiber delay line or high Q optical resonators. The latter can utilize active or passive cavities. Low phase noise in a delay line oscillator is ensured by a high Q feedback loop using long, low loss optical fiber. The oscillation frequency is determined using a narrowband microwave filter.

The OEO based on delay in an optical fiber loop suffers from multiple, closely-spaced oscillation modes that can pass through the narrowband microwave filter. To guarantee single-mode oscillation, an ultra-narrowband high Q microwave filter is needed, but such a filter is impossible to realize. Optical filtering could be incorporated, but filters that use optical resonators are difficult to implement and suffer from vibrational mode instability. Recently, Zhang and Yao[8] reported single-mode operation without an ultra-narrowband optical filter based on parity-time (PT) symmetry and two identical matching feedback loops, with one having a gain and the other having a loss of the same magnitude. As shown in ***Figure 4***, the PT-symmetric OEO utilizes polarization to implement tunable optical power splitting to the polarization sensitive balanced photo detector; however, even minor vibrations can stimulate strong modulation on the phase and polarization state of the light wave propagating in the long optical loop.

The measured phase noise plots reported by Zhang et al.,[8] as illustrated

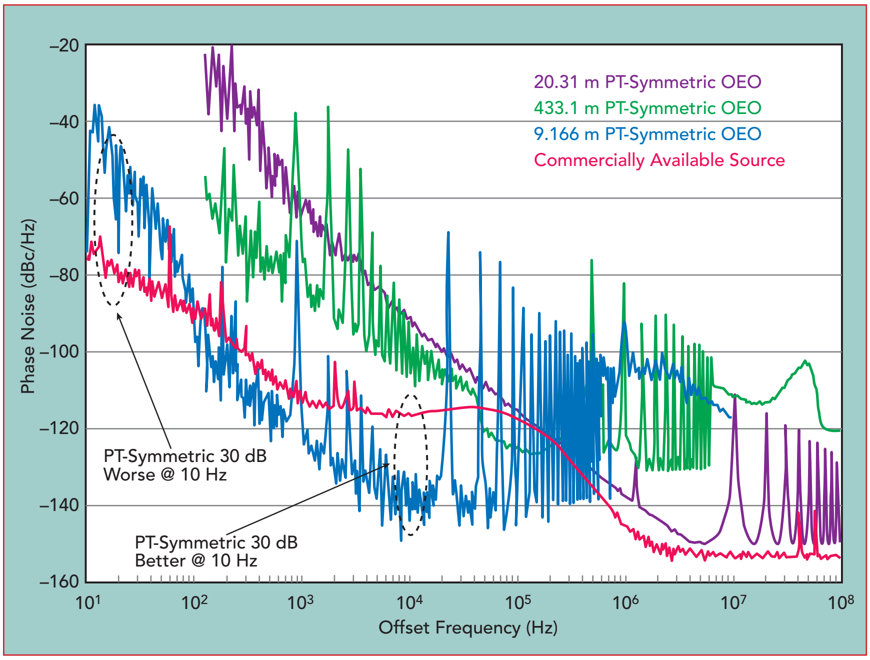

Fig. 5 Phase noise of the PT-symmetric OEO vs. a commercially available source, both at 9.76 GHz.[8]

in ***Figure 5***, compare the performance of the PT-symmetric OEO to a state-of-the-art commercially available electronically generated microwave signal source. The PT-symmetric OEO operates with three different loop lengths (20.31 m, 433.1 m and 9.166 km). Phase noise at 10 kHz offset from the 9.76 GHz carrier frequency is typically −93, −104 and −143 dBc/Hz, respectively. It is interesting to note that the PT-symmetric OEO topology improves phase noise performance at 10 kHz offset from the carrier but significantly degrades close-in performance compared to commercial available signal sources. Significant side modes exist due to resonance conditions associated with the 9.166 km delay line. These side modes degrade oscillator timing jitters, even

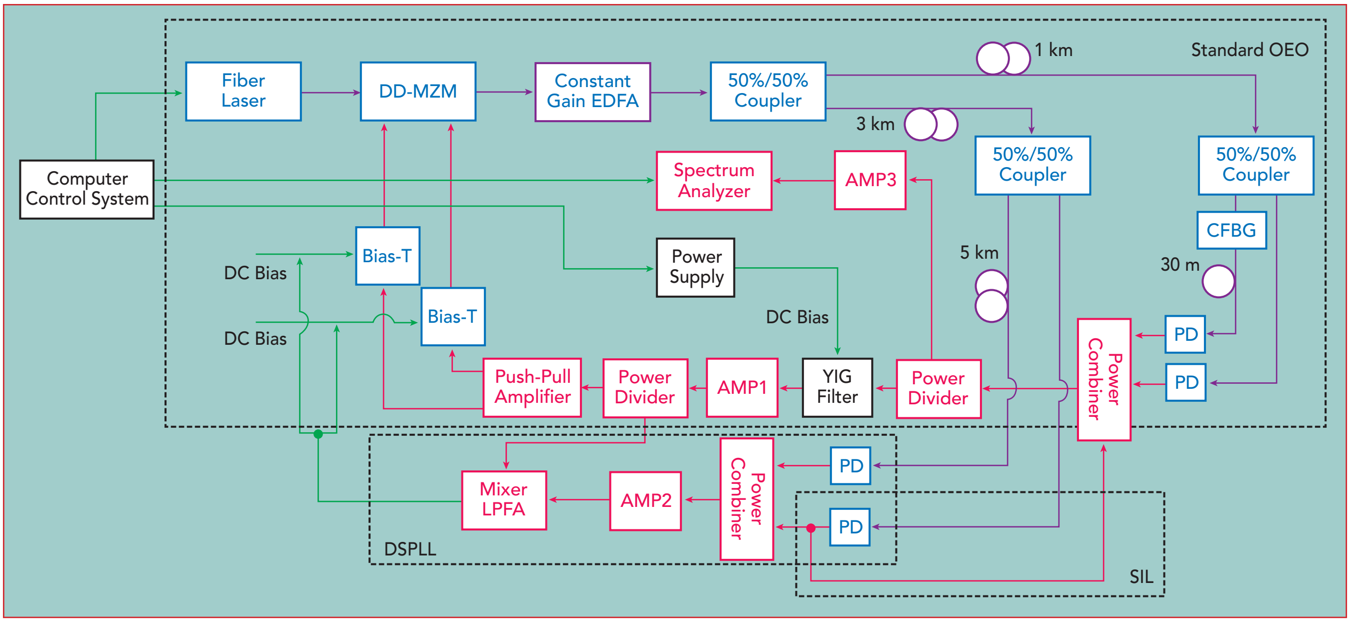

Fig. 6 SILDPLL synthesizer block diagram.

though they are reduced close-in to the carrier.

The suggested method to mitigate the poor close-in phase noise performances in a PT-symmetric OEO is to incorporate a polarization-insensitive optical power splitter and electrical feedback loop, to detect phase and polarization changes and perform real-time dynamic compensation. This can partially improve close-in phase noise performance; however, offsets greater than 10 kHz suffer degradation, and the approach lacks broadband tenability as well.

Current and future generation communication systems demand high frequency signal sources with tuning features to meet the criteria for broad bandwidth and high data transmission rates. The work described here offers solutions based on forced self-injection locking, double self phase-locking (SILDPLL) techniques.

SILDPLL OEO SYNTHESIZERS

Oscillator phase noise reduction can be achieved through injection locking (IL)[9] and phase-locked loops (PLL).[10] While IL is easy to implement, phase noise close to the carrier is degraded due to frequency detuning and a limited locking range.[11] On the other hand, a high gain loop filter enables the PLL to remove close-in phase noise significantly, while far-away offsets suffer from a higher noise. Sturzebecher et al.[12] demonstrated that in externally-forced oscillators, better phase noise characteristics for both close-in and far-away offset frequencies and a wider locking range are achieved by combining IL and PLL techniques. External reference sources are required, however, in the conventional injection locking phase-locked loop (ILPLL) topology, which limits the ultimate phase noise performance.

To bypass limitations imposed by an extremely stable external reference requirement, self-injection locking (SIL)[13] and the self phase-locked loops (SPLL)[14] have been proposed. SIL and SPLL are essentially feedback control loops where part of the output signal is delayed and used as the reference signal, eliminating the need for an external reference. The loop gain can be greatly enhanced in self-injection locking phase-locked loops (SILPLL) compared to SIL or SPLL alone, providing greater phase noise reduction. For long fiber delays, a large number of closely-spaced side modes at Δf = 200 kHz-km/L, where L is the fiber length in km, are expected in the forced oscillator spectra (as seen in Figure 5). Therefore, multiple feedback paths are introduced to cancel these side modes by using SILPLL, SILDPLL (two paths) and SILTPLL (three paths), depending upon requirements for side-mode suppression and corresponding timing jitter.

Figure 6 shows the block diagram of an SILDPLL OEO synthesizer. It uses SIL and double-sideband PLL techniques to minimize phase noise close-in and far-out from the carrier. A low relative intensity noise (RIN) fiber laser (TWL-C-HP-M) is used to provide a wavelength-tunable laser signal. The signal is transmitted through an optical fiber delay line, received by a photo detector (DSC50S) and passed through a narrow band filter. The narrowband filter is the core of the OEO and is used to select the oscillation frequency. In this work, a tunable YIG filter is used for wideband operation and for coarse tuning of the frequency synthesizer. Further improvement is achieved by incorporating a narrowband optical transversal filter realized with a chirped fiber Bragg grating (CFBG)[15-18] to provide narrowband microwave signal filtering. The optical transversal filter is wavelength dependent and provides frequency tuning as the wavelength of the fiber laser is tuned.

Besides the optical frequency selectivity of the YIG and optical transversal filter, SIL,[14] SPLL[15] and their combination SILPLL[19] are applied to reduce synthesizer phase noise, both close-in and far-out from the carrier. Figure 6 shows the SIL and DSPLL.[20-21] There are two paths for the modulated signal after the Mach-Zehnder modulator (MZM). One is the main loop of the OEO, and the other loop is split into two, creating 3 and 8 km dual phase-locking signals. The combined phase-

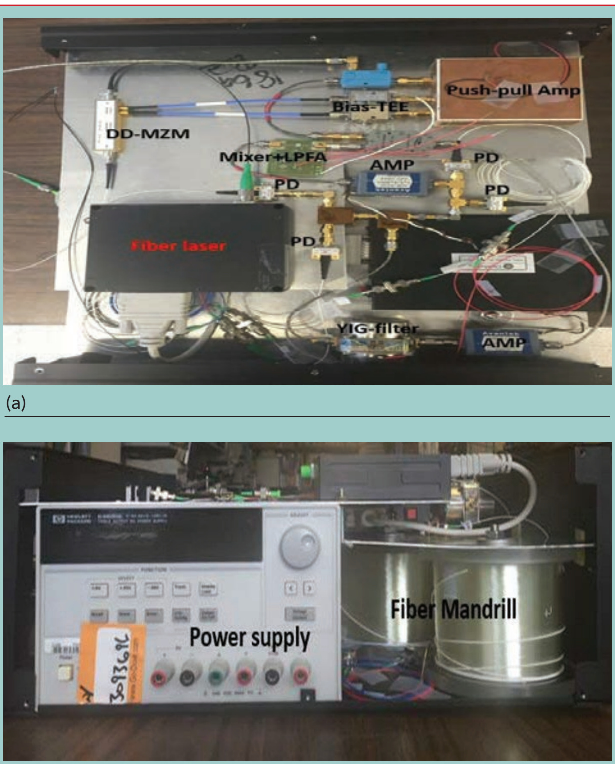

▲ Fig. 7 Top (a) and front view (b) of the X/K-Band SILDIL OEO synthesizer.

locking signal is then input to a custom-designed mixer and lowpass filter amplifier (LPFA) board (see ***Figure 7***). A double balanced mixer is integrated on this board with the LPFA, realized using opamp circuits, to work as a phase detector and lowpass portion of the PLL. The phase error of the OEO main loop is compared with the dual delay lines of the PLL, and the phase error signal is fed back to the bias port of the MZM. The SIL signal takes advantage of the PLL path and shares the same 3 km fiber used in the SPLL path. Dual delay lines of 3 and 8 km provide significant side-mode suppression. The 3 km SIL signal is tapped from one PLL signal and directly injected into the power combiner. The injected power level is expressed as

$$\rho = \sqrt{\frac{P_i}{P_O}},$$

with P_i the injected signal power and P_o the OEO power level.

The novelty of this approach is reflected in the design, implementation and testing of high frequency and resolution, 19-in. rack-mountable, X- and K-Band frequency synthesizers using SILDPLL OEOs. High resolution tuning is due to fine tuning of an optical transversal filter using a chirped fiber Bragg grating (CFBG) as a dispersive component for narrowband filtering. Second harmonic[22] generation is achieved by biasing the dual-drive MZM close to V_π to generate half rectified optical pulses. Performance of this synthesizer is evaluated by its measured close-to-carrier phase noise and its long-


Your Signal Integrity
Depends on NIC's Filters.
NIC
www.nickc.com
Innovative Solutions: DC-40GHz
3-4 Week Prototype Delivery
Preferred Supplier to Major OEMs
30+ Years of Success
LC Filters
Discrete & Monolithic Crystal Filters
Ceramic Filters
Integrated Assemblies
Switch Filter Banks
Cavity Filters & Diplexers
Radar | UAV | EW | Guidance & Navigation | Communications | GPS & Satellite
ISO 9001:2008
AS9100C
CERTIFIED
NIC NETWORKS INTERNATIONAL CORPORATION
913.685.3400
15237 Broadmoor
Overland Park, KS
e-mail: sales@nickc.com

term frequency stability over 60 minutes with a maximum frequency drift of 4 kHz.

SILDPLL OEO SYNTHESIZER DESIGN

The frequency synthesizer, shown in the block diagram of Figure 6 and the hardware of Figure 7, uses SIL and double-sideband PLL techniques simultaneously, with multiple signal paths supporting enhanced signal stability, as well as the application of modulation as needed. Signals are combined within the synthesizer with the aid of a custom-designed double balanced frequency mixer and LPFA assembly. The synthesizer design also incorporates an opamp circuit that works as a phase detector and lowpass portion of the PLL. The high resolution and wavelength-sensitive tuning is due to fine tuning by wavelength control of the fiber laser used as the optical source for the extremely narrowband optical transversal filter. The optical filter uses a CFBG as a dispersive component to achieve narrowband filtering. A current-tuned YIG filter used in cascade with the optical filter and CFBG provides coarse frequency tuning across wide tuning ranges in X- and K-Band. At X-Band, for example, the YIG filter tunes with a response of about 25 MHz/mA. Since the resolution of the current supply feeding the YIG filter is about 1 mA, the effective frequency tuning resolution of the YIG filter is 25 MHz. This combination of optical and electronic technologies results in relatively wide frequency tuning ranges with outstanding phase noise, both close-in and far-out from the carrier. A higher frequency tuning resolution and narrowband filtering is achieved by the dispersive CFBG transversal filter, as opposed to a fiber based filter.[23]

Fig. 8 **Phase noise measurement setup.**

Figure 8 shows the phase noise measurement setup for the synthesizer. A Keysight E3631A is adjusted in constant current mode for tuning the YIG filter, and a Rohde & Schwarz FSWP is used for the phase noise measurement. At X-Band, the single sideband (SSB)

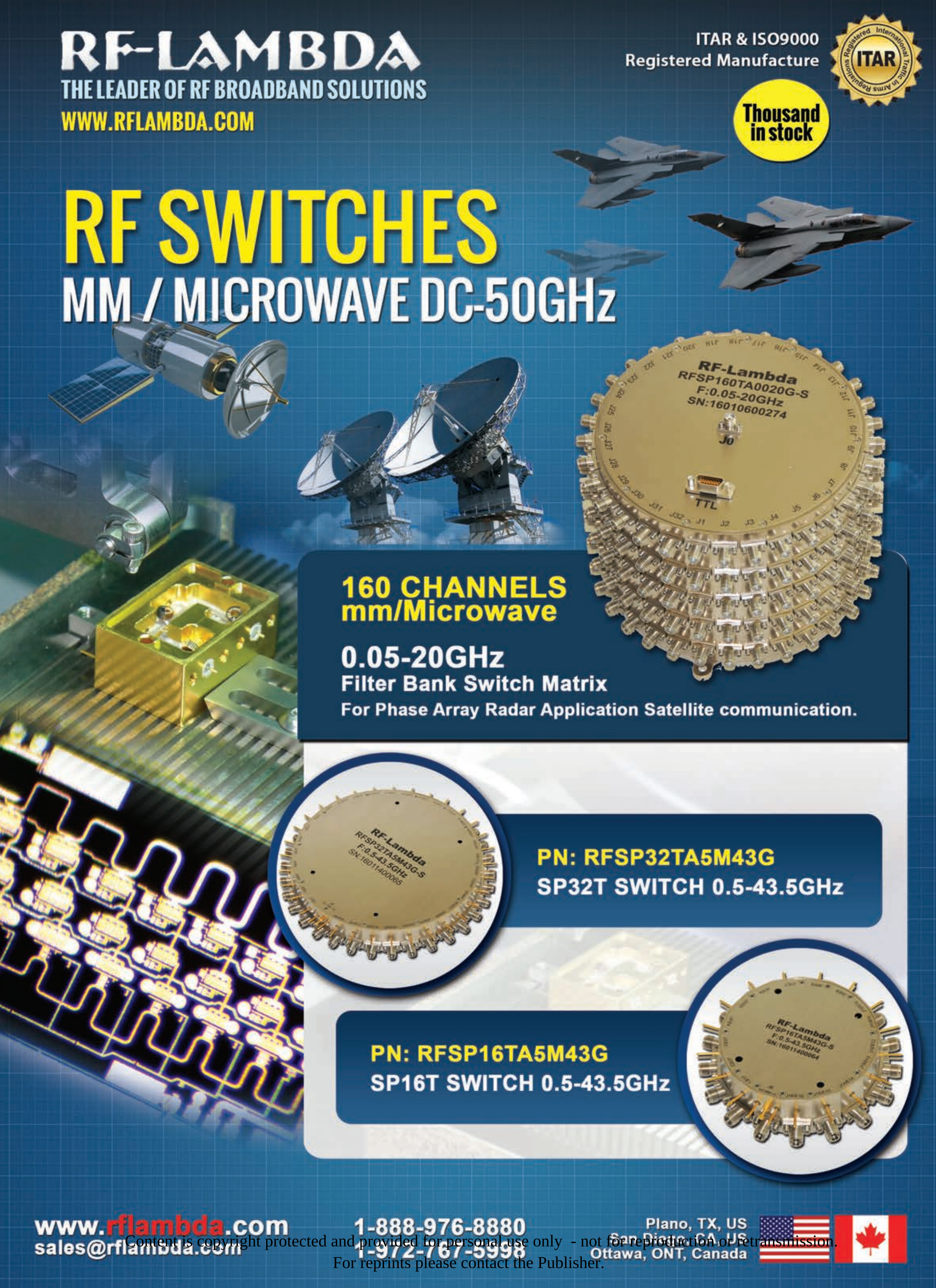
RF-LAMBDA
THE LEADER OF RF BROADBAND SOLUTIONS
WWW.RFLAMBDA.COM
ITAR & ISO9000
Registered Manufacture
ITAR
Thousand in stock
RF SWITCHES
MM / MICROWAVE DC-50GHz
RF-Lambda
RFSP160TA0020G-S
F:0.05-20GHz
SN:16010600274
J0
TTL
160 CHANNELS
mm/Microwave
0.05-20GHz
Filter Bank Switch Matrix
For Phase Array Radar Application Satellite communication.
RF-Lambda
RFSP32TA5M43G-S
F:0.5-43.5GHz
PN: RFSP32TA5M43G
SP32T SWITCH 0.5-43.5GHz
PN: RFSP16TA5M43G
SP16T SWITCH 0.5-43.5GHz
RF-Lambda
RFSP16TA5M43G-S
F:0.5-43.5GHz
www.rflambda.com
sales@rflambda.com
1-888-976-8880
1-972-767-5998
Plano, TX, US
San Diego, CA, US
Ottawa, ONT, Canada

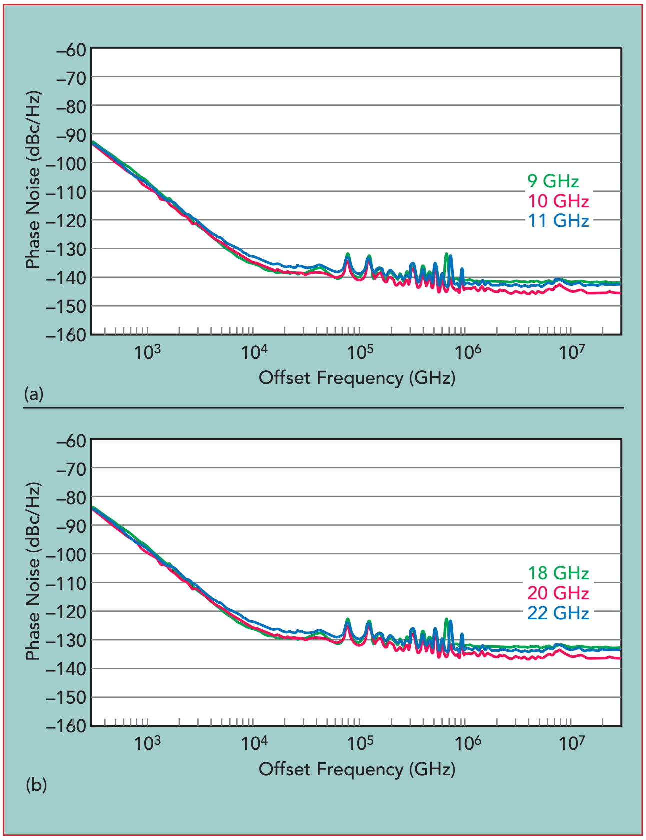

▲ **Fig. 9** **Measured phase noise of the X-Band (a) and K-Band (b) OEOs with SIL = 3 km and DSPLL = 3 and 8 km.**

phase noise is −110 dBc/Hz at 1 kHz from the carrier and −137 dBc/Hz at 10 kHz from the carrier for carrier frequencies from 8 to 12 GHz. In the time domain, this translates to 4.395 fs measured at side-mode markers of 35 and 200 kHz from the carrier. At K-Band frequencies, SSB phase noise is −103 dBc/Hz at 1 kHz from the carrier and −128 dBc/Hz at 10 kHz from the carrier for frequencies from 16 to 24 GHz. This translates to a time domain response of 6.961 fs measured at side-mode markers of 35 and 200 kHz from the carrier. For demonstration, the overall system is mounted in a 19-in. rack; the size can be reduced for specific applications. ***Figure 9*** shows X- and K-Band phase noise measurements for different fiber lengths.

In terms of size and power, the YIG filter is the dominant component in these opto-electronically driven frequency synthesizers. The main current consumer is the YIG filter, which draws 150 mA at +10 V_{DC} and consumes about 1.5 W power. The amplifier, with two channels, draws 80 to 160 mA at +10 V_{DC} and consumes as much as 1.6 W power. The mixer and LPFA, which use a combination of frequency translation and filtering to extract the RF/microwave signals from the higher frequency optical signals, draw about 110 mA (60 + 5 + 45 mA) from +15, +5 and −5 V_{DC} supplies, respectively. In stark contrast, the photo detector uses very low current and power, with its three cells each drawing about 10 mA (30 mA total) at +5 V_{DC} and using about 0.15 W power. The broadband dual-channel amplifier draws roughly 80 mA per channel from a +10 V supply, or 160 mA and 1.6 W total.

MONOLITHIC OEOs

Recently, Tang et al.[24] demonstrated an integrated OEO (see ***Figure 10***), where both the optical and electrical parts are packaged on a 5 × 6 cm^2 printed circuit board. The measured phase noise for an oscillation frequency of 7.30 GHz was −91 dBc/Hz at 1 MHz offset, with an injection current of 44 mA. The reported integrated solution is not attractive because of limited tuning and poor phase noise performance due to the high RIN of the directly modulated laser.

In this work, integrated topologies using monolithic fabrication techniques compatible with Si photonics are explored to reduce size and cost while improving temperature sensitivity. A chip-level multimode laser generates beat-notes at RF[25] but suffers from poor phase noise characteristics. The concept in ***Figure 11*** shows an alternative laser configuration, consisting of four

When Everything is Important... the NEW *Clarity™ Series* is the *Clear Choice*

Applications:

Research & Development Labs
VNA Test Port Extension Cables
High Volume Production Test
Bench or Portable Test equipment
RF Module Testing

Industry leading performance, unparalleled value, and stock to 4-week lead times.

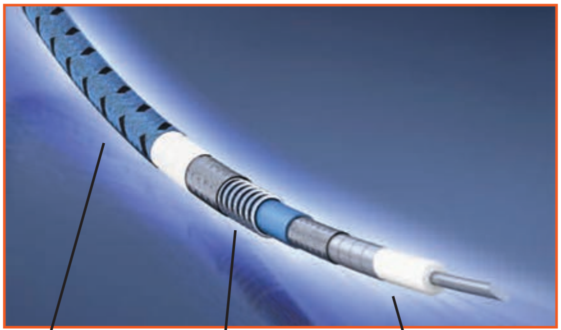

Phase stability <3.5º
Guaranteed up to 50,000 flexes
Super-sharp Sure-Grip™ knurl
Ergonomically designed Sure-Grip™ molding

TIMES MICROWAVE SYSTEMS
An Amphenol Company

World Headquarters: 358 Hall Avenue, Wallingford, CT 06492 • Tel: 203-949-8400, 1-800-867-2629 Fax: 203-949-8423
International Sales: 1+ 203 949 8503 • 1+ 800 867 2629
China Sales: TMC Building 4, No. 318 Yuanshan Road, Xinzhuang Industrial Park, Shanghai, China 201108 Tel: 86-21-5176-1209 Fax: 86-21-64424098

www.timesmicrowave.com

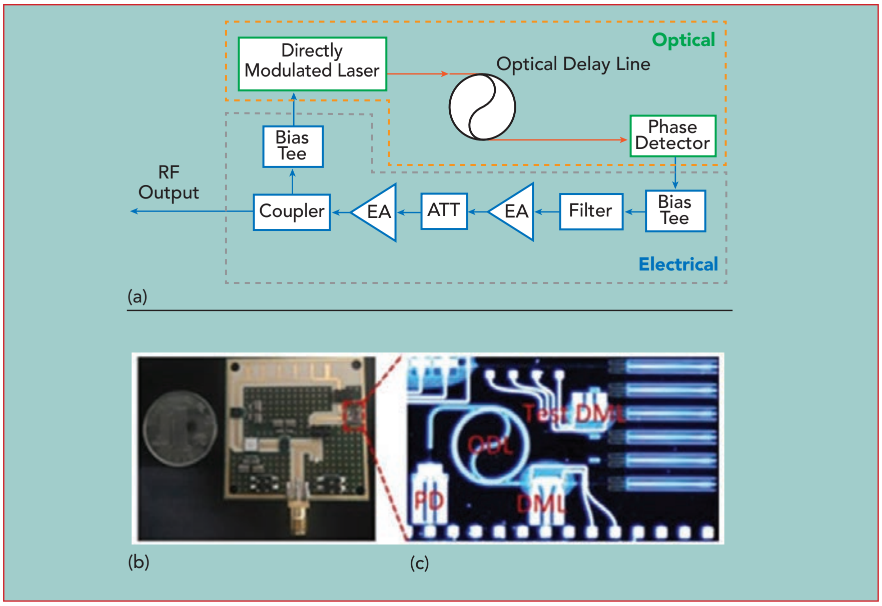

Fig. 10 IOEO block diagram (a), assembly (b) and photonic components (c).

sections[26] consisting of distributed Bragg reflector (DBR), gain, phase tuning and electro-absorption modulator. The DBR is used as a filter to select the laser output frequency.[27] The phase tuning section,[28] the phase modulator in the DBR laser, performs frequency tuning. Varying the DC bias voltages drives different output frequencies from each multi-mode laser.[29] The output Y-junction provides an input to a high speed photodetector for efficient detection of the ultra-stable RF beat note. Gain is provided by an InGaAsP-InAsP multi-quantum well structure for operation at about 1550 nm, where a threshold current of about 30 mA is estimated. Work is in progress for fabricating these designs in monolithically integrated components.[30]

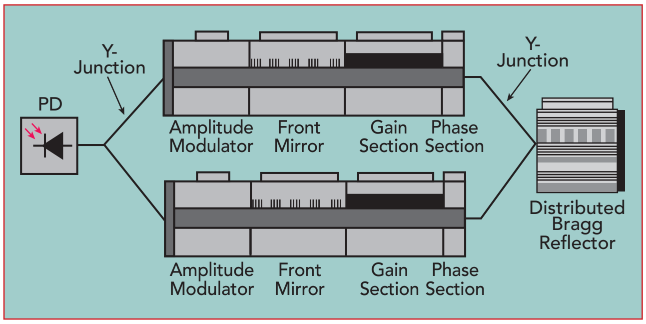

Fig. 11 Block diagram of RF beat-note generating laser system using DBR multi-mode laser pairs.[26]

CONCLUSION

The described SILDPIL OEO synthesizer in a 19-in. rack-mount enclosure is based on patented techniques[18-19] for portability; the size can be reduced for specific applications and requirements. Work is progressing to develop a monolithic integrated solution for hybrid optoelectronic systems that combines the integrated microwave and photonics circuits on-chip. Recent development of photonics integration material platforms, including SOI, InP and Si_3N_4, opens the way for an OEO on-chip for 5G applications.■

References

1. I. Suh and P. Roblin, "Model Comparison for 1/f Noise in Oscillators With and Without AM to PM Noise Conversion," *IEEE Transactions on Microwave Theory and Techniques*, Vol. 59, No. 12, December 2011, pp. 3129–3145.
2. K. C. Ho, C. F. Chan, C. S. Choy and K. P. Pun, "A Sub-Harmonic Oscillator Using an Injection-Locked DCO," *International Conference on Communications, Circuits and Systems*, June 2004.
3. A. K. Poddar and U. L. Rohde, Metamaterial Resonator Based Device, US9608564B2, U.S. Patent and Trademark Office, March 28, 2017.
4. A. Poddar, "Slow Wave Resonator Based Tunable Multi-Band Multi-Mode Injection-Locked Oscillator," *Habil-Thesis*, BTU-Cottbus, Germany, 2014
5. X. Yao and L. Maleki, "Optoelectronic Oscillator for Photonic Systems," *IEEE Journal of Quantum Electronics*, Vol. 32, No. 7, July 1996, pp. 1141–1149.

UNMATCHED DYNAMIC RANGE.
UNMATCHED PERFORMANCE.

VDI's Mini VNAX modules are one-quarter the volume of standard modules making them well suited for probe station and antenna measurement applications.

BRIDGING THE THz GAP JUST GOT SMALLER.

VDI's VNA Extenders provide high performance frequency extension of vector network analyzers from 26GHz to 1.5THz. These modules combine high test port power with exceptional dynamic range and unmatched stability.

VDI's mini-modules are reduced in size, but yield the same industry leading performance as our original designs. The compact form factor and simplified power supply make them the recommended solution for most applications.

Mini-modules are currently available in standard waveguide bands for 26GHz to 500GHz with higher frequency bands under development.

Waveguide Band (GHz)	**WR28** 26-40	**WR15** 50-75	**WR12** 60-90	**WR10** 75-110	**WR8** 90-140	**WR6.5** 110-170	**WR5.1** 140-220	**WR4.3** 170-260	**WR3.4** 220-330	**WR2.8** 260-400	**WR2.2** 325-500	**WR1.5** 500-750	**WR1.0** 750-1,100
Dynamic Range (BW=10Hz, dB, typ)	120	120	120	120	120	120	120	115	115	100	110	100	65
(BW=10Hz, dB, min)	110	110	110	110	110	110	110	100	105	80	100	80	45
Magnitude Stability (±dB)	0.15	0.15	0.15	0.15	0.15	0.25	0.25	0.3	0.3	0.5	0.5	0.8	0.5
Phase Stability (±deg)	2	2	2	2	2	4	4	6	6	8	8	10	6
Test Port Power (dBm)	10	13/6	13/6	11/6	6	9	-1	-2	-6	-10	-8	-25	-30

VDI

Virginia Diodes, Inc.
979 2nd St. SE, Suite 309
Charlottesville, VA 22902
434.297.3257

vadiodes.com

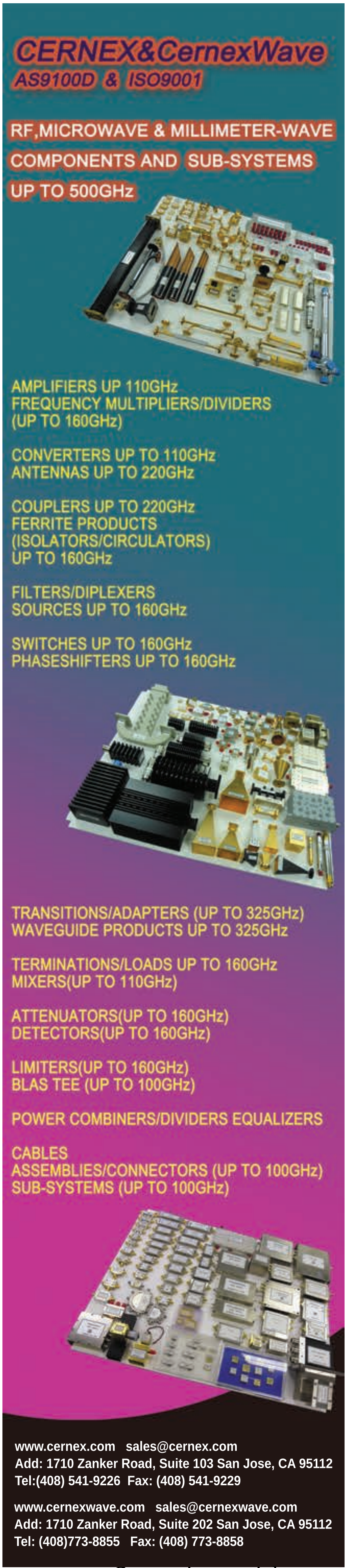

6. X. Yao and L. Maleki, "Converting Light into Spectrally Pure Microwave Oscillation," *Optics Letters*, Vol. 21, No. 7, April 1996, pp. 483–485.
7. X. Yao and L. Maleki, "Optoelectronic Microwave Oscillator," *Journal of the Optical Society of America B*, Vol. 13, No. 8, 1996, pp. 1725–1735.
8. J. Zhang and J. Yao, "Parity-Time–Symmetric-Optoelectronic Oscillator," *Science Advances*, Vol. 4, No. 6, June 2018, pp. 1–6.
9. H. Moyer and A. Daryoush, "A Unified Analytical Model and Experimental Validations of Injection-Locking Processes," *IEEE Transactions on Microwave Theory and Techniques*, Vol. 48, No. 4, April 2000, pp. 493–499.
10. C. McNeilage, E. N. Ivanov, P. R. Stockwell and J. H. Searls, "Review of Feedback and Feedforward Noise Reduction Techniques," *Proceedings of the IEEE International Frequency Control Symposium*, May 1998, pp. 146-155.
11. X. Zhou, X. Zhang and A. S. Daryoush, "A New Approach for a Phase Controlled Self-Oscillating Mixer," *IEEE Transactions on Microwave Theory and Techniques*, Vol. 45, No. 2, February 1997, pp. 196–204.
12. D. J. Sturzebecher, X. Zhou, X. S. Zhang and A. S. Daryoush, "Optically Controlled Oscillators for Millimeter-Wave Phased-Array Antennas," *IEEE Transactions on Microwave Theory and Techniques*, Vol. 41, No. 6, June/July 1993, pp. 998–1004.
13. H. Chang, "Phase Noise in Self-Injection Locked Oscillators–Theory and Experiment," *IEEE Transactions on Microwave Theory and Techniques*, Vol. 51, No. 9, September 2003, pp. 1994–1999.
14. G. Pillet, L. Morvan, M. Brunel, F. Bretenaker, D. Dolfi, M. Vallet, J. P. Huignard and A. Le Floch, "Dual-Frequency Laser at 1.5 µm for Optical Distribution and Generation of High-Purity Microwave Signals," *Journal of Lightwave Technology*, Vol. 26, No. 15, August 2008, pp. 2764–2773.
15. M. Aigle, G. Hechtfischer, W. Hohenester, R. Junemann and C. Evers, "A Systematic Way to YIG-Filter-Design," *37th European Microwave Conference*, October 2007.
16. Y. Jiang, P. P. Shum, P. Zu, J. Zhou, G. Bai, J. Xu, Z. Zhou, H. Li and S. Wang, "A Selectable Multiband Bandpass Microwave Photonic Filter," *IEEE Photonics Journal*, Vol. 5, No. 3, June 2013.
17. J. Mora, B. Ortega, A. Diez, J. L. Cruz, M. V. Andres, J. Capmany and D. Pastor, "Photonic Microwave Tunable Single-Bandpass Filter Based on a Mach-Zehnder Interferometer," *Journal of Lightwave Technology*, Vol. 24, No. 7, July 2006, pp. 2500–2509.
18. L. Zhang, A. Poddar, U. Rohde and A. Daryoush, "Analytical and Experimental Evaluation of SSB Phase Noise Reduction in Self-Injection Locked Oscillators Using Optical Delay Loops," *IEEE Photonics Journal*, Vol. 5, No. 6, December 2013.
19. L. Zhang, A. K. Poddar, U. L. Rohde and A. S. Daryoush, "Comparison of Optical Self-Phase Locked Loop Techniques for Frequency Stabilization of Oscillators," *IEEE Photonics Journal*, Vol. 6, No. 5, October 2014.
20. L. Zhang, A. K. Poddar, U. L. Rohde and A. S. Daryoush, "Self-ILPLL Using Optical Feedback for Phase Noise Reduction in Microwave Oscillators," *IEEE Photonics Technology Letters*, Vol. 27, No. 6, March 2015, pp. 624–627.
21. U. L. Rohde, A. K. Poddar and A. S. Daryoush, Self-Injection Locked Phase Locked Loop Optoelectronic Oscillator, US9088369B2, U.S. Patent and Trademark Office, December 28, 2012.
22. U. L. Rohde, A. K. Poddar and A. S. Daryoush, Integrated Production of Self-Injection Locked Self-Phase Locked Optoelectronic Oscillators, US9094133B2, U.S. Patent and Trademark Office, March 12, 2013.
23. T. Sun, L. Zhang, A. K. Poddar, U. L. Rohde and A. S. Daryoush, "Forced SILPLL Oscillation of X- and K-Band Frequency Synthesized Opto-electronic Oscillators," *IEEE International Topical Meeting on Microwave Photonics*, October/November 2016.
24. J. Tang, T. Hao, W. Li, D. Domenech, R. Baños, P. Muñoz, N. Zhu, J. Capmany and M. Li, "Integrated Optical Oscillator," *Optics Express*, Vol. 26, No. 9, April 2018, pp. 12257–12265.
25. J. E. Bowers, A. Beling, D. Blumenthal, A. Bluestone, S. M. Bowers, T. C. Briles, L. Chang, S. A. Diddams, G. Fish, H. Guo, T. J. Kippenberg, T. Komljenovic, E. Norberg, S. Papp, M. H. P. Pfeiffer, K. Srinivasan, L. Theogarajan, K. J. Vahala and N. Volet, "Chip-Scale Optical Resonator Enabled Synthesizer," *IEEE International Frequency Control Symposium*, May 2016.
26. L. A. Johansson, Y. A. Akulova, G. A. Fish and L. A. Coldren, "Sampled-Grating DBR Laser Integrated with SOA and Tandem Electro-Absorption Modulator for Chirp-Control," *Electronics Letters*, Vol. 40, No. 1, January 2004, pp. 70–71.
27. S. Joshi, C. Calò, N. Chimot, M. Radziunas, R. Arkhipov, S. Barbet, A. Accard, A. Ramdane and F. Lelarge, "Quantum Dash Based Single Section Mode Locked Lasers for Photonic Integrated Circuits," *Optics Express*, Vol. 22, No. 9, 2014, pp. 11254–11266.
28. J. S. Barton, E. J. Skogen, M. L. Masanovic, S. P. Denbaars and L. A. Coldren, "A Widely Tunable High-Speed Transmitter Using an Integrated SGDBR Laser-Semiconductor Optical Amplifier and Mach-Zehnder Modulator," *IEEE Journal of Selected Topics in Quantum Electronics*, Vol. 9, No. 5, September-October 2003, pp. 1113–1117.
29. L. Hou, R. Dylewicz, M. Y. Zulkifli bin Haji, P. Stolarz, B. Qiu and A. Catrina Bryce, "Monolithic 40-GHz Passively Mode-Locked AlGaInAs–InP 1.55-um MQW Laser With Surface-Etched Distributed Bragg Reflector," *IEEE Photonics Technology Letters*, Vol. 22, 2010, pp. 1503–1505.
30. A. S. Daryoush, "Highly Stable Forced Optoelectronic Oscillators and Roadmap to Integrated Clocks," *Quantum Sensing and Nano Electronics and Photonics XV*, Vol. 10540, 2018.

Planar Monolithics Industries, Inc.

Multi-Throw Solid State Switches

PMI's full line of RF & Microwave, Broadband Multi-Throw Solid-State Switches are available in Reflective or Absorptive configuration and up to SP128T. These models offer performance up to 50 GHz, high isolation, low insertion loss, fast switching speed and incorporate a TTL compatible driver for ease of system integration. PMI offers many other standard models with various options that are available at: http://www.pmi-rf.com/categories/switches

P20T-4G8G-80-T-515-SFF
P20T-7G18G-80-T-515-SFF-SP

P32T-0R5G18G-60-T-SFF

P16T-100M20G-60-T-512-SFF
P16T-100M20G-60-T-512-SFF-DEC
P16T-18G40G-90-T-512-SFF-DEC

P16T-100M40G-100-T-I-292
P16T-100M50G-100-T-I

PMI Model No.	FREQ Range (GHz)	Insertion Loss (dB)	Isolation (dB)	Switching Speed	Configuration	DC Voltage Supply / Current Drtaw	Size (Inches) / Connectors
P20T-4G8G-80-T-515-SFF https://www.pmi-rf.com/products-details/p20t-4g8g-80-t-515-sff	4 - 8	4 dB Max	80 dB Min	100 ns Typ	SP20T Absorptive	+5 VDC (±5%) @ 300 mA Max, +15 VDC (±2%) @ 200 mA Max	4.0" SQ X 0.63" SMA Female
P20T-7G18G-80-T-515-SFF-SP https://www.pmi-rf.com/products-details/p20t-7g18g-80-t-515-sff-sp 20 Output Ports are Amplitude Balanced to +/-0.25 dB Peak to Peak Max.	7 - 18	7.5 dB Max	65 dB Min	240 ns Typ	SP20T Absorptive	+5 VDC (±5%) @ 500 mA Max, -12 to -15 VDC (±2%) @ 200 mA Max	4.0" SQ X 0.63" SMA Female
P32T-0R5G18G-60-T-SFF https://www.pmi-rf.com/products-details/p32t-0r5g18g-60-t-sff	0.5 - 18	9.5 dB Max	70 dB Min	100 ns Max	SP32T Absorptive	+5 VDC @ 1600 mA, -5 VDC @ 20 mA	8.0" x 3.0" x 0.65" SMA Female
P16T-100M20G-60-T-512-SFF https://www.pmi-rf.com/products-details/p16t-100m20g-60-t-512-sff	0.1 - 20	8.5 dB Max	60 dB Min	150 ns Max	SP16T Absorptive	+5 VDC @ 750 mA Max, -12 VDC @ 200 mA Max	8.0" x 3.0" x 0.65" SMA Female
P16T-100M20G-60-T-512-SFF-DEC https://www.pmi-rf.com/products-details/p16t-100m20g-60-t-512-sff-dec	0.1 - 20	8.5 dB Max	60 dB Min	150 ns Max	SP16T Absorptive	+5 VDC @ 750 mA Max, -12 VDC @ 200 mA Max	8.0" x 3.0" x 0.65" SMA Female
P16T-18G40G-90-T-512-SFF-DEC https://www.pmi-rf.com/products-details/p16t-18g40g-90-t-512-sff-dec	18 - 40	12 dB Max	50 dB Min	150 ns Max	SP16T Absorptive	+5 VDC @ 750 mA Max, -12 VDC @ 200 mA Max	8.0" x 3.0" x 0.65" 2.92mm Female
P16T-100M40G-100-T-I-292 https://www.pmi-rf.com/products-details/p16t-100m40g-100-t-i-292	0.1 - 40	10 dB Typ	100 dB Typ	50 ns Typ	SP16T Absorptive	+5 VDC @ 800 mA Max, -5 VDC @ 700 mA Max	12.0" x 5.5" x 0.65" 2.92mm Female
P16T-100M50G-100-T-I https://www.pmi-rf.com/products-details/p16t-100m50g-100-t-i	0.1 - 50	16 dB Typ	70 dB Typ	100 ns Max	SP16T Absorptive	+5 VDC @ 800 mA Max, -5 VDC @ 700 mA Max	12.0" x 5.5" x 0.65" 2.4mm Female

- Amplifiers – Solid State
- Attenuators – Variable/ Programmable
- Couplers (Quadrature, 180° & Directional)
- Detectors – RF/Microwave
- DLVAs, ERDLVAs & SDLVAs
- DTOs, VCOs, PLO, DROs, & Frequency Synthesizers
- Filters & Switched Filter Banks
- Form, Fit, Functional Products & Services
- Frequency Discriminators & IFMs
- Integrated MIC/MMIC Assemblies (IMAs)
- IQ Vector Modulators
- Limiters – RF/Microwave
- Log Amplifiers
- Millimeter Wave Components (Up to 50 GHz)
- Miscellaneous Products
- Multifunction Integrated Assemblies (MIAs)
- Phase Shifters & Bi-Phase Modulators
- Power Dividers/Combiners (Passive & Active)
- Pulse Modulators (SPST)
- Rack & Chassis Mount Products
- Receiver Front Ends & Transceivers
- SDLVAs, ERDLVAs & DLVAs
- Single Side Band Modulators
- SMT & QFN Products
- Switch Matrices
- Switched Filter Banks
- Switches – Solid State
- Systems - Radar Sense & Avoid
- Systems – Fly Eye Radars
- Threshold Detectors
- USB Products

AMTA 2018

Antenna Measurement Techniques Association (AMTA)
Williamsburg Lodge, Williamsburg, VA, USA
November 4-9, 2018
Booth #109
amta2018.org

West Coast Operation:
4921 Robert J. Mathews Pkwy, Suite 1
El Dorado Hills, CA 95762 USA
Tel: 916-542-1401, Fax: 916-265-2597

East Coast Operation:
7311-F Grove Road
Frederick, MD 21704 USA
Tel: 301-662-5019, Fax: 301-662-1731

sales@pmi-rf.com • www.pmi-rf.com

ISO9001-2008 REGISTERED

INVITED PAPER

5G Brings New RF Challenges for Handsets

Ben Thomas
Qorvo, Greensboro, N.C.

Thanks, in part, to accelerated standards development, 5G is moving briskly toward worldwide deployment, bringing a multitude of new RF challenges for smartphone makers. Mobile operators are beginning to install infrastructure this year, and the first 5G handsets are promised in 2019. Although 4G LTE will remain the predominant cellular access technology for years, industry estimates suggest that sales of 5G smartphones will grow steadily. The latest Ericsson Mobility Report forecasts over 1 billion 5G mobile subscriptions by the end of 2023, accounting for 20 percent of mobile data traffic worldwide.

With the first 5G deployments on the horizon, smartphone manufacturers are under pressure to develop implementation strategies for adding 5G technology to handsets. This is no small task, since 5G adds an extraordinary level of RF complexity reflecting bandwidth, linearity and power management challenges.

5G LANDSCAPE

Early work on 5G specifications focused on enhanced mobile broadband (eMBB) as the first 5G use case. eMBB is expected to deliver data rates up to 20× today's LTE speeds. The first phase of 3GPP Release 15, published in December 2017 (see ***Figure 1***), included draft specifications for the non-standalone (NSA) 5G New Radio (NR). NSA uses an LTE anchor band for control, with a 5G NR band to deliver faster data rates (see ***Figure 2***). This is designed to let operators deliver 5G speeds more quickly by using their existing LTE networks.

In June 2018, 3GPP followed up with specifications for the 5G standalone (SA)

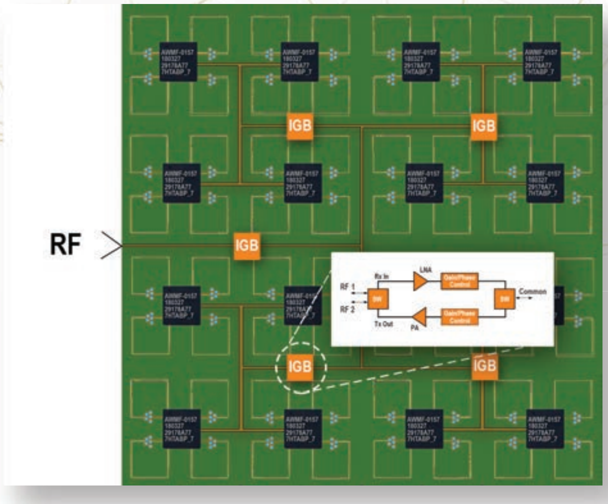
RF
IGB
IGB
IGB
IGB
IGB

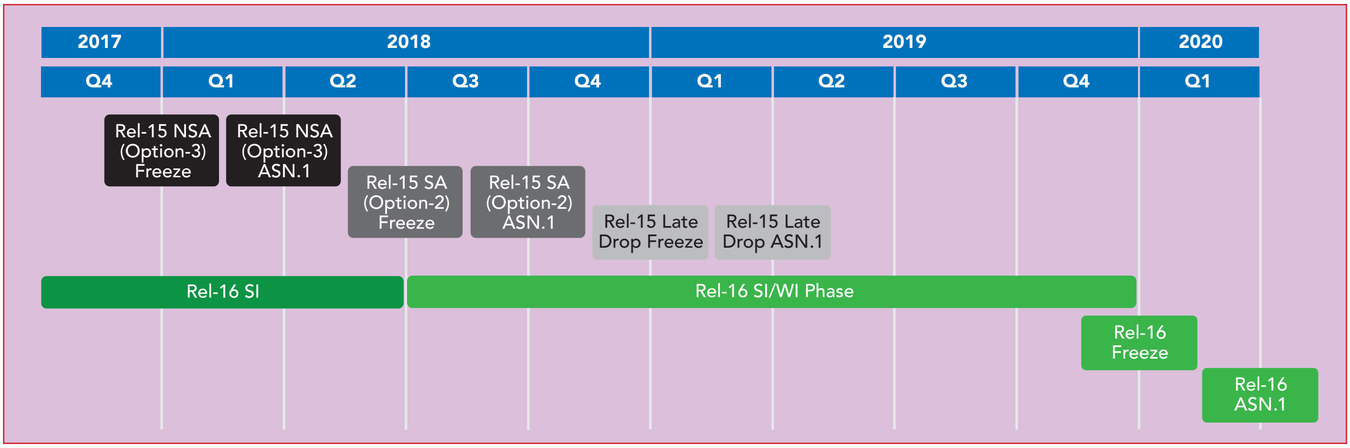

Fig. 1 3GPP 5G standards timeline.

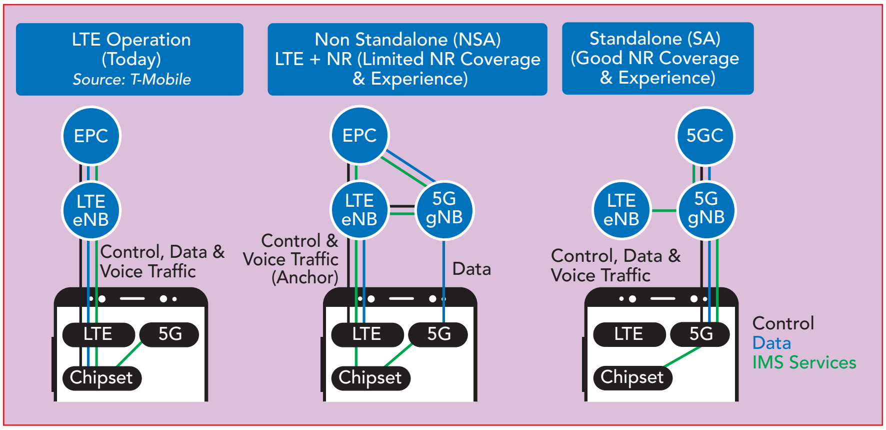

Fig. 2 NSA and SA implementation options compared with LTE.

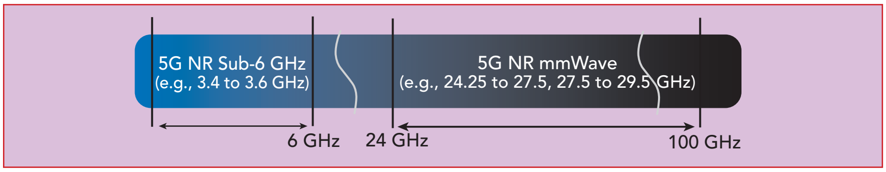

Fig. 3 The 5G spectrum will comprise new bands below 6 GHz and at mmWave frequencies.

NR, which removes the need for an LTE anchor and requires a full 5G network buildout. As shown in Figure 1, the standards group also defined a timeline for the next 18 months, including a "late drop" of additional Release 15 features and a work schedule for Release 16, which will begin to expand 5G specifications beyond mobile broadband to a vast range of new applications, including autonomous vehicles and the IoT.

To deliver the promise of faster data speeds and support increased capacity, 5G will massively increase the spectrum range and bandwidth used for cellular communications. Spectrum is being allocated in two frequency ranges: sub-6 GHz, designated FR1, and mmWave, designated FR2 (see ***Figure 3***). The initial mobile deployments will use

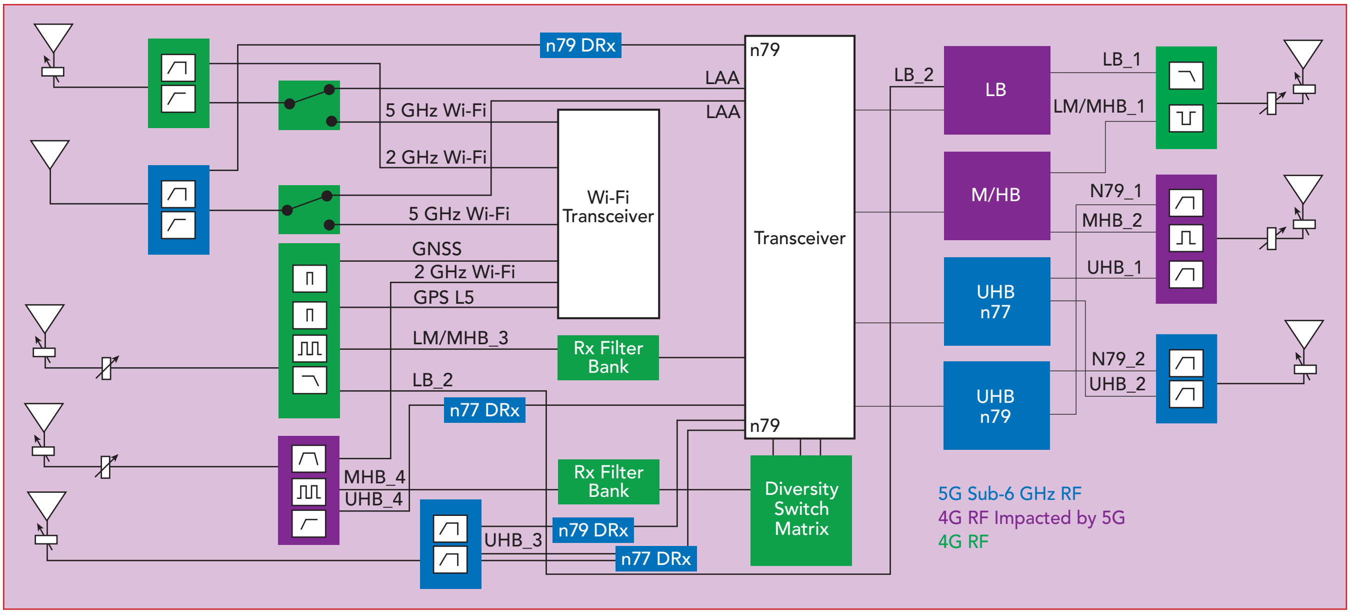

Fig. 4 Complexity of the RF front-end in the 5G smartphone, not including any mmWave bands.

FR1, which includes several new 5G bands above 3 GHz. The technical approach for supporting mmWave frequencies in handsets is being developed, but the technology is not as mature as for the sub-6 GHz bands.

In FR1, the maximum bandwidth for a single carrier is 100 MHz, 5× LTE's 20 MHz maximum. The 5G specifications mandate that handsets support two uplink and four downlink carriers in the bands above 1 GHz, for a total of 200 and 400 MHz, respectively. The Release 15 specifications include over 600 new carrier aggregation (CA) combinations, including many NSA permutations of 4G and 5G bands. The challenges managing this unprecedented bandwidth and CA combinations ripple through the entire RF subsystem. Adding to the complexity, 5G defines two alternative waveforms: CP-OFDM and DFT-s-OFDM. CP-OFDM offers very high spectral packing efficiency in resource blocks and good support for MIMO. DFT-s-OFDM, which is the same waveform used for the LTE uplink, provides less efficient spectral packing but greater range.

IMPACT ON HANDSET DESIGN

5G will have a huge impact on the handset RF front-end (RFFE). The standard requires handsets to squeeze additional RF complexity into essentially the same amount of space (see ***Figure 4***). Innovative approaches are needed to support the requirements for multiple simultaneous uplink and downlink connections, and the RFFE needs to support this massive bandwidth while providing very high linearity and managing power consumption.

NSA Dual-Connectivity

Although 5G NSA provides operators a way to accelerate 5G deployment, it adds RF complexity because it requires dual LTE and 5G connectivity. In some cases, the handset may be transmitting on one or more LTE bands while simultaneously receiving on a 5G band. This greatly increases the possibility that harmonics of the transmit frequencies will desensitize the receiver. One example is the CA combination of LTE bands 1, 3, 7 and 20 with the new 5G FR1 band n78. n78 occupies a much higher frequency range than the LTE bands and is very wide, from 3.3 to 3.8 GHz. This increases the potential that harmonics generated by transmission on one of the LTE bands will fall into the n78 frequency range. Filtering to attenuate the harmonics can increase RFFE insertion loss, driving up the required power amplifier (PA) output power and reducing total system efficiency.

Massive Bandwidth and New Waveforms

The combination of massive bandwidth, the new CP-OFDM waveform and higher output power presents significant challenges for RF linearity and power management. In 4G handsets, envelope tracking (ET) is widely used to minimize PA power consumption. ET optimizes efficiency by continuously

GaN SOLID-STATE MICROWAVE GENERATOR

Applications Plasma Generator MicrowaveCVD Reactor Microwave Heating & Drying Semiconductor Equipment

RFHIC's Solid-State Solutions

Although, most high-powered ISM systems utilize magnetron technology as the core component of microwave generators, it lacks controllability, has high maintenance costs, and has limited lifespan.
Transition over to solid-state technology and let RFHIC's latest array of high-powered solid-state microwave generators help you lower maintenance costs and optimize overall RF performance.

15kW

RIK0915K-40T
915 MHz

Key Features:

- Industrial 19" Rack Mount Type (16 SSPAs in One System Rack)
- Fully equipped with GaN Solid-State Power Amplifiers (SSPAs)
- 900-930 MHz, 15kW CW
- Power Supply Unit Included
- Water Cooling System

6kW

RIU256K0-40T
2.45 GHz

Key Features:

- Fully equipped with GaN Solid-State Power Amplifiers (SSPAs)
- 2.4-2.5 GHz , 6kW CW
- Power Supply Unit Included
- SSPA Head : 507x 392.4x192(LxWxH)
- Water Cooling System

Learn more at www.rfhic.com
rfsales@rfhic.com

RFHIC
www.rfhic.com

adjusting the PA's supply voltage to track the RF envelope. However, when 5G is first deployed, envelope trackers are only expected to support a maximum bandwidth of 60 MHz, which is not wide enough to support 100 MHz 5G carriers. As a result, PAs must operate in fixed voltage, average power tracking (APT) mode for wideband transmission, which will reduce efficiency and battery life.

Adding to the challenge, the new CP-OFDM waveform has much higher peak-to-average power ratio (PAR). Combined with the increased channel bandwidth, this requires greater PA back-off for 5G compared to LTE, to avoid exceeding regulatory limits and maintain the linearity required for high-quality data links. Finally, many operators are planning to implement the Power Class 2 standard to maximize the handset's operating range with 5G. Power Class 2 doubles the output power at the handset antenna to overcome the increased propagation losses of the higher frequency FR1 bands.

The combination of these three requirements—increased bandwidth, new waveform and higher output power—creates a very challenging linearity requirement for the PA design, with the potential for reduced efficiency in the transmit chain.

4 × 4 MIMO

While LTE requires two download pathways for receive diversity, 5G mandates four independent RF downlink paths for the bands above 1 GHz, to deliver higher data rates via 4× MIMO and CA. 5G also specifies two optional uplink paths in some bands. The challenge for handset manufacturers is how to fit these additional signal paths into the limited space allocated to the RFFE.

Increased integration is key to solving this problem, using integrated modules that typically combine PAs, switches and filters. In addition to saving space and increasing performance, integrated modules provide pre-tested RF building blocks that will help handset makers meet the industry's demanding handset development cycles. Unlike the previous transition from 3G to 4G, where handsets were largely implemented using discrete components, there is near unanimous agreement among manufacturers to use integrated RFFEs to speed their first 5G devices to market.

Space for Antennas

The rise in RF complexity is also driving up the number of antennas toward the practical limit achievable in a handset. To support 4× downlink MIMO, dual uplink MIMO, the wider range of frequency bands and requirements such as 2× Wi-Fi MIMO, the number of antennas is expected to increase from the three to five in today's LTE handsets to four to eight—or more—in 5G smartphones. At the same time, the industry's shift to full-screen smartphone designs is actually reducing the space available for antennas, by shrinking the bezel area that houses

the cellular antennas. The need to fit more antennas into less space means antennas must be smaller and, as a result, are less efficient.

These trends will drive the adoption of two categories of antenna solutions in the RFFE. One is antenna tuning, which enables each antenna to be tuned to the operating frequency band so that it is more efficient. To some extent, antenna tuning is already used in LTE handsets, largely to increase performance. With 5G, antenna tuning will become necessary to maintain performance, given the limited number of antennas and the broader range of frequencies they must support. The other antenna technology, antenna-plexers, will expand from being a high performance option used in some LTE handsets to a must-have technology in 5G. Antenna-plexers cover multiple frequencies with a single module that allows multiple RF pathways to simultaneously connect to the antenna, while preventing interference among the pathways. Currently used in some LTE handsets for routing CA signals, antenna-plexers will be essential in 5G handsets to support the massive number of dual-connectivity CA options defined in Release 15 and future releases.

SOLVING THE CHALLENGES

Behind the hype about 5G, the reality is that deployments are approaching more quickly than originally anticipated, increasing the pressure on smartphone manufacturers to add 5G functionality. The new standards introduce unprecedented RF challenges, including new levels of complexity, massive bandwidth, linearity and power management.

As 3GPP defines the 5G standards, Qorvo and other RFFE suppliers are supporting the effort, collaborating with the wireless infrastructure manufacturers, network operators, chipset providers and smartphone manufacturers. As with the previous technology transitions, innovative new RF solutions will be required to solve the complex challenges of 5G, enabling manufacturers to release new products to consumers.■

A Field-Effect Transistor That Avoids Pinch-Off

Alfred Grayzel
Planar Monolithic Industries Inc., Frederick, Md.

Greater efficiency and output power are proposed by providing a uniform depletion region along the channel to avoid pinch-off. A bias network to achieve this condition is described for a field-effect transistor (FET) with a segmented gate.

The efficiency of a FET is degraded when its drain voltage is greater than V_{Dsat}, the voltage at which pinch-off first occurs. Under this condition, the FET is in saturation, where the drain current is not a function of the drain voltage and is only a function of the gate voltage. To understand the degradation of efficiency, consider the behavior of a FET in saturation. When the drain voltage of a JFET, for instance, is equal to V_{Dsat}, pinch-off occurs exactly at the drain of the transistor (see ***Figure 1a***).[1] If the drain voltage is increased by ΔV, the point at which pinch-off occurs moves toward the source a distance ΔL (see ***Figure 1b***). Over the length, ΔL, the channel is completely depleted, and the resistance is quite large. Voltage, ΔV, is dropped across this depleted region and, due to its high resistivity, ΔL is very small. For ΔL << L, which represents the usual case, depletion from the source to the pinch-off point is essentially identical in shape, and the channel has approximately the same resistance from the source to the point where pinch-off occurs. The drain current, which is equal to V_{Dsat} divided by this resistance, hardly changes. This explains why the value of the drain current is nearly constant for drain voltages greater than V_{Dsat}. Over the length, ΔL, the resistance is quite large and the power dissipated in this resistance is equal to the product of the saturated current and ΔV. The voltage, ΔV, does not contribute to output power and simply degrades efficiency.

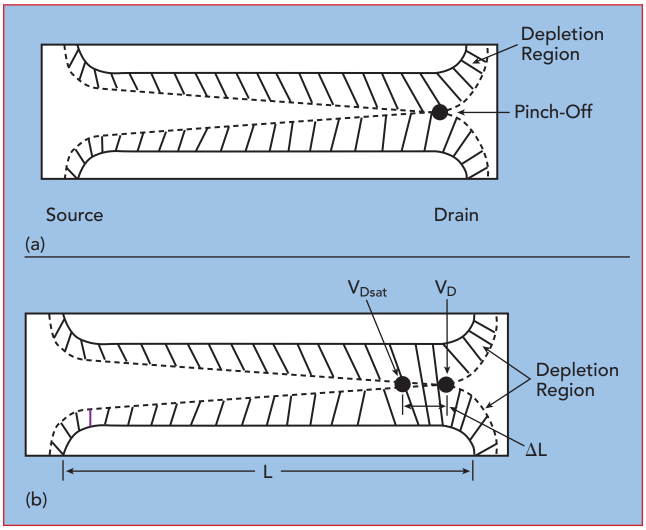

Fig. 1 **Channel of a JFET with the drain voltage equal to the pinch-off voltage (a) and the drain voltage exceeding the pinch-off voltage (b).**

Therefore, for high efficiency, pinch-off must be avoided, and the depletion region must be minimized. Ideally, for converting DC power to RF power, the channel should not be depleted for one-half the cycle and should be completely cut off for the other half. With an optimum load, this should yield maximum DC-to-RF efficiency. To accomplish this, a new FET has been proposed[2].

THE "GRAYZEL" JFET

Figure 2 shows a simplified schematic of a typical JFET with a drain-to-source DC voltage of 7 V. Points along the channel have voltage values of 0, 1, 2, 3, 4, 5, 6 and 7 V, as shown in the figure. The junction is progressively back-biased by these potentials, causing greater depletion at the drain than at the source. ***Figure 3*** shows a simplified schematic of the proposed device. The P+ region is divided into N sections that are insulated from one another, forming N, p-n junctions. As an illustrative example, in Figure 3, N = 8. Each p-n junction is biased

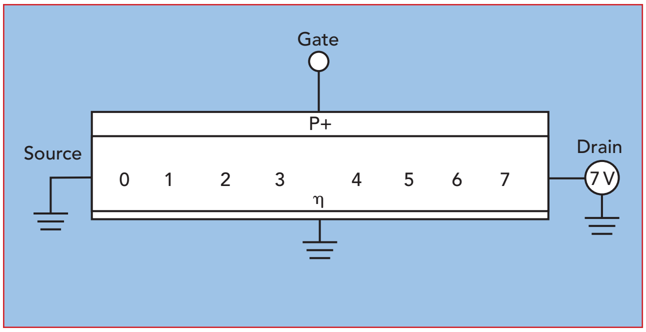

Fig. 2 Voltage drop across the channel of a typical JFET, with V_D = 7 V.

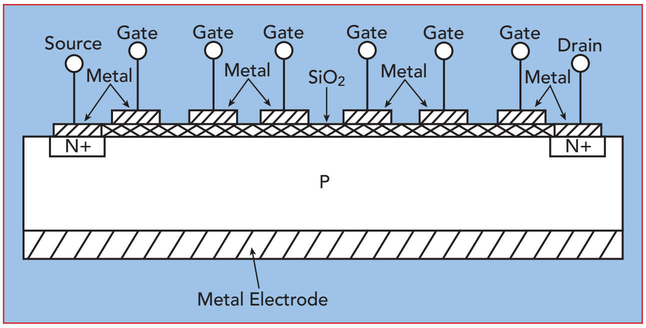

Fig. 4 Simplified cross-section of the proposed MOSFET.

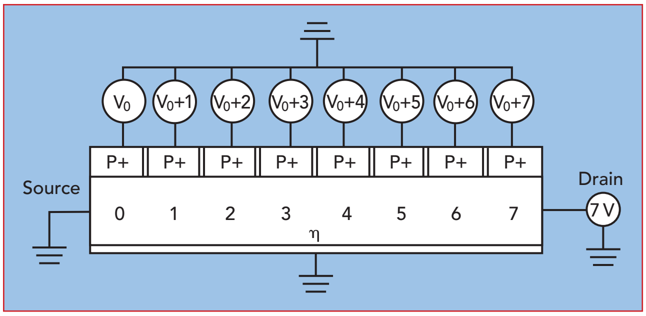

Fig. 3 Proposed JFET where the p-n junctions are individually biased and each junction is reverse biased at V_0.

to ground separately as shown in the figure; the first is biased at V_0 and the eighth at V_0 + 7 V. With a drain voltage of 7 V, all of the p-n junctions have the same DC voltage, V_0, across their junctions and hence, to a good approximation, the depletion region is uniform along the channel.

Dividing the gate into multiple sections is applicable to all types of FETs. ***Figure 4*** shows an example of a MOSFET with the gate divided into N = 6 sections. ***Figure 5*** shows a bias network with a drain voltage of 5V, biased such that each CMOS capacitor has a voltage of 5 V across it. The bias network consists of a 10 V DC voltage source and six resistors, which can be etched onto the chip.

ANALYSIS

Consider a case where the odd harmonics are short circuited and the even harmonics are open circuited by the load admittance Y(ω) and where, for half of the cycle, the FET is cut off and, for the other half, the depletion region in the channel is minimum width. The conductance is thus a square wave varying between 0 and G_0, where G_0 is the conductance when the depletion region in the channel is the minimum width. Let $\theta = 2\pi ft = \omega t$, where f is the fundamental frequency of the square wave. The Fourier series of the square wave is given by

$$G(t) = 0.5G_0 + g(t) \qquad (1a)$$

where

$$g(t) = (2G_0/\pi)\left(\cos\theta - \cos(3\theta)/3 + \cos(5\theta)/5 - \cos(7\theta)/7 + \ldots\right.$$

$$= (2G_0/\pi)\sum_{k=1}^{\infty}(-1)^{k-1}\cos[(2k-1)\theta]/(2k-1)] \qquad (1b)$$

The FET is terminated in an admittance $Y(\omega)$, which at the fundamental frequency has a value GL. The value of $Y(\omega) = 0$ at the even harmonics of the fundamental frequency and infinite at the odd harmonics. The drain voltage, therefore, has only even harmonics, and the drain current has only odd harmonics. The drain voltage, $V_D(t)$, has the form

$$V_D(t) = V_0 + v(t) \quad (2)$$

where

$$v(t) = V_1\cos(\theta) + \sum_{k=1}^{\infty} V_{2k}\cos(2k\theta) \quad (3)$$

The bias voltage V_0 in Equation 2 is the same for all of the segments when the proposed FET is biased as described. There is, however, a variation of the depletion region along the channel, due to v(t). This variation is small and, therefore, it is neglected in this analysis.

Equation 3 represents the voltage v(t) for the following reason. The value of the conductance of the channel is equal to G_0 when −90 degrees < θ < +90 degrees, and the channel is cutoff during the remainder of the cycle; therefore, current flows only when −90 degrees < θ < +90 degrees. Since the current is equal to $V_D(t)G(t)$, $V_D(t)$ has its maximum value centered at θ = 0 degrees and is the sum of cosines.

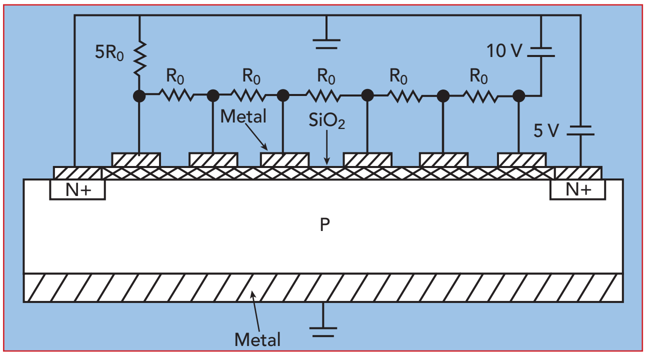

Fig. 5 **MOSFET bias network.**

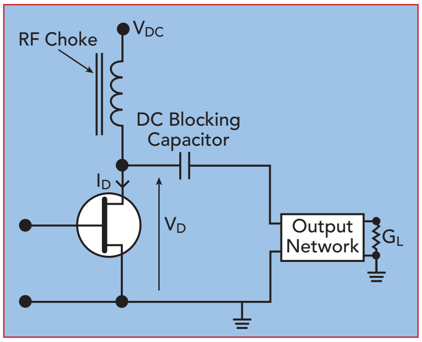

Fig. 6 **FET amplifier.**

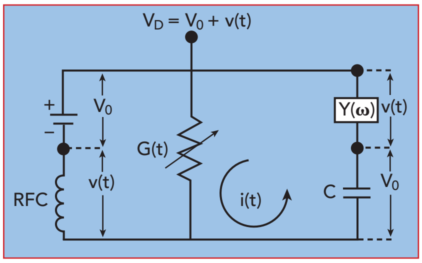

Fig. 7 **FET amplifier equivalent circuit.**

The proposed segmented-gate amplifier shown in ***Figure 6*** is analyzed with the aid of the circuit in ***Figure 7***. Voltage v(t) appears across the RF choke and across the load $Y(\omega)$, which is in series with blocking capacitor C. V_0 + v(t) appears across the nonlinear conductance G(t). The choke, which is in series with the DC battery, has voltage v(t) across it but negligible RF current flowing through it. Drain current $I_D(t) = I_0$ + i(t) is equal to the product $G(t)V_D(t)$. i(t) flows in a loop through the termination $Y(\omega)$. DC voltage, V_0, appears across the blocking capacitor C. The drain current is given by

$$I_D(t) = V_D(t)G(t) = [V_0 + v(t)][0.5G_0 + g(t)] = 0.5V_0G_0 + V_0 g(t) + 0.5G_0 v(t) + v(t)g(t) \quad (4)$$

Equations 2, 3 and 4 yield the terms in Equation 4

$$V_0 g(t) = (2V_0G_0/\pi)\left(\sum_{k=1}^{\infty} (-1)^{k-1}\cos[(2k-1)\theta]/[2k-1]\right) \quad (4a)$$

and

$$0.5G_0 v(t) = 0.5G_0\left[V_1\cos(\theta) + \sum_{k=1}^{\infty} V_{2k}\cos(2k\theta)\right]$$

$$v(t)g(t) = (2G_0/\pi)\left[V_1\cos(\theta) + \sum_{k=1}^{\infty} V_{2k}\cos(2k\theta)\right]\sum_{j=1}^{\infty}(-1)^{j-1}\cos[(2j-1)\theta]/(2j-1)$$

Ceyear

Designing and manufacturing world-class test and measurement products since 1968

Microwave/MMwave
- Signal Generators
- Signal and Spectrum Analyzers
- Network Analyzers
- Noise Figure Analyzers
- Microwave Power Meter
- RF/Microwave Comprehensive Testers
- Microwave Test Accessories

Optoelectronic
- Optical Spectrum Analyzers
- Optical Fiber Splicer
- OTDR
- Optical Sources
- Optical Power Meters
- Optical Attenuators
- Infrared & Ultraviolet Laser Tests

Communication
- Digital Communication
- Radio Communication
- Radio & TV Network

Fundamental
- Digital Oscilloscopes
- Photovoltaic Instruments
- Programmable Power

http://en.ceyear.com
sales@ceyear.com

Handheld Spectrum Analyzer
AV4024 Series
FREQUENCY RANGES FROM 9KHZ to 44 GHz (4 MODELS)

PRICE STARTING AT
$16,995
35% less than comparable models

- Low displayed average noise: -163dBm@1Hz RBW (typical)
- Excellent phase noise performance: -106dBc/Hz@100kHz frequency offset@1GHz carrier
- High sweep speed: for 1GHz span, sweep time <20ms
- Resolution bandwidth: 1Hz~10MHz
- Full-band pre-amplifier: standard configuration
- Easy user operation with 8.4 inch high definition LCD
- Various intelligent measurement functions: field strength, channel power, occupied bandwidth, adjacent-channel power ratio, tune & listen, carrier-to-noise ratio, emission mask.
- Various auxiliary test interfaces: 10MHz reference I/O, GPS antenna, zero span IF output, external triggering input, etc.
- Various measurement functions: spectrum analyzer, interference analyzer (spectrogram, RSSI), AM/FM/PM analyzer, channel scanner, high accuracy power meter etc.

Ceyear AuthorizedNorth American Sales & Support Centers:

Custom-Cal GLOBALTECH

(908) 328-3663
sales@cc-globaltech.com
www.cc-globaltech.com

The drain current is the sum of a DC term, odd harmonics and even harmonics

$$I_d(t) = I_0 + \sum\nolimits^{\infty}_{k=1}(I_{2k-1}) \cos(2k-1)\theta + \sum\nolimits^{\infty}_{k=1} I_{2k} \cos(2k\theta) \quad (5)$$

Using the identity cos(x)cos(y) = 0.5[cos(x + y) + cos(x − y)] in Equation 4a, the even harmonics can be written as

$$I_{2k} = G_0 \left[0.5V_{2k} - (2V_1/\pi)(-1)^k / \left(4k^2-1\right)\right] \quad (6)$$

Since the current at the even harmonics is zero, it is possible to solve for voltage V_{2k} by setting current $I_{2k} = 0$ in Equation 6, yielding

$$V_{2k} = (4/\pi)(V_1)(-1)^k / \left(4k^2-1\right) \quad (7)$$

Collecting the terms in cos(θ) in Equation 4, the value of the current at the fundamental frequency, I_1, is

$$I_1 = G_0 \left[2V_0/\pi + 0.5V_1 - (2/\pi) \cdot \sum\nolimits^{\infty}_{k=1}(-1)^k V_{2k} / \left(4k^2-1\right)\right] \quad (8)$$

Substituting Equation 7 into Equation 8 yields

$$I_1 = G_0 \left\{2V_0/\pi + V_1\left[0.5 - \left(8/\pi^2\right)\sum\nolimits^{\infty}_{k=1} 1/\left(4k^2-1\right)^2\right]\right\} \quad (9)$$

The term $[0.5 - (8/\pi^2)\, \Sigma^{\infty}_{k=1} 1/(4k^2 - 1)^2]$ converges in the limit to $(2/\pi)^2$ as k approaches infinity. (This limit was first estimated and then verified by a computer program.) Substituting $(2/\pi)^2$ for $[0.5 - (8/\pi^2)\, \Sigma^{\infty}_{k=1} 1/(4k^2 - 1)^2]$ in Equation 9 yields

$$I_1 = G_0\left[2V_0/\pi + (2/\pi)^2 V_1\right] \quad (10)$$

At the fundamental frequency $Y(\omega) = G_L$ and $I_1 = -(G_L)(V_1)$. Equating I_1 as given by Equation 10 to $-(G_L)(V_1)$, yields

$$2G_0V_0/\pi + G_0V_1(2/\pi)^2 = -G_LV_1 = -XG_0V_1 \quad (11)$$

where $X = G_L / G_0 = 1 / (G_0R_L)$.

Solving Equation 11 for V_1 yields

$$V_1 = -(2/\pi)V_0 / \left(X + (2/\pi)^2\right) \quad (12)$$

The DC current I_0 is found from Equation 4 to have two terms. The first term is $0.5(G_0)(V_0)$ and the second DC term results from the product $(2G_0/\pi)\cos(V_1\cos\theta)$.

$$I_0 = 0.5G_0V_0 + G_0V_1/\pi = 0.5G_0V_0\left[1 + (2/\pi)/(V_1/V_0)\right] \quad (13)$$

Substituting Equation 12 into Equation 13 yields

$$I_0 = 0.5G_0V_0X / \left(X + (2/\pi)^2\right) \quad (14)$$

The DC power is

$$P_0 = I_0V_0 = 0.5G_0V_0^2X / \left(X + (2/\pi)^2\right) \quad (15)$$

The output power at the fundamental frequency P_1 is

$$P_1 = 0.5G_LV_1^2 = 0.5G_L \cdot \left[(2/\pi)V_0 / \left(X + (2/\pi)^2\right)\right]^2 \quad (16)$$

The efficiency, EFF, is then

$$EFF = P_1/P_0 = (2/\pi)^2 / \left[X + (2/\pi)^2\right] \quad (17)$$

Figure 8 shows a plot of efficiency as a function of $X = G_L / G_0$.

This special case where the amplifier is terminated in an open circuit for the even harmonics and a short circuit for the odd harmonics gives good efficiency; however, it is not necessarily the optimum termination. An analysis similar to the one performed above, for the case where the amplifier is terminated in an open circuit for the odd harmonics and a short circuit for the even harmonics gives a

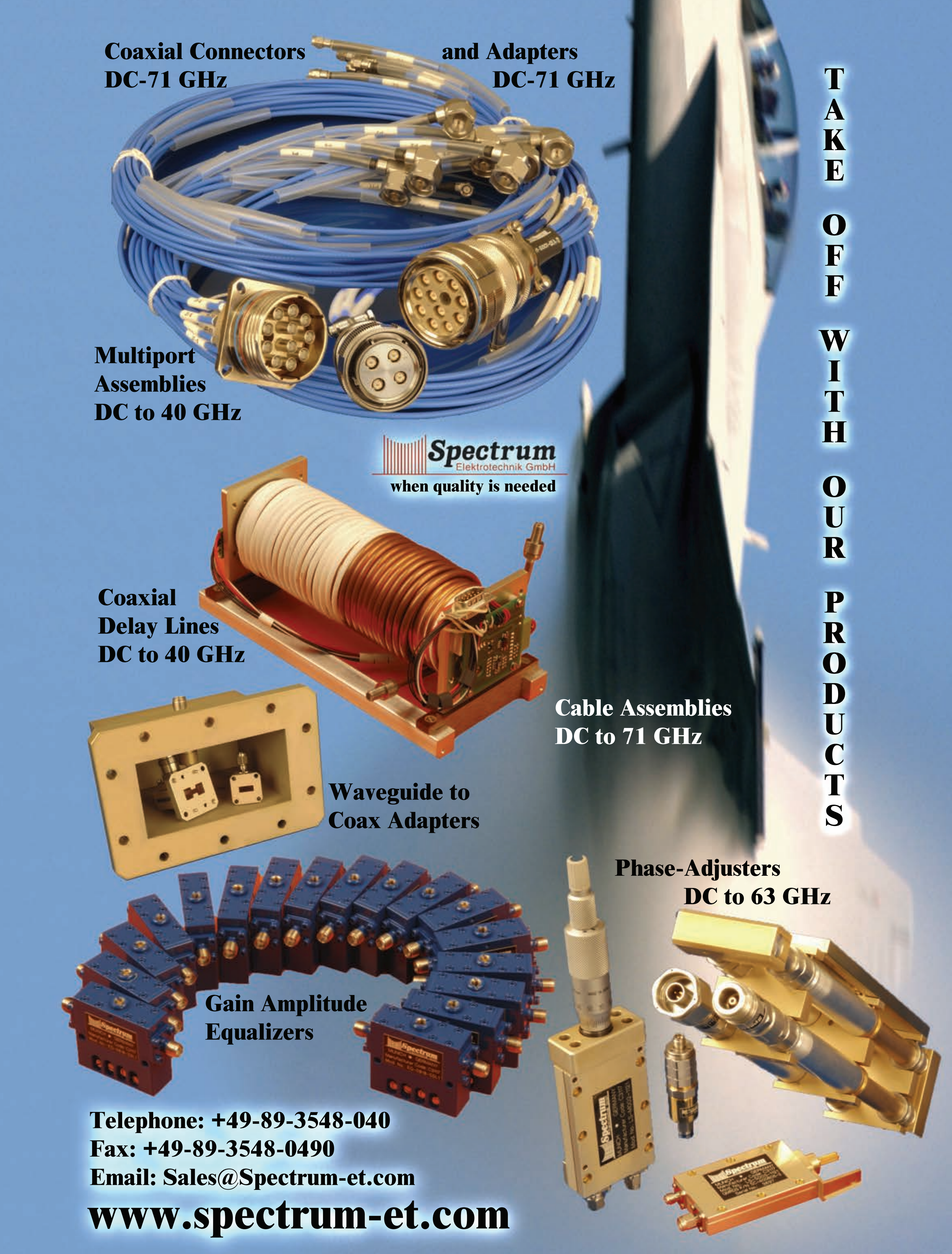
Coaxial Connectors
DC-71 GHz
and Adapters
DC-71 GHz
TAKE OFF WITH OUR PRODUCTS
Multiport
Assemblies
DC to 40 GHz
Spectrum
Elektrotechnik GmbH
when quality is needed
Coaxial
Delay Lines
DC to 40 GHz
Cable Assemblies
DC to 71 GHz
Waveguide to
Coax Adapters
Phase-Adjusters
DC to 63 GHz
Gain Amplitude
Equalizers
Telephone: +49-89-3548-040
Fax: +49-89-3548-0490
Email: Sales@Spectrum-et.com
www.spectrum-et.com
Hornet-06E

TechnicalFeature

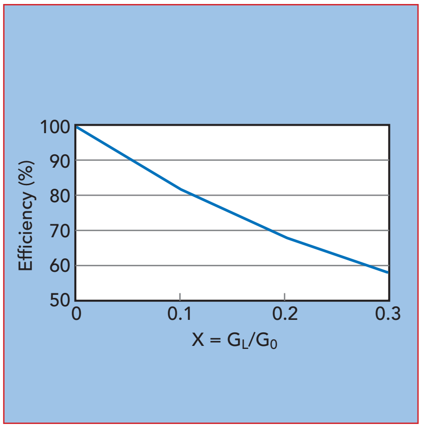

Fig. 8 Amplifier efficiency vs. X.

poorer result. An optimization is warranted to determine the best termination.

SUMMARY

A FET has greater efficiency and output power if pinch-off is avoided and the depletion region is made uniform along the channel. A bias network is presented for achieving this condition for a FET whose gate is segmented. Efficiency and output power are derived for the case where odd harmonics are short circuited and even harmonics are open circuited and where for half of the cycle the FET is off, while for the other half of the cycle the depletion region is minimum width.■

ACKNOWLEDGMENT

The author wishes to acknowledge the support provided by Ashok Gorwara, CEO, and the staff of Planar Monolithics Industries Inc.

Editor's Note

In a future issue of *Microwave Journal*, we hope to publish measured data confirming this theoretical FET structure.

References

1. R. F. Pierret, "Field Effect Devices: Modular Series on Solid State Devices," *Addison-Wesley Publishing Company*, 1983, pp. 5–15.
2. "Field Effect Transistor Which Can Be Biased to Achieve a Uniform Depletion Region," U.S. Patent 10,084,054.

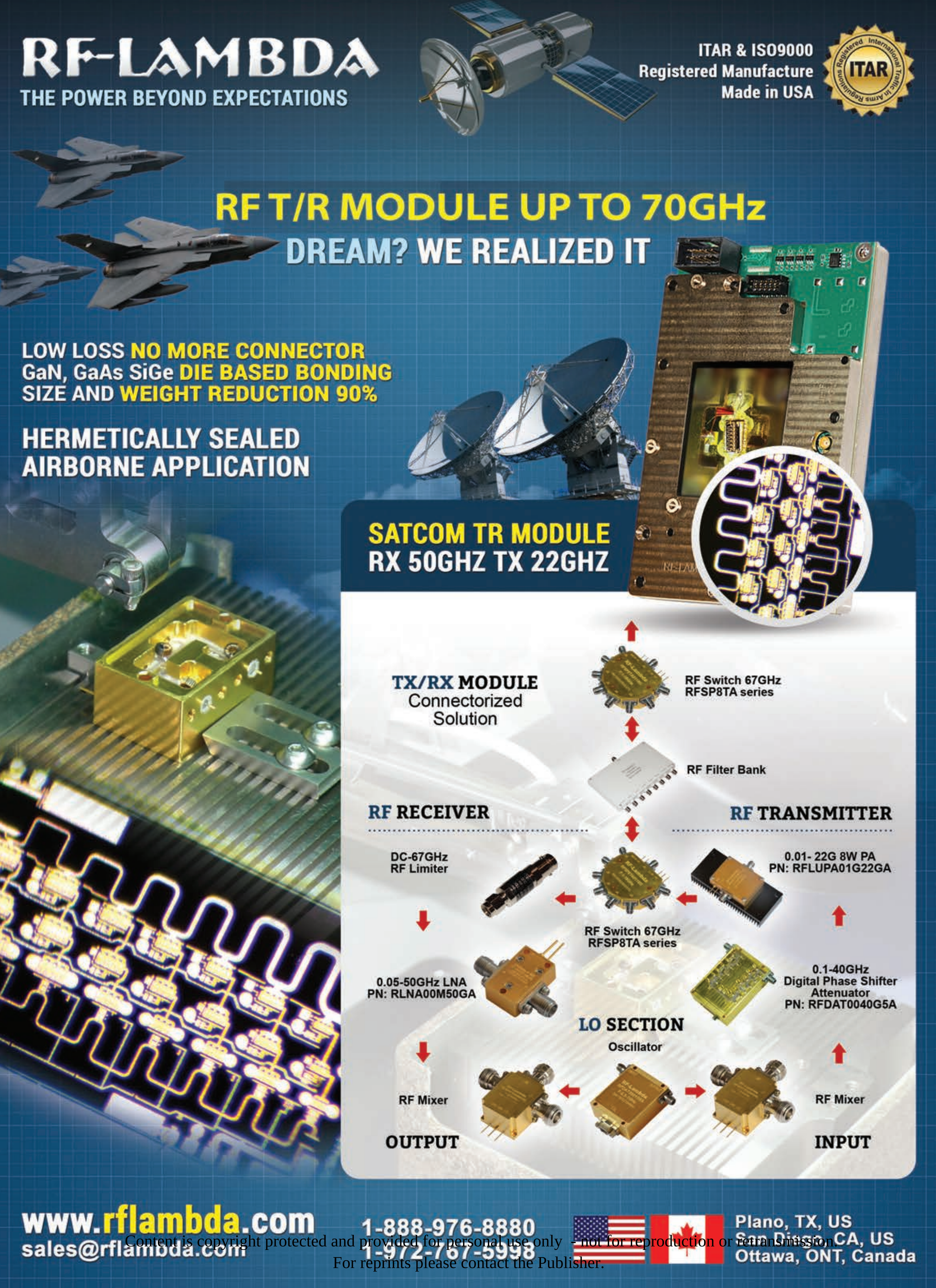
RF-LAMBDA
THE POWER BEYOND EXPECTATIONS
ITAR & ISO9000
Registered Manufacture
Made in USA
ITAR
RF T/R MODULE UP TO 70GHz
DREAM? WE REALIZED IT
LOW LOSS NO MORE CONNECTOR
GaN, GaAs SiGe DIE BASED BONDING
SIZE AND WEIGHT REDUCTION 90%
HERMETICALLY SEALED
AIRBORNE APPLICATION
SATCOM TR MODULE
RX 50GHZ TX 22GHZ
TX/RX MODULE
Connectorized
Solution
RF Switch 67GHz
RFSP8TA series
RF Filter Bank
RF RECEIVER
RF TRANSMITTER
DC-67GHz
RF Limiter
0.01- 22G 8W PA
PN: RFLUPA01G22GA
RF Switch 67GHz
RFSP8TA series
0.05-50GHz LNA
PN: RLNA00M50GA
0.1-40GHz
Digital Phase Shifter
Attenuator
PN: RFDAT0040G5A
LO SECTION
Oscillator
RF Mixer
RF Mixer
OUTPUT
INPUT
www.rflambda.com
sales@rflambda.com
1-888-976-8880
1-972-767-5998
Plano, TX, US
San Diego, CA, US
Ottawa, ONT, Canada

L-Band Microstrip Lowpass Filter with Small Size and Excellent Harmonic Suppression

Amirhossein Ghaderi and Saeed Roshani
Islamic Azad University, Kermanshah, Iran

A microstrip lowpass filter (LPF) with very small dimensions and an extremely wide rejection band has a cutoff frequency (f_c) of 1.89 GHz and suppresses the second to 34th harmonics (2.38 to 65 GHz) by greater than than 24 dB. The filter's simple topology consists of a symmetrical modified T-shaped resonator, a symmetrical modified flag-shaped (SMF) resonator and open-circuited stubs as suppression elements to achieve the ultra-wide stopband. Passband ripple is less than 0.15 dB. The overall dimensions are only $0.153\lambda_g \times 0.065\lambda_g$, where λ_g is the guided wavelength at f_c. The filter has a high figure of merit (FOM) of 32.465 and passband return loss better than 14.8 dB.

Microstrip LPFs with desirable properties—such as a wide stopband with high rejection and small size—are widely utilized in telecommunications systems to reject undesirable out-of-band peaks.[1-2] Raphika et al. reported on an LPF using an improved T-shaped resonator.[3] To increase the stopband width of this filter, four stepped-impedance stubs were used. Nevertheless, harmonic suppression was weak. Karimi et al.[4] developed a microstrip LPF with a suitable suppression level using T- and U-shaped resonators. To extend the stopband, radial stubs were added, even though this structure inherently has a narrow stopband and occupies a large area. Zhang and Li[5] introduced a dual-layer LPF, with large dimensions and a narrow stopband. The structures reported by Verma et al.[6] are simple, but they are large with narrow stopbands, as well. Kufa and Raida[7] introduced a conventional LPF using an open-circuited stub and an embedded, defected ground to reduce circuit dimensions; however, it had a slow transition band, enormous size and weak harmonic suppression. Several LPFs with high return loss in the passband were studied,[8-10] but they were challenged by wide transition bands and narrow stopbands. Attempts to increase the stopband width with defected ground planes have had limited success, and these filters were also large.[11-16] Hayati et al.[17] reported on a compact LPF with high return loss in the passband, using hexangular-shaped resonators. To have a high suppression level, rectangular stubs were utilized. However, this structure only suppressed up to the seventh harmonic. A symmetrical LPF by Mirzaee and Virdee[18] was limited by a gradual cutoff and large dimensions. The LPF by Liu et al.[19] suffered from a slow transition band and a narrow rejection band. Recently, a novel LPF with high return loss using symmetrical topology was presented.[20]

In this work, a novel LPF with high out-of-band suppression uses a symmetrical modified T-shaped resonator. Compact, an extremely wide stopband from 2.38 to 65 GHz, high return loss (14.8 dB) in the passband and a simple topology are beneficial properties.

FILTER DESIGN

The design sequence of the T-shaped resonator is shown in ***Figure 1***, including the layouts of resonator 1, resonator 2 and resonator 3 and their simulated $|S_{21}|$ responses. Resonator 1 is composed of two rectangular open stubs and one high impedance stub connected to a narrow transmission line. Resonator 1 has a slow transition band, with high passband ripple. With low impedance stubs added (resonator 2), a relatively sharp transition band is achieved. For a sharper transition band and negligible passband ripple, a symmetrical topology (resonator 3) is used.

The inductance and capacitance of a high-low impedance lossless line (see ***Figure 2a***) are computed using Equations 1 and 2, as is the capacitance of an open-circuited stub (see ***Figure 2b***).[2] The inductance of the stub is negligible.

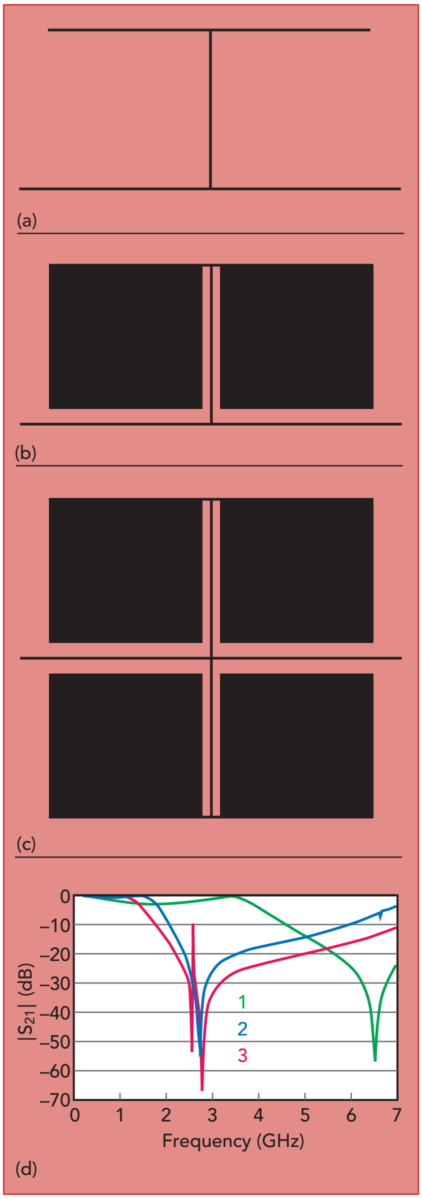

Fig. 1 Resonator layout: 1 (a), 2 (b), 3 (c) and simulated $|S_{21}|$ (d).

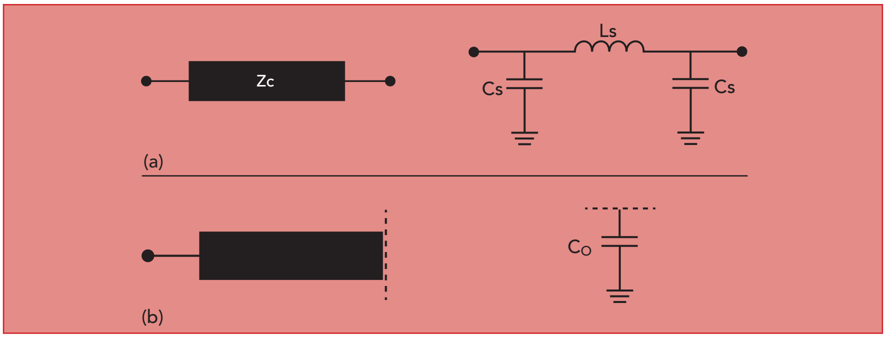

Fig. 2 Layout and L-C model of high-low impedance lossless line (a) and open-circuited stub (b).

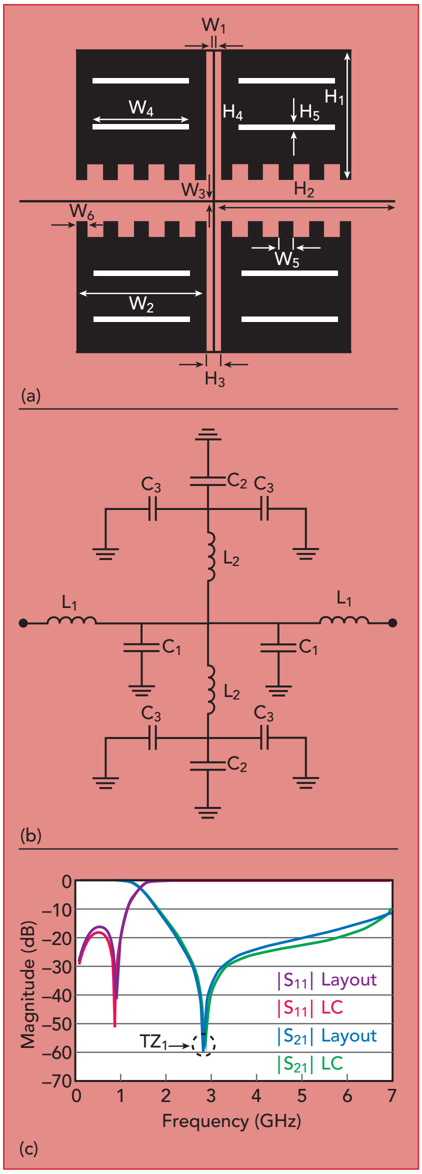

Fig. 3 Symmetrical modified T-shaped resonator layout (a), L-C model (b) and simulated responses (c).

TABLE 1				
L-C MODEL VALUES				
L_1 (nH)	L_2 (nH)	C_1 (pF)	C_2 (pF)	C_3 (pF)
6.634	2.377	0.298	0.088	0.6

$$l_S = \frac{1}{\omega}\times Z_C \times \sin\left(\frac{2\pi}{\lambda_g} l\right) \quad (1)$$

$$C_S = \frac{1}{\omega}\times \frac{1}{Z_C} \times \tan\left(\frac{\pi}{\lambda_g} l\right) \quad (2)$$

To develop the stopband, a symmetrical modified T-shaped resonator is used, as depicted in ***Figure 3a***, with the L-C model of the resonator shown in ***Figure 3b***. The inductances and capacitances of the transmission lines are designated as L_1 and C_1, respectively. L_2 and C_2 are the inductances and capacitances of the high impedance stubs, respectively. C_3 are the open-circuited low impedance stub capacitances. The inductances of the low impedance stubs are negligible. The L-C model values are found in ***Table 1***. EM and L-C simulation results (see ***Figure 3c***) show a transmission zero (TZ_1) at 2.83 GHz. The LPF is simulated with Advance Design System (ADS) software, assuming an RT-Duroid 5880 substrate (ε_r = 2.2, h = 0.381 mm and loss tangent = 0.0009). The physical dimensions of the resonator (in mm) are: H_1 = 3.3, H_2 = 8.75, H_3 = 0.42, H_4 = 3.55, H_5 = 0.137, W_1 = 0.1, W_2 = 3.43, W_3 = 0.1, W_4 = 2.46, W_5 = 0.38 and W_6 = 0.4. TZ_1 is calculated using the L-C model of ***Figure 3b***.

The ABCD matrix is defined for a two port network[1] as

$$\begin{bmatrix} V_1 \\ I_1 \end{bmatrix} = \begin{bmatrix} A & B \\ C & D \end{bmatrix} \begin{bmatrix} V_2 \\ I_2 \end{bmatrix} \quad (3)$$

where

$$A = \frac{V_1}{V_2}\Big|_{I_2=0} \quad B = \frac{V_1}{I_2}\Big|_{V_2=0} \quad (4)$$

$$C = \frac{I_1}{V_2}\Big|_{I_2=0} \quad D = \frac{I_1}{I_2}\Big|_{V_2=0} \quad (5)$$

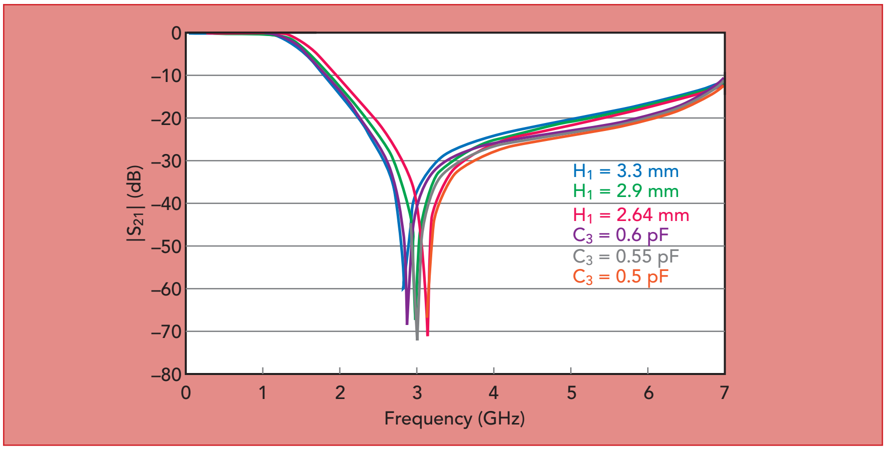

Fig. 4 Simulated TZ_1 of the symmetrical modified T-shaped resonator vs. H_1 and C_3.

TABLE 2

CUTOFF FREQUENCIES FOR DIFFERENT VALUES C_3 AND H_1

C_3 (pF)		0.6	0.55	0.5
H_1 (mm)		3.3	2.9	2.64
TZ_1 (GHz)	Simulated	2.872	2.998	3.124
	Calculated	2.876	2.995	3.129
	Error (%)	0.14	0.10	0.16
Cutoff Frequency (GHz)		1.423	1.486	1.550

According to Equations 4 and 5, the ABCD parameters of the proposed resonator are obtained from

$$A=\frac{S^4\left(8L_1L_2\left(2C_3+C_2\right)C_1\right)+S^2\left(8L_1C_1+L_2\left(2C_3+C_2\right)+2L_1\left(2C_3+C_2\right)\right)+1}{1+S^2L_2\left(2C_3+C_2\right)} \quad (6)$$

$$B=\frac{S^5\left(8L_1^2L_2\left(2C_3+C_2\right)C_1\right)+S^3\left(2L_1L_2\left(2C_3+C_2\right)+8C_1L_1^2+2L_1^2\left(2C_3+C_2\right)\right)+2SL_1}{1+S^2L_2\left(2C_3+C_2\right)} \quad (7)$$

$$C=\frac{S^3\left(8L_2\left(2C_3+C_2\right)C_1\right)+S\left(8C_1+2\left(2C_3+C_2\right)\right)}{1+S^2L_2\left(2C_3+C_2\right)} \quad (8)$$

$$D=\frac{S^4\left(8L_1L_2\left(2C_3+C_2\right)C_1\right)+S^2\left(8L_1C_1+L_2\left(2C_3+C_2\right)+2L_1\left(2C_3+C_2\right)\right)+1}{1+S^2L_2\left(2C_3+C_2\right)} \quad (9)$$

From the ABCD parameters, S_{21} is[1]

$$S_{21}=\frac{2}{A+B/Z_0+CZ_0+D} \quad (10)$$

The S_{21} of the proposed resonator is

$$S_{21}=\frac{\left(Z_0\left(L_2\left(2C_3+C_2\right)S^2+1\right)\right)}{\left(Z_0+L_1S\right)\left(\begin{array}{l}4C_1Z_0S+Z_0\left(2C_3+C_2\right)S+4C_1L_1S^2+L_1\left(2C_3+C_2\right)S^2+L_2\left(2C_3+C_2\right)S^2+\\4C_1L_1L_2\left(2C_3+C_2\right)S^4+4C_1L_2Z_0\left(2C_3+C_2\right)S^3+1\end{array}\right)} \quad (11)$$

The transmission zero (TZ_1) is extracted from Equation 11

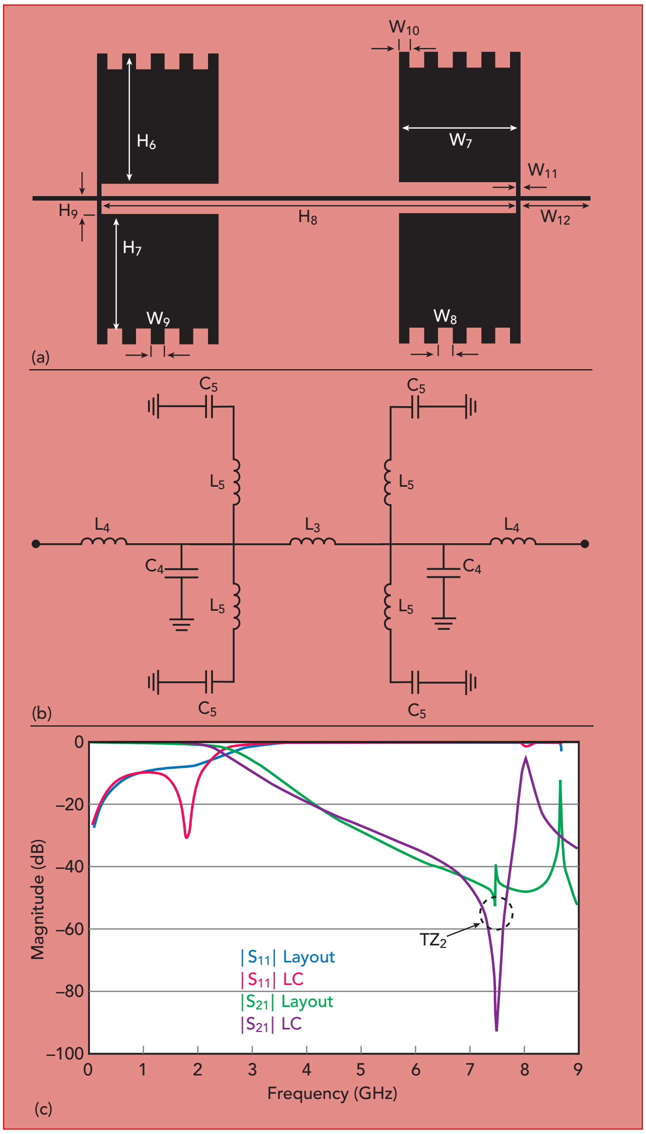

Fig. 5 Layout (a), L-C model (b) and simulated responses (c) of the SMF resonator.

TABLE 3

L-C MODEL VALUES

Parameters	L_4 (nH)	L_5 (nH)	C_4 (pF)	C_5 (pF)	L_3 (nH)
Values	0.470	3.000	2.325	0.150	4.193

$$TZ_1 = \frac{1}{2\pi\sqrt{(2C_3 + C_2)L_2}} \quad (12)$$

According to Equation 12, TZ_1 is a function of C_3, where C_3 is the capacitance of H_1. By reducing the length of H_1, TZ_1 and the cutoff frequency move higher in frequency (see ***Figure 4***). As a result, the cutoff frequency is adjusted by TZ_1. For a low cutoff frequency, TZ_1 is tuned to 2.872 GHz. Cutoff frequencies for different values of C_3 and H_1 are summarized in ***Table 2***.

Symmetrical Modified Flag-Shaped Resonator

Figure 5a shows the layout of the SMF resonator, and the L-C model is shown in ***Figure 5b***. Inductances and capacitances of the transmission line are L_3, L_4 and C_4, respectively. L_5 is the sum of the high impedance and low impedance stub inductances. C_5 is the open-circuited low impedance stub capacitance. The capacitances of the high impedance stubs are negligible. The L-C model values are presented in ***Table 3***. EM and L-C simulation results are shown in ***Figure 5c*** and agree with the model. The SMF resonator creates a transmission zero (TZ_2) at 7.6 GHz. The physical dimensions of this structure (in mm) are: W_7 = 3, W_8 = 0.29, W_9 = 0.41, W_{10} = 0.25, W_{11} = 0.1, W_{12} = 3.25, H_6 = 3.24, H_7 = 2.97, H_8 =13.61 and H_9 = 0.37.

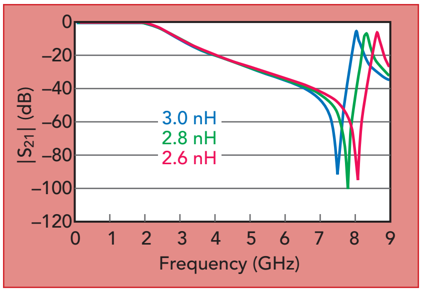

Fig. 6 Simulated $|S_{21}|$ of the SMF resonator vs. L_5.

From Equation 10, the S_{21} of the SMF resonator is calculated as

$$S_{21} = \frac{\left(2Z_0\left(C_5L_5S^2+1\right)^2\right)}{\left(\left(1+\left(2C_5Z_0+4C_4Z_0\right)S+\left(C_5L_5+2C_5L_4+4C_4L_4\right)S^2+4Z_0C_5C_4L_5S^3+4C_5C_4L_4L_5S^4\right)\left(2Z_0+\left(L_3+2L_4\right)S+\left(C_5L_5L_3+2C_5L_4L_3+4C_4L_4L_3+2C_5L_4L_5\right)S^3+\left(2C_5Z_0L_3+4C_4Z_0L_3+2C_5Z_0L_5\right)S^2+4C_5C_4L_5L_3Z_0S^4+4C_5C_4L_5L_4L_3S^5\right)\right)} \quad (13)$$

TZ_2 is extracted from Equation 13

$$TZ_2 = \frac{1}{2\pi\sqrt{\left(C_5L_5\right)}} \quad (14)$$

According to Equation 14, TZ_2 is tuned by L_5 (see ***Figure 6***).

To have a wide stopband, the symmetrical modified T-shaped resonator and SMF resonator are combined, as shown in ***Figure 7a***. The EM simulation of the combined resonator is shown in ***Figure 7b***.

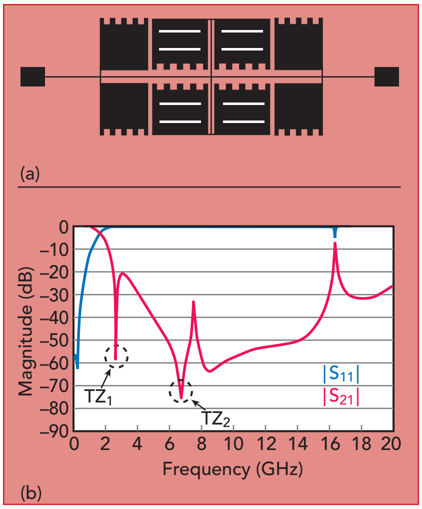

Fig. 7 Layout (a) and simulated responses (b) of the combined resonator.

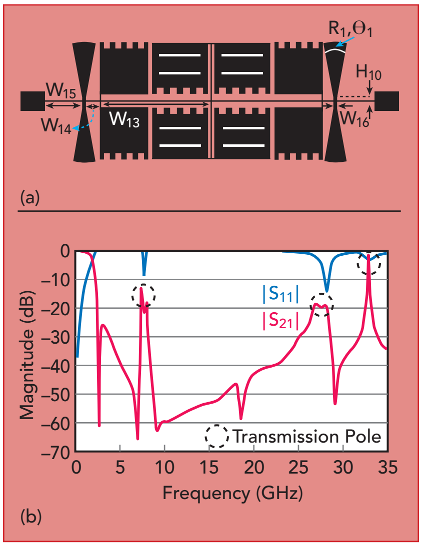

Fig. 8 Layout (a) and simulated responses (b) of the primitive LPF.

This structure has two transmission zeros (TZ_1 and TZ_2) at 2.7 and 6.6 GHz, respectively.

Primitive and Improved LPF

To increase the transition band sharpness, four radial stubs are added to the combined resonator (see ***Figure 8***). The primitive LPF has a sharp transition band; however, the stopband is narrow. The physical dimensions of this structure (in mm) are: W_{13} = 6.73, W_{14} = 0.88, W_{15} = 2.33, W_{16} = 0.64, H_{10} = 0.25, R_1 = 4.06 and θ_1 = 20 degrees.

According to Figure 8b, the stopband is limited by transmission poles. To achieve a wider stopband, four open-circuited stubs are added as suppressing elements, producing several transmission zeros (see ***Figure 9***). The circuit layout and EM simulation are shown in ***Figures 10a*** and ***10b***, respectively. This improved LPF has a high return loss, and the stopband is extended to more than 35 GHz. The physical dimensions (in mm) are: W_{17} = 1.5, W_{18} = 0.1, W_{19} = 1.52, H_{11} = 2.79 and H_{12} = 0.76.

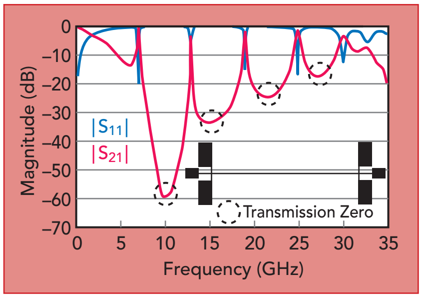

Fig. 9 Simulated transmission zeros from four additional open-circuited stubs.

The final filter design employs four semi-circular stubs (see ***Figure 11***). It has an ultra-wide stopband (2.38 to 65 GHz) with high attenuation (24 dB) up to the 34^{th} harmonic. The physical dimensions (in mm) are: W_{19} = 0.69, W_m = 1.17, H_m = 1.5, R_2 = 0.25 and θ_2 = 180 degrees.

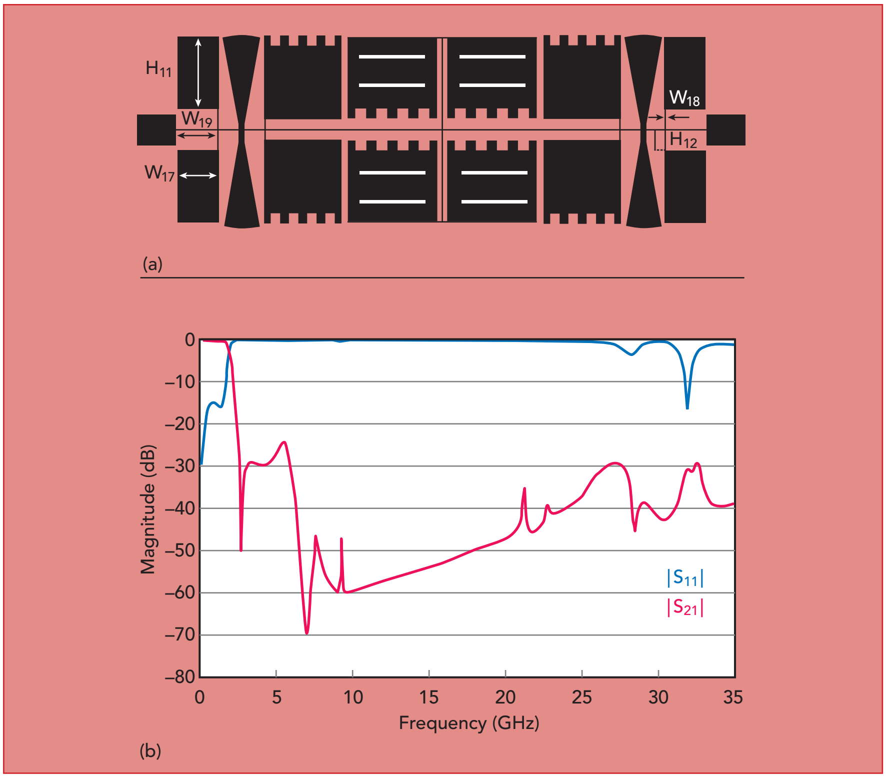

Fig. 10 Layout (a) and EM simulation (b) of the improved LPF.

SIMULATION AND MEASUREMENT

The LPF was simulated using ADS software, fabricated on RT-Duroid 5880 (ε_r = 2.2, h = 0.381 mm, loss tangent = 0.0009) and tested with a Keysight 8757A network analyzer (see Figure 11c). It exhibits an ultra-wide stopband from 2.38 to 65 GHz, with 24 dB suppression up to the 34th harmonic. The final filter has a 3 dB cutoff frequency of 1.89 GHz and high return loss (14.8 dB) in the passband. Overall dimensions are only 17.7 mm × 7.5 mm (0.153λ_g × 0.065λ_g). With these features, it is useful for wireless applications, according to the specifications listed by Hayati et al.[17] This filter and other reported works are compared in ***Table 4***. This filter has the widest stopband, the smallest size and the highest FOM.

In Table 4, the transition band

TABLE 4

LPF PERFORMANCE COMPARISON

Reference	ξ	RSB	SF	NCS	AF	Harmonic Suppression	FOM
3	94	1.261	2	0.243 × 0.169	1	4	5.772
4	135	1.64	2.2	0.160 × 0.200	1	11	15.221
5	159	1.146	2	-	2	3	-
6	48.57	1.5	2	0.160 × 0.080	2	9	11.383
13	95.5	1.359	2	0.540 × 0.480	2	5	500.5
14	78	1.6	2	0.160 × 0.100	2	15	7.800
15	-	1.125	2	0.450 × 0.350	2	5	-
16	29.3	1.53	2.4	0.0075	2	10	7.172
17	84.69	1.51	2	0.143 × 0.156	1	7	11.625
18	58.6	1.43	2.5	0.220 × 0.110	1	7	8.657
19	52.8	1.529	2	0.081 × 0.113	1	10	17.640
20	97.4	1.87	2	0.100 × 0.190	1	29	19.172
This Work	72	1.86	2.4	0.153 × 0.065	1	34	32.465

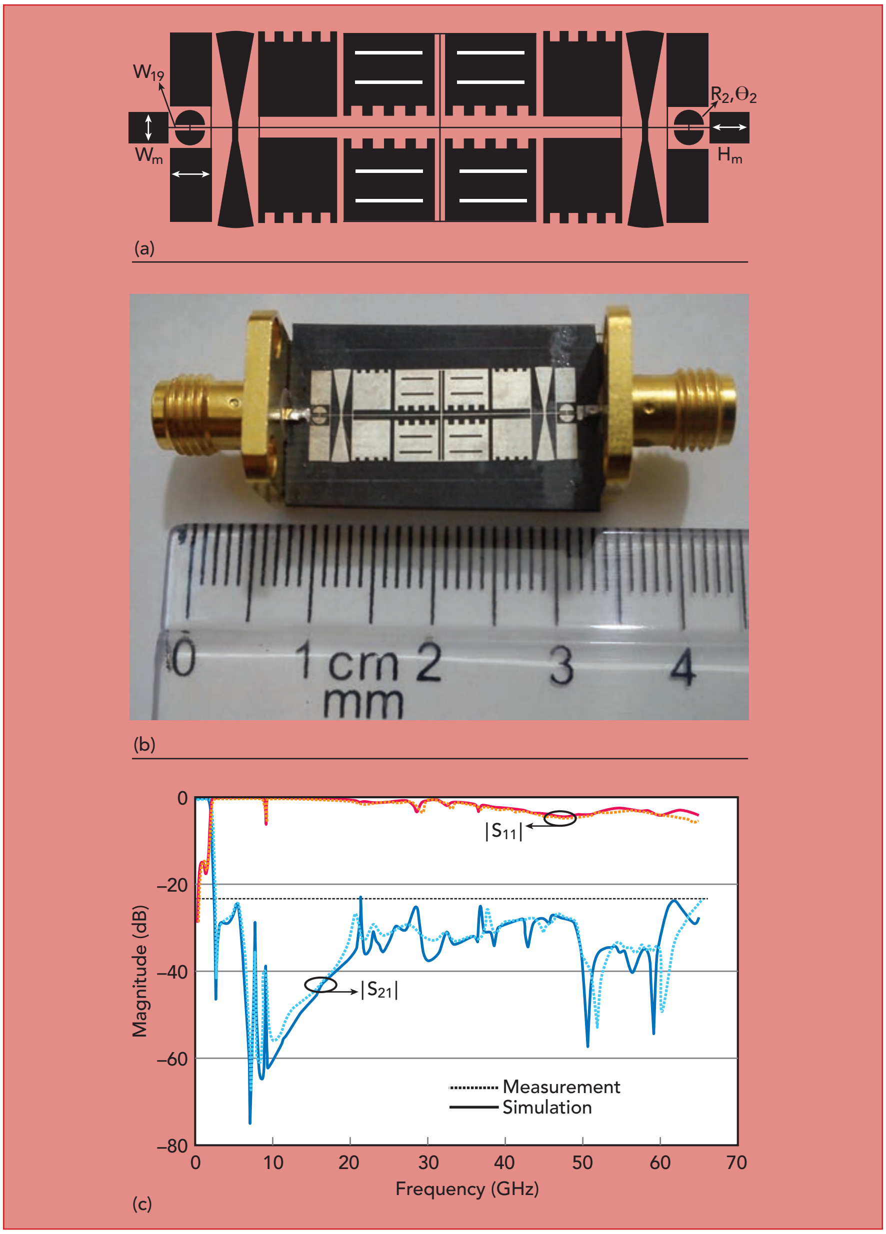

Fig. 11 Layout (a), fabricated filter (b) and simulated vs. measured performance (c) of the completed LPF.

sharpness (ξ) is defined as

$$\xi = \frac{\alpha_{max} - \alpha_{min}}{f_s - f_c} (dB/GHz) \qquad (15)$$

where α_{min} and α_{max} are suppression points of –3 and –40 dB, respectively. f_s is the frequency corresponding to α_{max}, and f_c is the frequency corresponding to α_{min}. The relative stopband bandwidth (RSB) is

$$RSB = \frac{\text{stopband bandwidth}}{\text{stopband center frequency}} \qquad (16)$$

The suppressing factor (SF) is

$$SF = \frac{\text{suppression level}}{10} \qquad (17)$$

The normalized circuit size (NCS) is

$$NCS = \frac{\text{physical dimensions (length x width)}}{\lambda_g^2} \qquad (18)$$

For 2D and 3D circuits, the architecture factor (AF) is defined as 1 and 2, respectively, and the FOM is

$$FOM = \frac{RSB \times \xi \times SF}{AF \times NCS} \qquad (19)$$

CONCLUSION

An ultra-wide rejection band LPF using symmetrical modified T-shaped and flag-shaped resonators has been manufactured and tested. The stopband width is 62.62 GHz (from 2.38 up to 65 GHz) with more than 24 dB suppression. This configuration has the best performance for harmonic suppression (from the second to 34th) and the smallest size compared to other recent work.■

References

1. D. M. Pozar, *Microwave Engineering*, Third Edition, Wiley, New York, 2005.
2. J. S. Hong and M. J. Lancaster, *Microstrip Filters for RF/Microwave Applications*, Wiley, New York, 2004.
3. P. M. Raphika, P. Abdulla and P. M. Jasmine, "Planar Elliptic Function Lowpass Filter with Sharp Roll-Off and Wide Stopband," *Microwave and Optical Technology Letters*, Vol. 58, No. 1, January 2016, pp. 133–136.
4. Gh. Karimi, A. Lalbakhsh, Kh. Dehghani and H. Siahkamari, "Analysis of Novel Approach to Design of Ultra-Wide Stopband Microstrip Lowpass Filter Using Modified U-Shaped Resonator," *ETRI Journal*, Vol. 37, No. 5, October 2015, pp. 945–950.
5. P. Zhang and M. Li, "A Novel Sharp Roll-Off Microstrip Lowpass Filter with Improved Stopband and Compact Size Using Dual-Plane Structure," *Microwave and Optical Technology Letters*, Vol. 58, No. 5, May 2016, pp. 1085–1088.
6. A. K. Verma, N. Chaudhari and A. Kumar, "Improved Performance Step Impedance Lowpass Filter," *International Journal of Electronics and Communications (AEÜ)*, Vol. 67, March 2013, pp. 761–770.
7. M. Kufa and Z. Raida, "Lowpass Filter with Reduced Fractal Defected Ground Structure," *IET Electronics Letters*, Vol. 49, No. 3, January 2013, pp. 199–201.
8. H. R. Khakzad, S. H. Sedighy and M. K. Amirhosseini, "Design of Compact SITLs Low Pass Filter by Using Invasive Weed Optimization (IWO) Technique," *Applied Computational Electromagnetics Society Journal*, Vol. 28, No. 3, March 2013, pp. 228–233.
9. K. Li, M. Zhao, Y. Fan, Z. Zhu and W. Cui, "Compact Lowpass Filter with Wide Stopband Using Novel Double-Folded SCMRC Structure with Parallel Open-Ended Stub," *Progress In Electromagnetics Research Letters*, Vol. 36, November 2012, pp. 77–86.
10. S. S. Karthikeyan and R. S. Kshetrimayum, "Compact and Wide Stopband Lowpass Filter Using Open Complementary Split Ring Resonator and Defected Ground Structure," *Radioengineering*, Vol. 24, No. 3, September 2015, pp. 708–711.
11. A. Boutejdar, A. Omar and E. Burte, "High-Performance Wide Stop Band Lowpass Filter Using a Vertically Coupled DGS-DMS-Resonators and Interdigital Capacitor," *Microwave and Optical Technology Letters*, Vol. 56, No. 1, January 2014, pp. 87–91.
12. M. Xiao, G. Sun and X. Li, "A Lowpass Filter with Compact Size and Sharp Roll-Off," *IEEE Microwave and Wireless Components Letters*, Vol. 25, No. 12, December 2015, pp. 790–792.
13. Y. Zhang, L. Jin and L. Li, "Design of LPF Using Hi-Lo Interdigital DGS Slot," *Institute of Electronics, Information and Communication Engineers Electronics Express*, Vol. 13, No. 9, March 2016, pp. 1–6.
14. F. C. Chen, H. T. Hu, J. M. Qiu and Q. X. Chu, "High-Selectivity Lowpass Filters with Ultrawide Stopband Based on Defected Ground Structures," *IEEE Transactions on Components, Packaging and Manufacturing Technology*, Vol. 5, No. 9, September 2015, pp. 1313–1319.
15. A. Boutejdar, "Design of Broad-Stop Band Low Pass Filter Using a Novel QUASI-YAGI-DGS-Resonators and Metal Box-Technique," *Microwave and Optical Technology Letters*, Vol. 56, No. 3, March 2014, pp. 523–528.
16. S. Majidifar, "Design of High Performance Miniaturized Lowpass Filter Using New Approach of Modeling," *Applied Computational Electromagnetics Society Journal*, Vol. 31, No. 1, January 2016, pp. 52–57.
17. M. Hayati, M. Gholami, H. S. Vaziri and T. Zaree, "Design of Microstrip Lowpass Filter with Wide Stopband and Sharp Roll-Off Using Hexangular Shaped Resonator," *IET Electronics Letters*, Vol. 51, No. 1, January 2015, pp. 69–71.
18. M. Mirzaee and B. S. Virdee, "Realisation of Highly Compact Planar Lowpass Filter for UWB RFID Applications," *IET Electronics Letters*, Vol. 49, No. 22, October 2013, pp. 1396–1398.
19. S. Liu, J. Xu and Z. Xu, "Compact Lowpass Filter with Wide Stopband Using Stepped Impedance Hairpin Units," *IET Electronics Letters*, Vol. 51, No. 1, January 2015, pp. 67–69.
20. S. Roshani, "A Compact Microstrip Low-Pass Filter with Ultra Wide Stopband Using Compact Microstrip Resonant Cells," *International Journal of Microwave and Wireless Technologies*, September 2016, pp. 1–5.

Amirhossein Ghaderi *received his B.S. degree in electronics engineering in 2015 from Islamic Azad University (with honors), and is currently working toward his M.S. degree. His current research interests include microwave passive circuits and RF integrated circuit design.*

Saeed Roshani *received his B.S. degree in electrical engineering from Razi University in 2008, his M.S. degree in electrical engineering from Shahed University in 2011 and his Ph.D. in electrical engineering from Razi University in 2015. He is currently an assistant professor in the Department of Electrical Engineering at Islamic Azad University. His research interests include microwave and mmWave devices and circuits, as well as low power and small size integrated circuit design.*


MEETING DEMAND FOR CONNECTIVITY
ANYTIME, ANYWHERE!

Oscilloscope with 110 GHz Front-End Eliminates Frequency Interleaving

Keysight Technologies Inc.
Santa Rosa, Calif.

Technologies like terabit optical data communications, next-generation digital bus standards, high speed I/O and new wireless standards are demanding higher bandwidth and more accurate measurements in multi-channel test systems. Similarly, emerging mmWave applications are demanding wider bandwidths. For example, 802.11ay uses about 4 GHz of bandwidth at 60 GHz. High signal integrity is needed for measurements such as error vector magnitude (EVM), especially over multi-GHz signal bandwidths with high-order modulation.

To address these needs, Keysight has designed a 110 GHz oscilloscope with custom ASICs to achieve more signal integrity than any other oscilloscope in its class. The technology has been leveraged and optimized down to 13 GHz models, providing extreme signal integrity in a wide range of bandwidth options, enabling high speed digital design and wireless. Keysight's Infiniium UXR-Series oscilloscopes are the first oscilloscopes to achieve greater than 40 GHz bandwidth without frequency interleaving, which adds noise and distortion to the signal being tested.

JOURNEY OF A SIGNAL

To understand the technology within Keysight's new oscilloscopes, follow the signal flow through a UXR (see ***Figure 1***). The signal enters through the channel, a challenge when developing a high bandwidth oscilloscope, as reflections in the channel cause measurement inaccuracy. The 33 GHz and below models use robust 3.5 mm connectors (only accurate below 40 GHz), Keysight's traditional AutoProbe II interface to support traditional SMA connections and Infiniium probes that may already be on the lab bench. The 40 to 70 GHz models use 1.85 mm connector technology, which is a little more delicate but extends the bandwidth. To support 80 GHz and above, Keysight uses 1 mm connectors, the industry standard for mmWave technology to 110 GHz. While these connectors are traditionally more fragile like all 1 mm connectors, they require adaptors to connect to traditional probes, but users testing at these frequencies will likely connect cables directly to the 1 mm input to maintain signal integrity, rather than using hand-held probes.

From the front-end connector, the signal flows to a mechanical attenuator and then into the preamplifier, the first component of the front-end module. While this may sound simple, it is one of the key distinctions between UXR oscilloscopes and other high bandwidth oscilloscopes. The front-end module consists of a proprietary Keysight InP chipset protected from noise and interference with a Faraday cage (see ***Figure 2***), custom designed to handle 110 GHz signals while keeping noise to a minimum. This is a key distinction, because the hardware can support the full bandwidth of the oscilloscope. Other high bandwidth oscilloscopes must use frequency interleaving to achieve the full bandwidth because the IC technology within the oscilloscopes is limited. Frequency interleaving can double—even triple—an oscilloscope's bandwidth beyond the raw capability of the chipset. The tradeoff is additional circuitry, adding significant noise and distortion which are amplified by the preamp. With interleaving, digital signal processing stitches the signal components

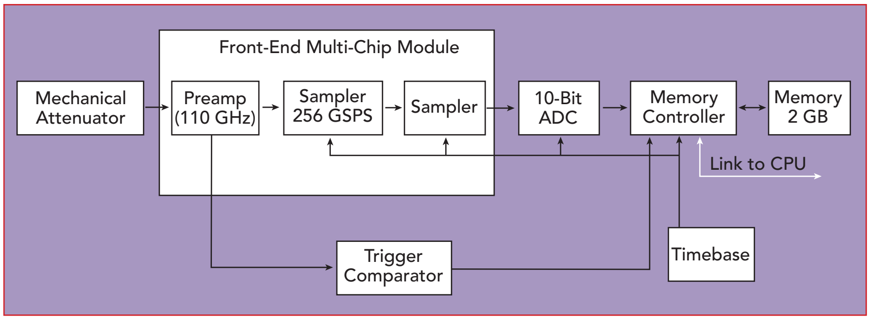

Fig. 1 Simplified block diagram of the UXR oscilloscope.

back together, which may add more noise to the signal. This all happens in the front-end of the oscilloscope before data acquisition. Using a preamp with a frequency range to 110 GHz without attenuation, the UXR foregoes frequency interleaving, preserving the signal under test. One of the trade-offs to designing hardware to support higher bandwidth without frequency interleaving is time-to-market. However, the improvement in performance is well worth the design effort.

After the attenuator and the preamp, the signal flows to a 256 GSPS sampler (also designed uniquely for the UXR using InP) and a trigger comparator. The 256 GSPS high speed sampler "slows" the signal for the rest of the system, using a process called time interleaving. Unlike frequency interleaving, time interleaving is carefully controlled with the oscillator board. Signal acquisition uses an array of 10-bit analog-to-digital converters (ADC), with each ADC operating at 64 GSPS. 10-bit ADCs provide 4× the vertical resolution of 8-bit ADCs. After being converted to digital, the signal is sent to Keysight's new memory controller reading and writing to a modern 2.5D memory storage device with 2 GB of deep memory. The trigger comparator sends trigger information to the memory controller, which enables filtering, de-embedding, triggering and other advanced hardware features. It even has a bus for plotting the waveform, reducing the work done in the FPGA to speed the performance of the oscilloscope. The memory controller sends this data to the FPGA, which communicates to the CPU over PCI Express to display the signal and measurements on the screen of the oscilloscope. Each 110 GHz channel has its own acquisition board, ensuring the full bandwidth and memory depth on each channel.

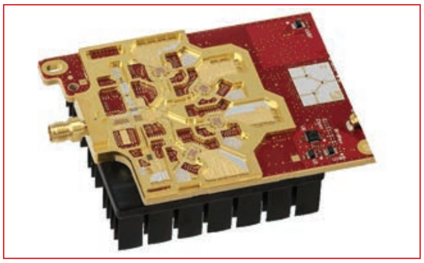

Fig. 2 The 110 GHz front-end module.

This oscilloscope design has enabled new industry "bests." The UXR provides:

- Four full bandwidth channels with up to 110 GHz of bandwidth.
- As low as 210 µV rms noise at 10 mV/division.
- Only 25 fs rms of intrinsic jitter at 1 µs/div.
- Less than an additional 10 fs rms of inter-channel intrinsic jitter.
- Up to 6.8 effective bits.

WHY DOES THIS MATTER?

For emerging mmWave applications to 110 GHz, high performance digital oscilloscope technology offers an additional tool to gain insight when analyzing wideband mmWave signals. Directly digitizing mmWave signals, then post-processing them with application software enable direct measurement of wideband mmWave signals, complementing the traditional approach using an external down-converter with a lower bandwidth oscilloscope. The UXR's accuracy—up to 6.8 effective bits—enables wideband EVM measurements of higher-order modulation signals, such as 802.11ay.

As anyone in the high speed digital industry knows, test margins are decreasing as new generations of technology become the standard. Design cycles are shorter, and compliance is more difficult as the limits of existing hardware are reached. Previously, there was so much time between bit transfers that set up and rise time tests were only required to pass specification. Now, passing compliance requires pre- and post-channel equalization as well as strict mask test validation. Millivolts of noise can make the difference between passing or failing. The UXR's signal integrity reduces the risk of failing from excessive oscilloscope noise and jitter. With a noise floor as low as 210 µVrms at 10 mV/division and only 25 fs of intrinsic jitter, signal eyes will be wider, leading to more confidence passing compliance tests.

In terabit and optical research, next-generation technology breakthroughs have been prohibited by limited test equipment. Higher modulation standards require measurement systems with extreme signal integrity, high bandwidth and multiple channels to decipher complete coherent receiver designs. Daisy chained single channel instruments can be too costly and highly inaccurate. Inter-channel jitter between daisy chained measurement devices can impede the ability to clearly view signals. Four high bandwidth channels with only femptoseconds of inter-channel intrinsic jitter enable optical measurements not previously possible.

The UXR was designed piece by piece, with the intention to enable research in various applications with new industry-best specifications. Keysight's new technology blocks enable the UXR to revert to traditional, clean oscilloscope design practices without frequency interleaving, increasing the signal fidelity in every category.

Keysight Technologies Inc.
Santa Rosa, Calif.
www.keysight.com/find/UXR

Content is copyright protected and provided for personal use only - not for reproduction or retransmission.
For reprints please contact the Publisher.

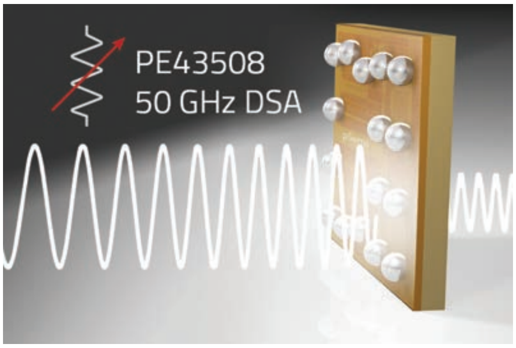

9 kHz to 50 GHz Single-Chip SOI Digital Step Attenuator

pSemi Corp.
San Diego, Calif.

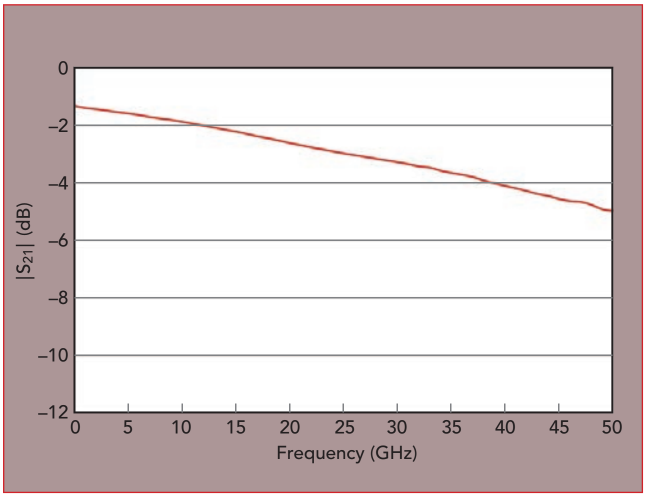

▲ Fig. 1 **PE43508 $|S_{21}|$ vs. frequency**

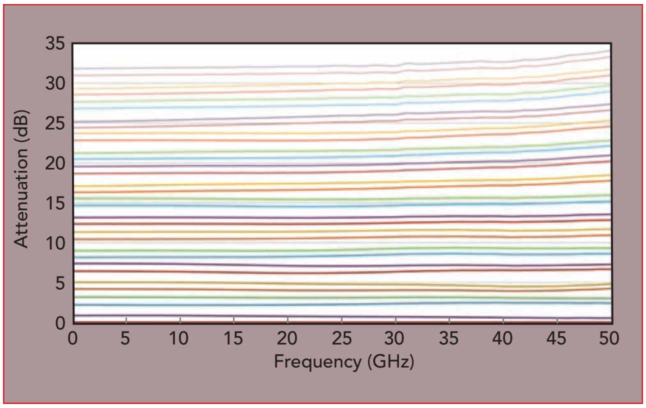

▲ Fig. 2 **Normalized attenuation states vs. frequency.**

With the rollout of 5G, the mobile industry will expand beyond sub-6 GHz to support mmWave frequencies. mmWave signals often suffer increased attenuation passing through walls and structures, and semiconductor device technologies are inherently frequency-limited, creating both system design and implementation difficulties. Overcoming these hurdles requires technologies like beamforming and massive MIMO, backed by commercially viable and reliable passive components tailored to the high frequency signal chain.

To serve the evolving mmWave demands of 5G, pSemi (formerly Peregrine Semiconductor) has introduced several high frequency components, including a 40 GHz switch (PE42524) and two 60 GHz switches (PE42525 and PE426525). The newest product in this portfolio is a 50 GHz digital step attenuator (DSA): PE43508. These monolithic ICs are ideal for applications, such as test and measurement and 5G wireless infrastructure, and can be used in more traditional high frequency applications, such as very small aperture satellite terminals.

pSemi's mmWave switches and new DSA are manufactured on the company's UltraCMOS® platform, a patented variation of silicon on insulator (SOI) technology, and contain industry-leading innovations in RF SOI switch design. The PE43508 DSA is based on the 300 mm UltraCMOS 12 tech-

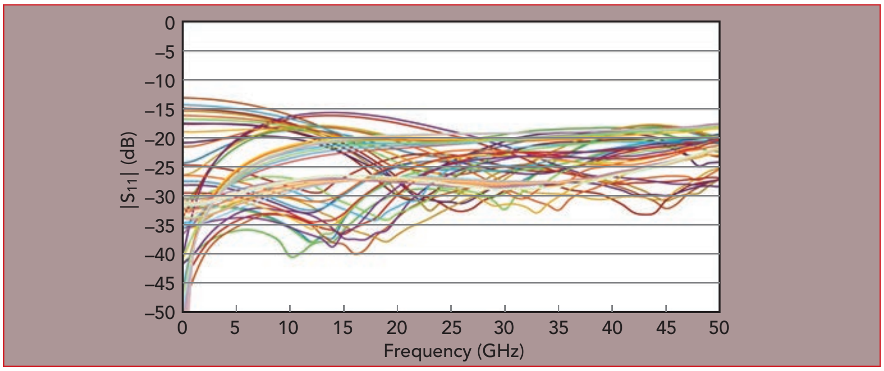

▲Fig. 3 $|S_{11}|$ vs. frequency.

nology platform that delivers R_{on}-C_{off}, a key figure of merit for RF switches, of 80 fs, surpassing the SOI competition.

Traditionally, GaAs solutions have ruled the high frequency domain, but the pSemi mmWave portfolio proves that RF SOI can deliver high performing and reliable solutions at mmWave frequencies. Introduced in 2015, the PE42524 was the industry's first RF SOI switch to operate up to 40 GHz, and it offered design engineers the first alternative to GaAs switches at K- and Ka-Band. The PE42525 and PE426525 surpassed this milestone by supporting a wider frequency range from 9 kHz to 60 GHz, delivering exceptional performance in all key RF parameters and attaining a fast switching speed of only 8 ns.

DSA FEATURES

Now, pSemi has broadened its mmWave portfolio with the introduction of the PE43508, the industry's first single-chip DSA to support the 9 kHz to 50 GHz frequency range. Single-chip DSAs are a product category pSemi first introduced in 2004—since proven to be more optimal in RF performance than discrete components. In an RF chain, a DSA controls the signal amplitude by setting the desired attenuation to deliver the proper power level to the next component in the signal chain. The goal is to control the signal level accurately, with minimal attenuation error.

The PE43508 is a 6-bit, 50 Ω DSA with a 31.5 dB attenuation range in 0.5 and 1 dB steps. It features low insertion loss, low attenuation error and good return loss, and it maintains a monotonic response across the entire frequency range. ***Figure 1*** shows the 0 dB attenuation (reference state) insertion loss through 50 GHz at room temperature. ***Figure 2*** shows the attenuation versus frequency for each 1 dB step, where the attenuation is normalized to the reference state (i.e., the measured insertion loss minus the loss of the reference state at the same frequency). ***Figure 3*** plots $|S_{11}|$ for all attenuation states, and ***Figure 4*** shows the attenuation error for all states.

Leveraging pSemi's patented HaRP™ technology enhancements, the DSA delivers high-power handling and high linearity. At room temperature, the PE43508 has a maximum CW input power of +28 dBm from 1 to 50 GHz, with a typical input IP3 of +51 dBm at 16 GHz and a 1 dB compression point of +32 dBm at 50 GHz. Other features are a fast switching time of 350 ns, with glitch-safe attenuation state transitions—meaning no increased power spike during a state transition. The PE43508 has an extended temperature range from −40°C to +105°C, an HBM ESD rating of 1 kV and an easy-to-use digital control interface supporting both serial addressable and parallel programming. The DSA supports 1.8 V control signals and has an optional V_{SS_EXT} bypass mode to improve spurious performance.

Offered as a flip chip die, the PE43508 uses lead-free solder ball technology for the signal and ground interconnects. Solder reflow profiles common to lead-free surface-mount assembly can be used to achieve uniform and reliable attachment. Since the material composition of the DSA is similar to alumina (Al_2O_3), the coefficients of thermal expansion for the two materials are similar, 5 to 7 ppm/°C (or 5 to 7 × 10^{-6}/°K), ensuring a mechanically reliable and robust interconnect. The PE43508 is configured with a 500 μm minimum ball pitch. While thin film technologies can readily meet the line width and spacing critical dimensions (CD) of 100 μm or less, thick film and PCB processes generally require far less stringent CDs to achieve reasonable and consistent manufacturing yields. The comparatively wide 500 μm ball pitch of the PE43508 is intended to support the larger CD requirements and enable assembly of the die directly to RF PCB boards. pSemi has written an application note, available on their website, discussing the recommended landing patterns and assembly process for obtaining peak performance with alumina and PCB assemblies.

Volume production quantities, evaluation kits and samples of the PE43508 are available. In 1000 quantity orders, the PE43508 is priced at $50.

pSemi Corp.
San Diego, Calif.
www.psemi.com
sales@psemi.com

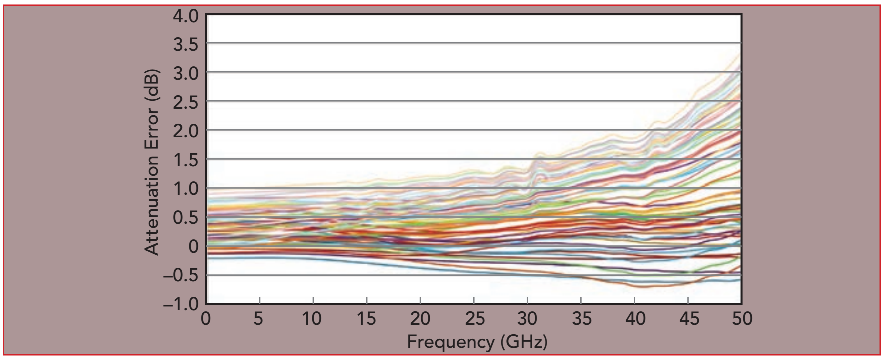

Fig. 4 Attenuation error vs. frequency.

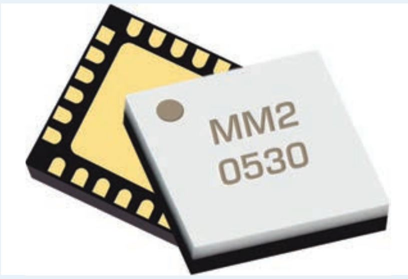

Mixer Vanquishes Up-Converted Spurs in Difficult Frequency Plans

The MM2-0530SM from Marki Microwave is the most versatile, high performance, surface mount mixer for X- through K-Band ever produced. It is the world's first truly triple balanced MMIC mixer covering these bands in one device. The MM2-0530SM provides exceptional spurious cancellation and port-to-port isolation for RF and LO frequencies from 5 to 30 GHz and IF frequencies from 2 to 20 GHz. These massively overlapping bands, along with outstanding performance, make the mixer ideal for the difficult frequency plans encountered in test & measurement, electronic warfare and synthesizer/LO generator applications.

There are three major categories of passive diode mixers: single balanced, double balanced and triple balanced, with each additional layer of balance increasing design complexity. The IF balun layout of the MM2-0530SM proved to be the most challenging Marki has released. Another major challenge arose from the overlapping LO, RF and IF bands, meaning that LO-to-IF and RF-to-IF isolation are extremely important. The MM2-0530SM offers LO-to-IF and RF-to-IF isolation of 25 to 45 dB, significantly better than competing double balanced mixers with IF isolation of 15 to 30 dB. This translates to dramatically improved IF harmonics and spurs. For example, with a 0 dBm input signal, the MM2-0530SM has typical third IF harmonic suppression of 90 dBc, compared to 51 dBc for a good double balanced mixer.

The MM2-0530SM is available with two diode levels, tailored to the desired tradeoff between linearity and LO drive power. The MM2-0530HSM offers +28 dBm input IP3 and +19 dBm P1dB with an LO drive between 16 and 22 dBm, while the MM2-0530LSM has +19 dBm input IP3 and +9 dBm P1dB and requires only 9 to 17 dBm LO drive. Datasheets, application notes and pricing are available from the website.

Marki Microwave Inc.
Morgan Hill, Calif.
www.markimicrowave.com

55 MHz to 15 GHz, Single Chip Synthesizer Delivers Low Phase Noise, Spurs

To support a diverse range of applications in aerospace and defense, wireless infrastructure, microwave point-to-point links, test & measurement and satellite terminals, Analog Devices has developed a wideband synthesizer with an integrated VCO that delivers excellent performance and flexibility. Using a fractional-N architecture, the ADF5610 generates frequencies from 57 MHz to 14.6 GHz and achieves the lowest phase noise of a single chip synthesizer. Compared to alternative solutions that use multiple, narrowband, GaAs VCOs and PLLs, the ADF5610 uses 50 percent less power, fits in a smaller footprint and offers a simpler board design, with the benefits of a lower cost bill of materials and reduced time-to-market.

Fabricated on ADI's proprietary, SiGe BiCMOS process, the ADF5610 provides RF output power of +6 dBm, high system modulation bandwidth and very low BIT error rates. It has industry-leading VCO phase noise of −114 dBc/Hz at 100 kHz offset and −165 dBc/Hz at 100 MHz offset at 10 GHz, with a low normalized phase noise floor of −232 dBc/Hz. The integrated PLL provides fast frequency hopping and lock times below 30 μs with the appropriate loop filter. Integer boundary spurious levels are typically better than −45 dBc in-band.

The synthesizer is programmable using control software and the integrated SPI interface, compatible with 1.8 V logic and contains hardware and software power-down modes. The ADF5610 is biased with separate +3.3 V supplies for the analog, digital and charge pump circuitry and a +5 V supply for the VCO. Packaged in a 7 mm x 7 mm LFCSP, the IC operates from −40°C to +85°C.

Design-in is easy, fully supported by Analog Devices' comprehensive, easy-to-use PLL synthesizer design and simulation tool, the ADIsimPLL™. Using ADIsimPLL, designers can assess phase noise, lock time, jitter and other parameters.

VENDORVIEW

Analog Devices Inc.
Norwood, Mass.
www.analog.com

Scalable Coaxial Components Reach 110 GHz

Anritsu has extended its component offering by introducing new W1 coaxial components. The W1 family expands Anritsu's existing line of passive components with attenuators, power dividers, power splitters and a directional coupler covering up to 110 GHz. These metrology-grade components enable the best performance and repeatability for mmWave measurements.

These new components provide an alternative to waveguide for broadband and mmWave measurements. For example, the test setup for intermodulation distortion (IMD) requires a power divider/combiner to combine two tones. Using a 110 GHz coaxial power divider with a native W1 interface, the user avoids waveguide, reducing interconnects and measurement uncertainty. Depending on the geometry between the interfaces to the device being tested, waveguide geometries can be complex. This is not a problem with a coaxial power divider, whether using an inline or 90 degree connector. Another benefit of using a coaxial power divider covering DC to 110 GHz: it is not band limited.

Designing broadband, mmWave component solutions poses several design challenges when achieving the tight mechanical and electrical specifications. Substrate behavior must be accounted for, as well as attaining the tight mechanical tolerances when manufacturing W1 connectors. Anritsu addresses both with its on-site thin film lab and machine shop capable of precision machining.

Anritsu's new W1 coaxial components ensure better measurements by providing metrology-grade solutions, delivering a coaxial interface for broadband and mmWave systems, reducing complexity and increasing performance repeatability.

VENDORVIEW

Anritsu
Morgan Hill, Calif.
www.anritsu.com/en-US/components-accessories

Virtual Model Inspector for 3D EM Solver

The Virtual Model Inspector (VMI) from IMST is a new application for the HTC VIVE virtual reality system. It allows the user to move freely through scaled version of electromagnetic (EM) structures, providing a fascinating experience of inspecting the structure's geometry from all perspectives. This enables an unprecedented layout check and design verification of simulation models, a crucial step before going into production. In addition to the geometry, the VMI also visualizes the 3D simulation results, e.g., EM fields in different planes. The VMI will be offered as an add-on module for the 3D EM solver EMPIRE XPU 7.7. Every simulation model in EMPIRE can be experienced virtually with the VMI software.

EMPIRE XPU helps designers with demanding RF design challenges, such as antennas, passive circuits, packages, waveguide and finding EMC/EMI problems. Because of IMST's innovative XPU technology, EMPIRE XPU enables accurate, full, 3D EM modeling of structures larger and more complex than handled by conventional EM simulation tools. The XPU technology enables full parallel computation on modern PCs and yields higher simulation speed than using GPU supercomputers. Just-in-time code generation and caching save 50 percent of the memory used compared to other finite-difference time-domain simulators.

This fast and highly efficient simulation technique combined with the VMI enables design cycles to be accelerated, particularly for challenging applications like 5G and 77 GHz automotive radar.

IMST GmbH
Kamp-Lintfort, Germany
www.imst.com

Unlock All Your RF & EMC Testing Needs

VENDORVIEW

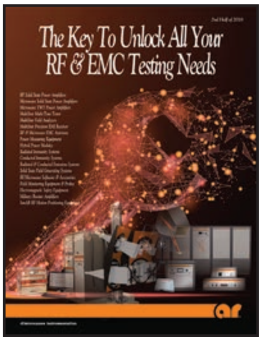

AR RF/Microwave Instrumentation's comprehensive catalog includes virtually everything necessary for RF and EMC testing. Find important information on everything from RF/microwave amplifiers to antennas, probes, analyzers, accessories and integrated test systems that make testing quicker, easier and more accurate. Discover innovative new products like MultiStar Field Analyzers, Test Systems and Receivers that use groundbreaking technology to perform multiple tasks simultaneously, reducing test times from days to hours. The latest developments in hybrid power modules and dual band technology are also represented here.

AR RF/Microwave Instrumentation
www.arworld.us

Frequency Sources Short Form Catalog

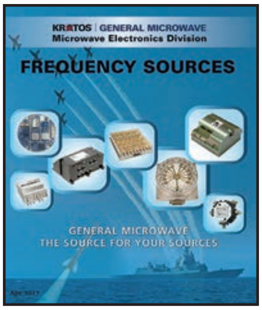

General Microwave Corp. has designed and manufactured cutting-edge microwave frequency sources since 1987. This Short Form Catalog includes sources ranging from free running voltage and digitally controlled oscillators to fast (1 usec) indirect synthesizers, company profile and a wideband frequency modulation applications and techniques tutorial. Specially featured is the Series SM60 family of fast indirect synthesizers capable of analog and digital frequency modulation, while center frequency remains in the pure locked mode.

General Microwave Corp.
www.kratosmed.com

New Brochure

K&L Microwave has been a key supplier to space programs since the Apollo 17 lunar sounder experiment in 1972. K&L has supported customers with high-reliability filter products for integration into flight equipment, providing bandpass, highpass, lowpass and bandstop configurations. As a supplier of custom filter products, K&L has the expertise and resources for determining how best to meet customer space flight requirements. A highly trained engineering staff utilizes specialized in-house and purchased software tools to identify and realize advantageous designs. Download their new brochure and find out how K&L can be "Your Partner in Space."

K&L Microwave
www.klmicrowave.com

Filter Designer 3D Flyer

VENDORVIEW

CST Filter Designer 3D is a complete synthesis tool for narrow bandpass and diplexer filters. It offers a range of solutions throughout the design process of a coupled-resonator filter—regardless whether it is implemented in planar, waveguide or dielectric media. CST Filter Designer 3D together with the simulation capabilities of CST MICROWAVE STUDIO® offers the complete technology for your filter design requirements. Learn more about this powerful tool in their flyer.

SIMULIA, Dassault Systèmes
www.cst.com/solutions/articles/cst-filter-designer-3d

HiRel Broadband Conical Inductors

Gowanda's HiRel Conicals offer predictable frequency response from 40 MHz to 50+ GHz, current ratings to 6A, scalability, low-to-high volumes, unique footprints, ultra-low insertion loss and return loss, in both standard and application-specific designs. Their unique construction helps to limit the effects caused by stray capacitance. They also offer < 1 percent TML per ASTM E595 outgas testing. For needs that go beyond off-the-shelf components, the company maintains a leadership role in custom SMT and flying lead conical solutions to address customer requirements.

Gowanda Electronics
www.gowanda.com/conical

Benchtop Test Solutions Product Guide

VENDORVIEW

Mini-Circuits' has innovated a line of products for these functions that are smaller, faster, easier to control and much more affordable than other options typically available in the industry. Their benchtop test and measurement modules offer the ease of control via USB or Ethernet and include programmable attenuators, power sensors, frequency counters, switch modules, signal generators and control products. Depending on the application, these units may be used as standalone solutions or easily integrated as building blocks to build scalable testing platforms customized to each user's individual needs.

Mini-Circuits
www.minicircuits.com

CatalogUpdate

Innovative T&M Instruments at Budget-Friendly Price

VENDORVIEW

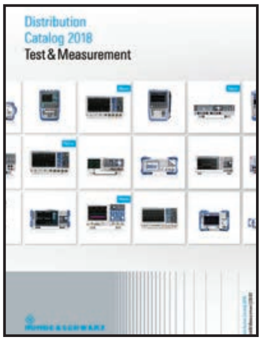

Whatever your job is, you do not always need the ultimate high-end T&M equipment. What you need are precise, reliable, universal measuring instruments. That is what you get from Rohde & Schwarz: The instruments combine practical features with excellent measurement characteristics; they are easy to use and easy on the budget. The Distribution Catalog 2018 presents a lot of new instruments of outstanding quality and innovation at a budget-friendly price (Order number: PD 3606.6463.42).

Rohde & Schwarz GmbH & Co.
www.rohde-schwarz.com

Interface Gauge Kits

VENDORVIEW

A small investment will help to avoid trouble, means checking interfaces of connectors. The connector gauge kits of Spectrum Elektrotechnik GmbH are easy to use with direct reading and self-checking, measure the interface dimensions of coaxial connectors. The kits consist of gauges with especially developed dial indicators to mate with the individual connectors. A master setting gauge adjusts the dial indicator to zero, before mating with a connector to measure the interfaces. The gauges are sold as kits, individual components or replacement parts. Calibration service is provided as well.

Spectrum Elektrotechnik GmbH
www.spectrum-et.com

Updated Broadcast Catalog

VENDORVIEW

SPINNER has published an updated version of its Broadcast Catalog. The company has added band 3 DAB high-power filters for power levels up to 10 kW and band 3 DAB high-power combiners for max 20 kW. All SPINNER UHF CCS combiners in the catalog come with new 3 dB couplers for better return loss. Direct access units for systems from 6 1/8 in. EIA to 9 3/16 in. EIA are now available in a new, more compact design which are easier to install. SPINNER's new 50 kW SmartLoad with indoor or outdoor cooler is also included.

SPINNER
www.spinner-group.com

NEW PRODUCTS

FOR MORE NEW PRODUCTS, VISIT WWW.MWJOURNAL.COM/BUYERSGUIDE
FEATURING VENDORVIEW STOREFRONTS

COMPONENTS

Low PIM Cavity Filters

VENDORVIEW

MCV Microwave introduces two new series of low PIM cavity filters covering UHF, LTE and CBRS frequency bands from 350 MHz to 3.5 GHz. Standard low PIM series feature 163 dBc at 2 tone 43 dBm with 90 to 120 dB isolation. Ultra-low PIM series provide 173 dBc at 2 tone 43 dBm with the same high isolation as the standard low PIM series. Custom wideband designs are available for PIM test bench applications.

MCV Microwave
www.mcv-microwave.com

Broadband 3-Way Type N Power Dividers

VENDORVIEW

MECA Electronics' latest new product offering, non-binary 3-way broadband of power divider covering 0.5 to 6 GHz (803-4-3.250WWP) encompassing public safety through ISM bands. With typical performance of: VSWR of 1.30:1, isolation 17 dB, insertion loss 1.2 dB and exceptional amplitude and phase balance of 1 dB and 12 degrees max. This is in addition to the family of 2-, 4-, 8- and 16-way splitters in various connector styles and IP60 and 67/68 ratings. Made in the U.S. with 36 month warranty.

MECA Electronics Inc.
www.e-MECA.com

2-Way Splitter

VENDORVIEW

The MRFSP8525 2-way splitter is designed for applications that require small, low cost and highly reliable surface mount components.

Applications may be found in broadband, wireless and other communications systems. These units are built lead-free and RoHS compliant. S-parameters are available on request.

MiniRF
www.minirf.com

High-Power Ka Circulators

The M Wave Design Corp. 28DPIA12xx differential phase circulator line offers high-power handling with low insertion loss (< 0.40 dB over a 4 GHz B/W). The circulator has integrated waveguide runs and will handle up to 250 W average and 80 kW peak without special cooling provisions.

M Wave Design Corp.
www.mwavedesign.com

RF Surge Protection Devices

PolyPhaser has released an innovative line of RF surge protection devices engineered and tested to protect equipment from high-altitude electromagnetic pulse (HEMP) and high-level RF weapons. The PolyPhaser HEMP tested product family includes solutions that protect sensitive equipment from intentional electromagnetic interference (IEMI) as specified by the Department of Homeland Security.

PolyPhaser
www.polyphaser.com

6-Way Power Divider

Response Microwave Inc. announced the availability of its new compact 6-way power divider for use in various X-Band applications. The new RMPD6.6000-18000Sf covers the 6 to 18 GHz band offering typical electrical performance of 1.6 dB max insertion loss, VSWR of 1.70:1 max, amplitude unbalance of 0.8 dB and min isolation of 16 dB. Average power handling is 30 W and the unit is operational over the −40°C to +85°C range. Mechanical package is 3.0 × 1.9 × 0.39 in., plus stainless steel SMA female connectors. Alternate power division configurations available on request.

Response Microwave Inc.
www.responsemicrowave.com

Ka-Band 4 Channel Downconverter

VENDORVIEW

RFE Inc. has designed a convenient, cost-effective solution for translating wideband 18 to 40 GHz RF signals into the 6 to 18 GHz domain (via two separate converter banks) giving extended frequency coverage to many existing systems.

RFE Inc.
www.rfe-mw.com

Multiplexers

VENDORVIEW

RLC Electronics' multiplexers are available in 2, 3 or 4 channel versions. Adjacent passbands may be designed for a contiguous or non-contiguous response. For passband frequencies below 2 GHz, lumped element designs will often achieve the desired response in the smallest package. At higher frequencies (up to 40 GHz), distributed coaxial structures are employed to realize the lowest possible loss. The unit pictured above is a diplexer that covers both L-/S-Band frequencies, as well as Ku frequencies, and exhibits low loss (< 0.5 dB per channel). This unit has been fully qualified to operate under military environments and is currently used on an airborne application.

RLC Electronics Inc.
www.rlcelectronics.com

Voltage Controlled Oscillator

The USSP1570-LF is designed to cover the frequency range of 1540 to 1600 MHz while tuning over 0.5 to 2.5 VDC. This unmatched VCO features extremely low-power consumption by operating off a 2.7 VDC supply and drawing a mere 7 mA of current all while housed within an ultra-small footprint measuring 0.2 × 0.2 × 0.04 in. This VCO features a spectrally clean signal of −90 dBc/Hz at 10 kHz offset.

Z-Communications
www.zcomm.com

CABLES & CONNECTORS

40 GHz Skew Matched Cable Pairs

Fairview Microwave Inc. has released a new line of 40 GHz skew matched cable pairs designed for bit-error-rate testing, eye diagrams and differential signals at data rates of 10 to 28 Gbps. Fairview's new line of skew matched cables consists of three extremely flexible models that are 100 percent tested for skew match. Performance specs include an impressive VSWR of 1.4:1 and 1 ps delay match.

Fairview Microwave Inc.
www.fairviewmicrowave.com

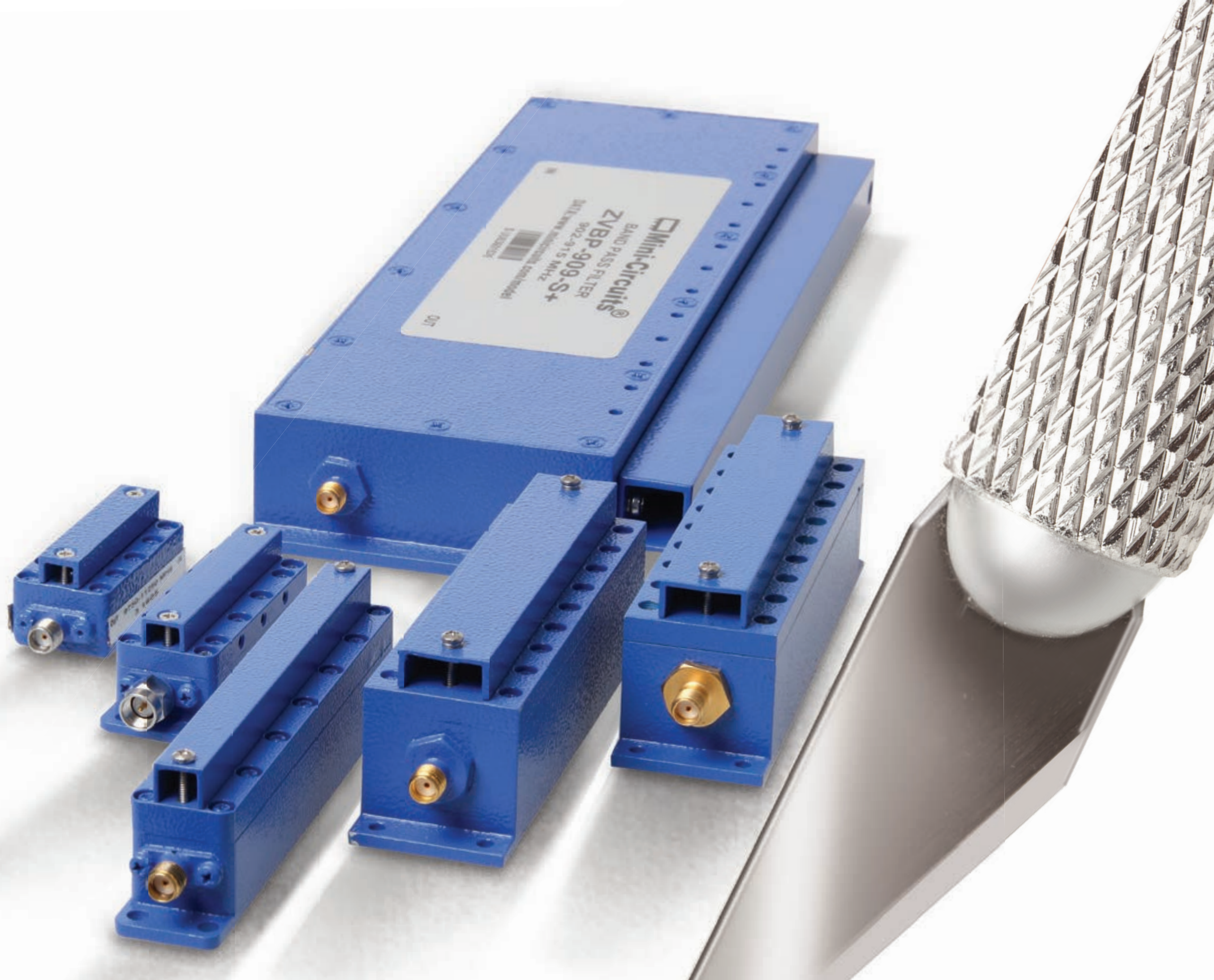
Mini-Circuits
ZVBP-909-S+

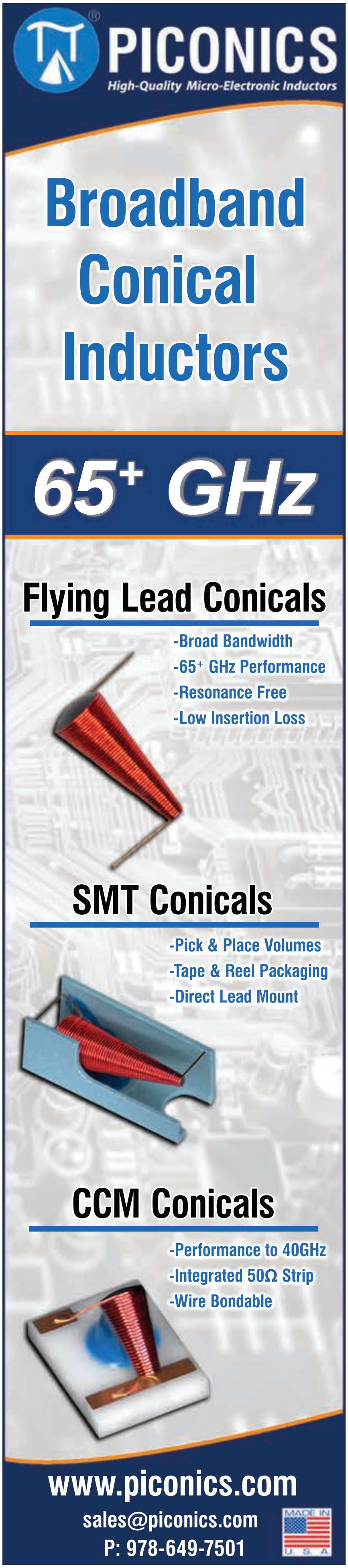

NewProducts

Removable Vertical Launch Connectors

VENDORVIEW

Pasternack has introduced a new line of solderless vertical launch connectors that are ideal for high speed networking, computing and telecommunications applications. Pasternack's new series of vertical launch connectors consists of 12 models that provide VSWR as low as 1.3:1 and maximum operating frequency of up to 50 GHz, depending on the model. These launches boast a reusable clamp attachment and can be used for microstrip or stripline.

Pasternack
www.pasternack.com

Precision Adapters

VENDORVIEW

RF Superstore is excited to announce the addition of precision RF adapters to its large selection of in-stock interconnect RF components. The 3.5 mm male or female to 7 mm adapter options made with passivated stainless steel are priced below $150.

RF Superstore
www.rfsuperstore.com

Solderless PCB Connectors

For a variety of standard applications up to 70 GHz Rosenberger provides cost-effective, economic solderless PCB connectors which can be easily assembled to PCBs by using screws (standard screws included). The product range consists of RPC-3.50 (up to 26.5 GHz), RPC-2.92 (up to 40 GHz), RPC-2.40 (up to 50 GHz) and RPC-1.85 (up to 70 GHz) straight female connectors characterized by low return loss values and high mating cycles (≥ 500). Typical test & measurement applications are semiconductor chip testing fixtures or PCB-characterization.

Rosenberger Hochfrequenztechnik GmbH & Co. KG
www.rosenberger.com/us_en

Coax Connector Type 2.2-5

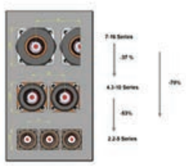

The innovative 2.2-5 connector series offers very low PIM values of −166 dBc at 2 × 43 dB, while solving the low space requirements of modern MIMO antennas, small cell concepts and innovative DAS (Distributed Antenna Systems). A typical 2.2-5 flange saves up to 53 percent in space compared to 4.3-10, and even 70 percent over the 7-16 connector. Despite its compact design, the 2.2-5 is designed for low attenuation cables of up to ½ in.

Telegärtner Karl Gärtner GmbH
www.telegaertner.com

AMPLIFIERS

GaN Solid-State Power Amplifier

Model Number SSPA 16.75-20.25-40 is a high-power, GaN solid-state power amplifier that operates from 16.75 to 20.25 GHz. It is packaged in an enclosure that is optimized for high shock and vibration requirements. Nominal output power is 40 W typical. Typical power gain is 46 dB min. Input and output VSWR is 2.0:1 max. This SSPA can be blanked on and off in less than 10 uSec. OIP3 is 51 dBm min.

Aethercomm
www.aethercomm.com

100 kHz to 1000 MHz U Series Amplifier, Now Up To 250 W

VENDORVIEW

AR's new family of "U" (Universal) Series RF solid-state Class A power amplifiers now includes a 250 W model that covers the 100 kHz to 1000 MHz frequency range. These amplifiers are ideal for EMC, laboratory use, antenna and component testing, Watt meter calibration, medical/physics research and more. This compact, high performance and affordable amplifier joins a family of products available in 1, 2.5, 10, 25 and 50 W output levels that covers 10 kHz to 1000 MHz.

AR RF/Microwave Instrumentation
www.arworld.us/html/u-series-amplifiers.asp

1 W, Solid-State, Medium Power Amplifier Module

VENDORVIEW

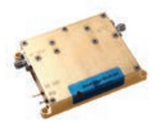

Introducing MPA1004, an ultra broadband 0.5 to 26.5 GHz medium power solid-state amplifier for all lab applications. The MPA1004 module produces 1 W of CW power with a gain of 30 dB. This is a state-of-the-art power amplifier module that features Exodus' instantaneous ultra-wideband module with built-in protection circuits for superb reliability and ruggedness. It is a design suitable for EW, EMI/RFI testing, phased arrays and any application requiring small size and high-power density.

Exodus Advanced Communications
www.exoduscomm.com

SGA/SGN Series SSPAs

KRATOS General Microwave's SGA/SGN Series SSPAs offer GaAs/GaN

technology reliability that can be customized to meet specific pulse or CW output powers. The product line supports both X- and Ku-Band applications with bandwidths up to 10 percent and offers peak power outputs up to 400 W. Designed for demanding defense, aerospace and SATCOM applications. General Microwave SSPAs have excellent power efficiency with demonstrated field proven performance and reliability. General Microwave's vertical integration process affords flexible layouts and architectures to meet individual specifications for electrical, mechanical and environmental parameters.

Kratos General Microwave
www.kratosmed.com

Low-Current MMIC LNA Die Covers 10 to 13 GHz

VENDORVIEW

Mini-Circuits' PMA2-133LN-D+ is a MMIC low noise amplifier die covering the 10 to 13 GHz range. This model operates on a 3 to 5 V supply with just 13 mA current

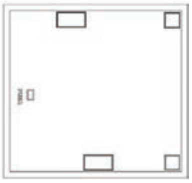

consumption at 3 V, and provides 1.3 dB noise figure, +28.6 dBm IP3, 8.9 dB P1dB and 14.1 dB gain. The amplifier is designed with a built-in shut-down feature to conserve DC power consumption when the amplifier is not in use. The amplifier die is supplied in small-quantity gel-paks of 5, 10, 50 or 100 KGD (Known Good Dice), as well as partial and full production wafers.

Mini-Circuits
www.minicircuits.com

6 to 18 GHz, Low Noise Amplifier

VENDORVIEW

PMI Model No. PE2-19-6G18G-1R6-16-12-SFF is a low noise amplifier (LNA) which operates between 6 to 18 GHz. This LNA

provides 19 dB of small signal gain while maintaining a low noise figure of only 1.6 dB. The P1dB output power of 15 dBm enables the LNA to function as a LO driver for balanced, I/Q or image reject mixers. This model also features I/Os that are DC blocked and internally matched to 50 Ohms.

Planar Monolithics Industries Inc.
www.pmi-rf.com

SOURCES

Ku- and Ka-Band BUCs and SSPAs

The ATOM series of Ku- and Ka-Band BUCs and SSPAs are among the smallest, lightest, most energy efficient transmitters available. ATOM's high efficiency reduces power consumption significantly, delivering considerable lifetime operational cost savings. This series is ideal for applications such as airborne, comms on the move and TWTA replacement. Its special options include complete customization, baseplate cooling, 1275D surge protection, EMI filtering and internal reference with auto-sensing, backed by excellent availability and short lead times.

Norsat International
www.norsat.com

C-Band GaN SSPA Transmitter

RFHIC Corp. introduces the RRT56575K0-67, 5.6 to 5.7 GHz GaN SSPA transmitter for radar system applications. The RRT56575K0-67 has an output power of 5 kW, 30 percent power consumption efficiency, 67 dB gain and a 10 percent duty cycle. The RRT56575K0-67 is designed and manufactured utilizing RFHIC's GaN HEMT technology, providing excellent power density, high breakdown voltage and high efficiency. Upon customer's needs, the transmitter shelf can be easily integrated without phase matching. Digital monitor and control features are available upon request.

RFHIC Corp.
www.rfhic.com

4G/LTE Embedded Cellular Module

Richardson RFPD Inc. announced the availability and full design support capabilities for a new 4G/LTE embedded cellular module from Sierra Wireless. The EM7565 offers global 4G/LTE coverage on 24 LTE bands. It provides uplink speeds up to 150 Mbps, downlink speeds up to 600 Mbps and support for carrier aggregation and 256-QAM. The module also supports LTE-LAA and 3.5 GHz CBRS band. The EM7565 dramatically improves network performance and enables businesses to use one module for global 4G networks.

Richardson RFPD Inc.
www.richardsonrfpd.com

1 GHz Low Noise Phase Locked Translator

The KFCTS1000-10-5 is a 1 GHz phase locked frequency source featuring excellent

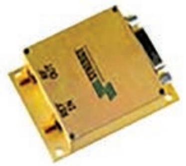

phase noise performance. Phase noise at 10 kHz offset is –141 dBc/Hz and at 100 kHz offset is –158 dBc/Hz. Spurious products are suppressed by 80 dB and output power is +5 dBm min. Power supply requirements are +5 V at 60 mA and +12 V at 10 mA max. The reference input requirements are 10 MHz at a signal level of +1 to +3.3 V.

Synergy Microwave Corp.
www.synergymwave.com

E LEARNING CENTER

Presented by: Microwave Journal

October Short Course Webinars

Technical Education Training.............................. 10/9
An Overview of Glass-Weave Impact on Millimeter-Wave PCB Performance
Sponsored by: Rogers Corp.

Technical Education Training........................... 10/24
Choosing the Right RF Technology for 5G Infrastructure
Sponsored by: NXP Semiconductors

Register to attend at mwjournal.com/webinars

Past Webinars On Demand

Distributed Wi-Fi (Wi-Fi Mesh): A Key to Smarter Homes

Sponsored by: RFMW / Qorvo

Presented by: Cees Links, General Manager of Qorvo's Wireless Connectivity Business Unit

microwavejournal.com/events/1774

How to Optimize Filter Designs for 5G Mobile Front-Ends

Sponsored by: onscale

Presented by: Gerry Harvey, VP of Engineering, OnScale and Ryan Diestelhorst, VP of Strategy, OnScale

microwavejournal.com/events/1799

mmWave Silicon Technologies: Tackling Performance, Integration & Affordability for 5G

Sponsored by: GLOBALFOUNDRIES

Presented by: Shankaran Janardhanan, Director of RF SOI, FDX™ RF and RF CMOS Offerings, GLOBALFOUNDRIES

microwavejournal.com/events/1794

MACOM's Technology Advantage Enables Mainstream 5G Cost Structures, Energy Efficiency, Range and Form Factors

Sponsored by: MACOM — Partners from RF to Light

Presented by: Michael Ziehl, VP and GM for RF Power and Basestations, MACOM

microwavejournal.com/events/1782

NewProducts

ANTENNAS

SENCITY® Rail Multi Antenna

VENDORVIEW

The unique rooftop antenna meets the special requirements of rail applications and enables a fully connected fleet, leading to improved customer satisfaction for Train Operating Companies (TOC). Designed to improve rail connectivity and drive productivity, the antenna aids the transition to a digital railway, able to deliver connected services to passengers such as Wi-Fi, real-time passenger information and live seat reservations. It can also benefit train-to-ground solutions for rail employees, such as on-board ticketing and remote train control management.

Huber + Suhner
www.hubersuhner.com

Airborne Radar Radome

Meggitt recently produced large, disk-shaped radomes for a radar application. This 14 × 4 ft. radome operates over a wide frequency range with very low insertion loss and electromagnetic reflection. The composite radome is a multi-layer construction that optimizes electrical performance while providing high mechanical strength for a demanding airborne environment. The radome is fully qualified for subsonic airborne applications, is resistant to rain erosion and hail and has an integral lightning protection system.

Meggitt Baltimore Inc.
www.meggittbaltimore.com

Monopole Blade Antenna

PIDSO GmbH announces a new blade antenna design. The antenna is linear polarized, very lightweight and environmental resistant. The frequency range is from 1.9 to 2.6 GHz and typical gain value is around 3 dBi. The small form factor making the antenna ideal for low-visibility, aerodynamic or tactical applications such as motorsports (currently in usw at DTM), unmanned vehicles or other applications where size, weight and performance are most critical.

PIDSO GmbH
www.pidso.com

F-Band X9 Frequency Extender

VENDORVIEW

Model STE-SF908-00-S1 is an F-Band X9 frequency extender that uses an input

frequency range of 10 to 15.56 GHz at +5 dBm along with harmonic generation and filtering to produce a 90 to 140 GHz RF signal at –3 dBm. The extender is designed and manufactured as a bench top unit to extend the low frequency synthesizer or sweeper without losing all of the functionalities and features. The extender also features adjustable legs to allow for an easy test setup.

SAGE Millimeter
www.sagemillimeter.com

MATERIALS

Low Loss Microwave Laminate

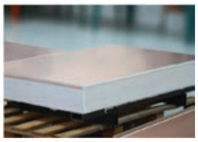

CLP 240 is an innovative low loss copper clad microwave laminate. CLP 240 is manufactured using proprietary hybrid continuous lamination technology developed in-house. This system based on blended Polyolefin resins provides an excellent value solution to designers and manufacturers of wireless panel antennas. Typical production applications are subscriber and infrastructure antennas up to 5.8 GHz. Good PIM performance (at 2 GHz band) and prototype mmWave antenna designs up to 40 GHz have been successfully demonstrated by customers.

Tadbik Advanced Technologies
www.tadbik.com

TEST & MEASUREMENT

Ace Calibration Extender

The ACE-1000A is a calibration solution that allows customers to self-calibrate their Kaelus PIM analyzers in the field. With successful calibration, the ACE calibration extender will extend your analyzer's calibration while reducing downtime to one hour and increasing productivity by retaining instruments in the field.

Kaelus
www.www.kaelus.com

Doppler Measuring System

Spacek Labs Model DS-940HD is a cost-effective, Doppler measuring system. Center frequency is 94 GHz with ±50 MHz bias tuning. Output power is 20 mW. The Gunn oscillator incorporates a GaAs diode, bias is +4.5 to +5.5 VDC at 1 A typ. Delivered with a WR-10 horn antenna, isolator, circulator and a Spacek Labs W-Band detector, DW-2, for real-time Doppler measurements including directional indication. Systems available from 18 to 110 GHz in standard waveguide bands.

Spacek Labs
www.spaceklabs.com

MICRO-ADS

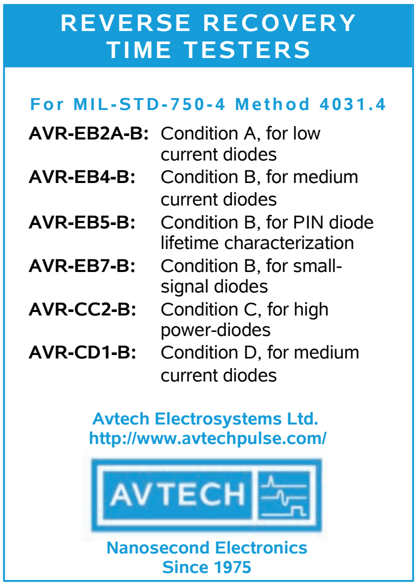

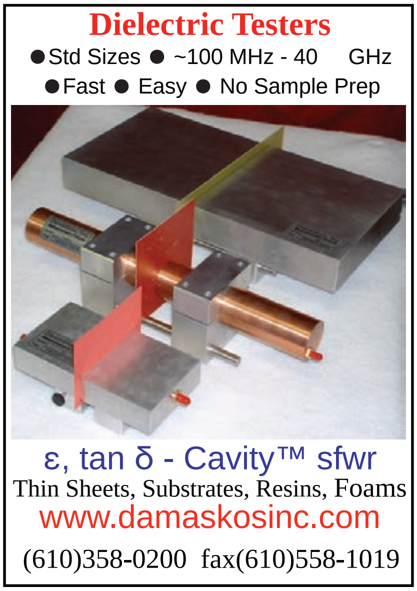

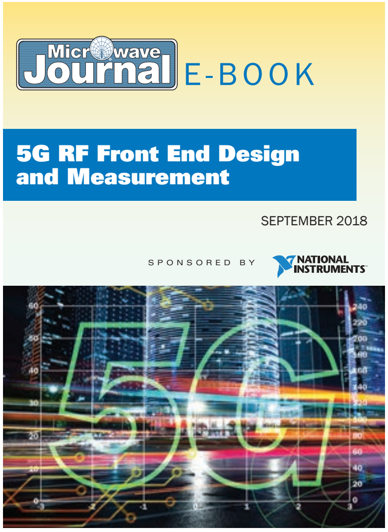

Download @ mwjournal.com

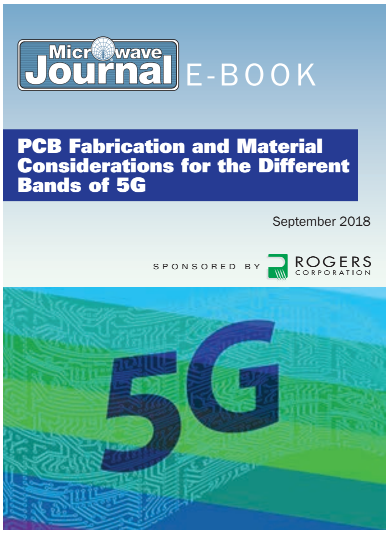

Download @ mwjournal.com

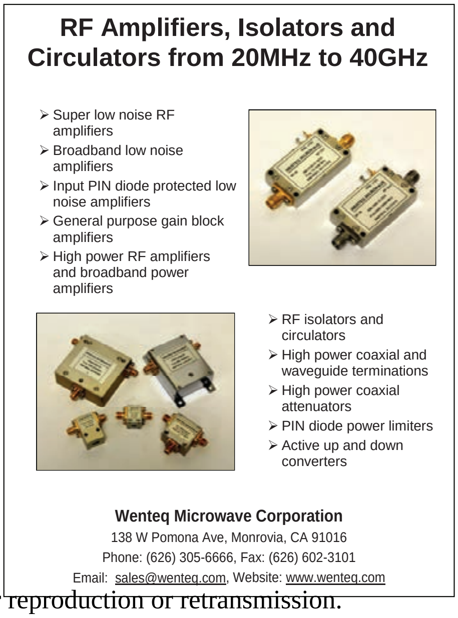

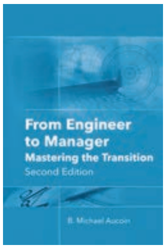

From Engineer to Manager: Mastering the Transition, Second Edition

B. Michael Aucoin

"This book is a must-read if you're an engineer, an upward-bound engineer thinking about transitioning to a leadership position in management, a professional in any discipline pursuing a future in management or a student.

It offers clear and understandable fundamentals for transitioning from engineer to leadership in management—no seven steps to utopia, but guidelines that clearly define the requirements. The author, B. Michael Aucoin, with his experience from practice and research is uniquely qualified—he provides you with what it takes to make a successful transition to leadership in management. Read it, study it and as you grow in leadership responsibility, use it as a reference."

—Gerard H. Gaynor, 3M Director of Engineering, Retired; IEEE Life Fellow

Providing clear, expert guidance to help engineers make a smooth transition to the management team, this newly revised and updated edition of an Artech House bestseller belongs on every engineer's reference shelf. The author's 30-plus year perspective indicates that, while most engineers will spend the majority of their careers as managers, most are dissatisfied with the transition. Much of this frustration is the result of lack of preparation and training.

Supplemental material, such as templates, exercises and worksheets are available at no additional cost at: www.engr2mgr.com.

Contents: Principle 1: Mastering Relationships; Principle 2: Seeing the Big Picture; Principle 3: Getting Things Done; Principle 4: Communicating Effectively; Principle 5: Using Assets Wisely; Principle 6: Taking It to the Next Level.

To order this book, contact:

Artech House
www.artechhouse.com
Email: artech@artechhouse.com
US 800-225-9977
UK +44 (0)20 70596 8750

ISBN: 978-1-63081-543-1
360 pages

Special New Release Prices
$82 – US Now Available
£67 – UK Available November 2018


IMS
Connecting Minds. Exchanging Ideas.
IMS2019
2-7 JUNE 2019
BOSTON 2019
THE HUB OF MICROWAVES
BOSTON CONVENTION & EXHIBITION CENTER
BOSTON, MASSACHUSETTS
Submit your Paper Today!
Secure your Booth Space Now!
www.ims-ieee.org
IEEE
MTT-S

Advertising**Index**

Sales Representatives

Microwave Journal
Frequency Matters.

Eastern and Central Time Zones
Jaime Leger
Northeast Reg. Sales Mgr.
(New England, New York, Eastern Canada)
685 Canton Street
Norwood, MA 02062
Tel: (781) 619-1942
FAX: (781) 769-5037
jleger@mwjournal.com

Michael Hallman
Eastern Reg. Sales Mgr.
(NJ, Mid-Atlantic, Southeast, Midwest, TX)
4 Valley View Court
Middletown, MD 21769
Tel: (301) 371-8830
FAX: (301) 371-8832
mhallman@mwjournal.com

Pacific and Mountain Time Zones
Brian Landy
Western Reg. Sales Mgr.
(CA, AZ, OR, WA, ID, NV, UT, NM, CO, WY, MT, ND, SD, NE & Western Canada)
144 Segre Place
Santa Cruz, CA 95060
Tel: (831) 426-4143
FAX: (831) 515-5444
blandy@mwjournal.com

International Sales
Richard Vaughan
International Sales Manager
16 Sussex Street
London SW1V 4RW, England
Tel: +44 207 596 8742
FAX: +44 207 596 8749
rvaughan@horizonhouse.co.uk

Germany, Austria, and Switzerland (German-speaking)
WMS.Werbe- und Media Service
Brigitte Beranek
Gerhart-Hauptmann-Street 33,
D-72574 Bad Urach
Germany
Tel: +49 7125 407 31 18
FAX: +49 7125 407 31 08
bberanek@horizonhouse.com

Korea
Young-Seoh Chinn
JES Media International
2nd Floor, ANA Bldg.
257-1, Myungil-Dong
Kangdong-Gu
Seoul, 134-070 Korea
Tel: +82 2 481-3411
FAX: +82 2 481-3414
yschinn@horizonhouse.com

China
Shenzhen
Michael Tsui
ACT International
Tel: 86-755-25988571
FAX: 86-755-25988567
michaelt@actintl.com.hk

Shanghai
Linda Li
ACT International
Tel: 86-021-62511200
lindal@actintl.com.hk

Beijing
Cecily Bian
ACT International
Tel: +86 135 5262 1310
cecilyb@actintl.com.hk

Hong Kong, Taiwan, Singapore
Mark Mak
ACT International
Tel: 852-28386298
markm@actintl.com.hk

Japan
Katsuhiro Ishii
Ace Media Service Inc.
12-6, 4-Chome,
Nishiiko, Adachi-Ku
Tokyo 121-0824, Japan
Tel: +81 3 5691 3335
FAX: +81 3 5691 3336
amskatsu@dream.com

Ed Kiessling • Traffic Manager/Inside Sales • 685 Canton Street, Norwood, MA 02062 • Tel: (781) 619-1963 FAX: (781) 769-6178 • ekiessling@mwjournal.com

PRECISION ATTENUATORS

2 W to 100 W

50 W & 100 W models

NEW
BW-E Series 65 GHz models

DC-65 GHz from $31[95] ea. (1-49)

Customers trust Mini-Circuits' BW-family precision fixed attenuators for accuracy, reliability, and repeatability. Now, we've expanded your choices by adding the BW-E series, covering even more applications from DC up to 65 GHz! With fixed attenuation values from 3 to 20 dB, these new, ultra-wideband models feature 1.8mm connectors and provide outstanding attenuation accuracy, excellent VSWR, and RF power handling up to 1W. Our full "BW" family of fixed precision attenuators now includes over 70 models with attenuation values ranging from 1 to 50 dB and power handling from 1 to 100W to meet your requirements with performance you can count on.

Visit minincircuits.com for free data, curves, quantity pricing, designer kits, and everything you need to find the right BW attenuator for your needs. All models are available off the shelf for delivery as soon as tomorrow!

RoHS compliant

Mini-Circuits®

www.minicircuits.com P.O. Box 350166, Brooklyn, NY 11235-0003 (718) 934-4500 sales@minicircuits.com 518 Rev F

FABS and LABS

Ultra-Low Phase Noise is Their Business at Holzworth

In 2004, Holzworth Instrumentation was born as a one person, 200 sq. ft. garage shop in Boulder, Colo. At that time, Jason Breitbarth, now president and CTO, was in the conceptual phase of creating something that would change the face of test & measurement equipment with a specific focus on phase noise analysis. Breitbarth was well versed in the challenges of making valid phase noise measurements using the limited number of high cost test set options that were then available for measuring phase noise at the time. In 2007, he teamed up with Joe Koebel, VP business development, and Leyla Bly, director of interface development, to help the company expand and refine the designs for production.

During the early development of Holzworth's first phase noise test set, the architecture needed a compact, broadband RF synthesizer module for use as a tunable LO within the analyzer. This RF synthesizer needed to have excellent phase noise and spectral performance. With no viable solutions available on the general market, Holzworth needed to do their own design. This early RF synthesizer requirement helped shape the company into what it is today, a well-known provider of innovative product solutions primarily in phase noise analysis and RF synthesis. The company now supplies phase noise analyzers, RF synthesizer modules, multi-channel phase coherent RF synthesizers, low noise amplifiers, mixers/phase detectors, power splitters, frequency dividers, frequency multipliers and electronic phase shifters.

Holzworth's manufacturing facility was setup to handle high volume throughput from original conception, to the current 6,000 sq. ft. facility. The founders knew that long term growth and overall success would depend on establishing a low overhead manufacturing environment that could support high volume. Therefore, an automated test equipment (ATE) approach was adopted early on. By fully automating manufacturing processes from initial PCB turn on and burn-in, through full production testing, it allowed for the original staff of less than five employees then to focus on product design, rather than spending time on manual production test operations. The founders knew that if the big semiconductor manufacturers could handle volumes that can instantaneously increase by millions of any given chipset, it would have to work equally as well for a test equipment manufacturer.

Holzworth manufacturing relies heavily on U.S.-based, ISO certified contract manufacturers to build most of their PCBs, but does all of the integration, test and calibration at its factory in Boulder to ensure high quality. It is ultimately the dedication and skill set of both the Holzworth engineering and manufacturing teams that have created the level of success that Holzworth realizes today. The factory staff is 100 percent responsible for correcting any errors made by a contract manufacturer as well as the rapid prototyping of new designs. The ability to place 01005 sized SMT components as well as placing and reworking large BGA array assemblies in house with > 95 percent yields are just a few examples of the critical skills necessary for product development as well as maintaining timely customer shipments.

Holzworth's tag line is "Ultra-Low Phase Noise is Our Business," but the ability to manage high throughput manufacturing for timely delivery of high performance and highly reliable products is critical.

www.Holzworth.com

EDICON 2019

Electronic Design Innovation Conference
电子设计创新大会

Reserve your booth now to reach engineers in China working on RF, microwave, and high-speed digital designs

April 16-18

China National Convention Center

Beijing China

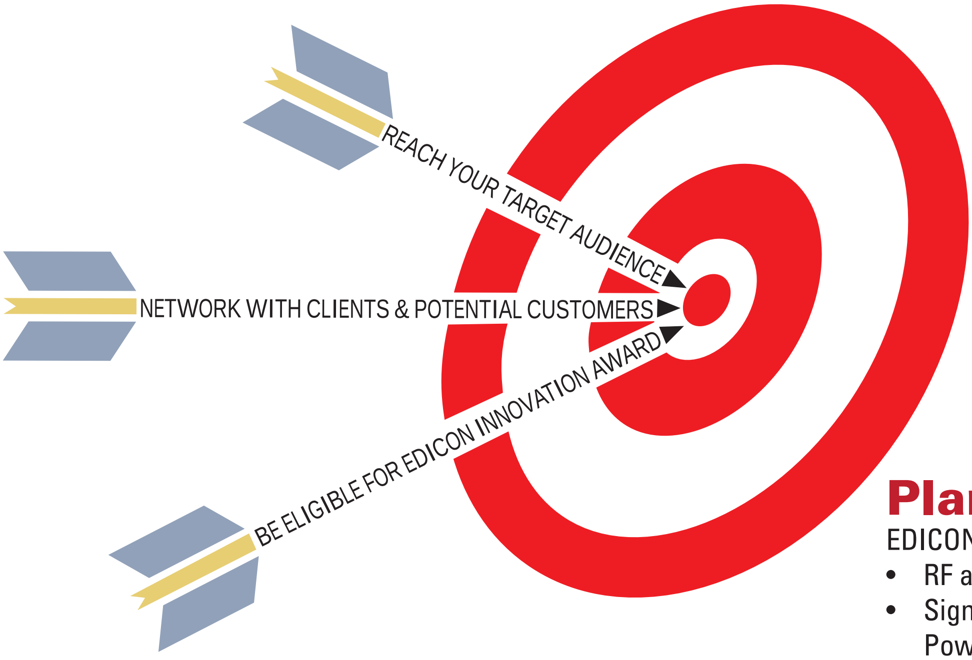

Plan to Exhibit!

EDICON attendees work in:

- RF and Microwave
- Signal Integrity and Power Integrity
- High-Speed Digital Design
- Semiconductors
- Test & Measurement
- Materials and Packaging
- EDA/CAD
- EMC/EMI

Sign up now to choose your booth! **EDICONCHINA.com**

Host Sponsor: KEYSIGHT TECHNOLOGIES

Diamond Sponsor: ROHDE&SCHWARZ

Corporate Sponsor: NATIONAL INSTRUMENTS

Organized by: horizon house® Microwave Journal China 微波杂志

WERLATONE®

True RMS In-Line Power Meters

✓ No Calibration Required
✓ 40 dB Dynamic Range
✓ Optimal Accuracy
✓ Compact & Easily Transportable

Instantaneous & Simultaneous

- Local and/or Remote Monitoring
- Forward Power Reading/Monitoring (Watts or dBm)
- Reverse Power Reading/Monitoring (Watts or dBm)
- VSWR Reading (Watts, Return Loss, Rho)

VSWR Alarm

- Alarm Level Set By Customer
- Customer can Set Up Audio/Visual Alarm via Alarm Relay Contacts
- Signal Sent to Closed Loop

Temperature Monitoring (with Alarm)

- One Sensor, Internal Measurement, within Power Meter
- One Sensor, External Measurement, To Be Placed By Customer

General Purpose Inputs (6 ea) Multiple Use

- Eg. Track Switch Closures (Assign to Interlock Group)
- Eg. Trigger Alarm Relay (Sends Email Alert)
- Eg. RF Presence Status/Alarm (Safety Feature)
- Eg. Alarm, Activated Switch

Accessories

- Single Channel and Multi-Channel Displays (1U Rack, Graphical User Interface)
- RF Digital Dashboard Spreadsheet Software, (Simultaneously Monitor Outputs of 30+ Power Meters)
- PC Based Graphical User Interface Windows XP/7/8/10 Compatible

Accuracy

- ± 1% to Customer Calibration Standard, at Preselected Frequencies
- ± 5% over a Multi-Octave Bandwidth
- Werlatone Calibration Traceable to **(NIST)** **National Institute of Standards and Technology**

Power

- AC Power Adapter (100/240 50-60 Hertz V AC)
- POE (Passive Over Ethernet, Optional POE Injector Kit Available)
- Via RS485 (Via Single Channel or Multi-Channel Displays)

Interface (Via)

- TCP/IP - SNMP and Browser Interface via Local Area Network
- RS232, Serial
- RS485 - Form Addressable Serial Network
- User ID and Password Protected for Access and Control
- Multiple units can be Networked and Simultaneously Monitored On-Site or Remotely (TCP/IP/SNMP/Serial)

✓ RoHS Compliant Design Available
✓ Custom Connector Configurations Available

Werlatone, Inc. 17 Jon Barrett Road Patterson, NY 12563 845-278-2220 sales@werlatone.com www.werlatone.com